Critical Load Serving Capability by Microgrid Operation

A Thesis

Presented in Partial Fulfillment of the Requirements for the

Degree of Master of Science

with a

Major in Electrical Engineering

in the

College of Graduate Studies

University of Idaho

by

Pavan Kumar Penkey

Major Professor: Brian K. Johnson, Ph.D.

Committee Members: Herbert L. Hess, Ph.D., Michael B. Lowry, Ph.D.

Department Administrator: Mohsen Guizani, Ph.D.

July 2016

AUTHORIZATION TO SUBMIT THESIS

This thesis of Pavan Kumar Penkey, submitted for the degree of Master of Science with a major in Electrical Engineering and titled "Critical Load Serving Capability by Microgrid Operation," has been reviewed in final form. Permission, as indicated by the signatures and dates given below, is now granted to submit final copies to the College of Graduate Studies for approval.

Major Professor: _____ Date: _____
Brian K. Johnson, Ph.D.

Committee Members: _____ Date: _____
Herbert L. Hess, Ph.D.

_____ Date: _____
Michael B. Lowry, Ph.D.

Department Administrator:
_____ Date: _____
Mohsen Guizani, Ph.D.

ABSTRACT

In order to improve the resilience of power systems, utilities are interested in developing the capability to form microgrids when abnormal situations occur. In some cases, the microgrid is used to minimize the adverse impacts on the most critical loads, such as hospitals, government offices, and police stations. The costs associated with failure to supply critical loads are significant. Therefore, the ability to create a microgrid largely using existing generation assets with only the addition of control devices can result in improved reliability, greater level of services, and in significant savings during major events. For instance, a significant portion of the power supply to a major city in the northwest region of North America comes through a single 500kV line. If the line goes down, under some circumstances the city grid could go down. The main objective of this thesis is to perform a study establishing the feasibility of forming a microgrid to supply high priority loads in the city, while disconnected from the main grid and using hydroelectric and solar generation available in the area. These transitions will occur while establishing and maintaining stability of the microgrid. Modeling and analysis of the microgrid network is done in Powerworld® simulation software that proved the possibility of forming the microgrid. The model development and validation are described along with the analysis and results of several studies.

ACKNOWLEDGEMENTS

This thesis becomes reality with the kind support and help of many individuals. I would like to take the privilege to thank all of them.

I would like to express my special gratitude to my advisor, Dr. Brian Johnson, for imparting his knowledge and expertise in this study. His valuable time and advices have led me an inspirational journey towards my degree completion. He has provided all possible resources required during the rigorous study and he has motivated me to achieve this success by his influential personality.

I extend my sincere thanks to Dr. Herbert Hess and Dr. Michael Lowry for serving on my committee and for providing indispensable advice, time and support towards the completion of this research.

I would like to thank Erik Lee, Randy Gnaedinger, and Tracy Rolstad for their valuable inputs towards implementation of the project and their guidance in making this possible.

I appreciate Nathan Gaul, Matt Phillips, and Kennedy Caisley for several in-depth discussions about the simulation results. It was pleasure working with such enthusiastic students, which has kept me proactive in my study. I thank Lorrae Fox from University of Idaho Writing center and Yashashree Wase for their help in drafting and formatting this thesis. In addition, I am grateful to my colleagues at University of Idaho for enlightening discussions.

With the upmost importance, I thank my family, friends and Indian Students' Association at University of Idaho for supporting during the highs and lows of this strenuous journey. Without your blessings and love, I would not have expected this success. Lastly, I thank University of Idaho for providing me the competent platform to conduct my research.

DEDICATION

This work is dedicated to my beloved family, and

my parents, Amma and Nanna, my young brother, and

my cousin Sridhar Bandi

TABLE OF CONTENTS

LIST OF FIGURES

LIST OF TABLES

CHAPTER 1. INTRODUCTION

1.1 PROBLEM STATEMENT

The U.S Presidential Policy Direction 21 defines resilience as "the ability to prepare for and adapt to changing conditions and withstand and recover rapidly from disruptions. Resilience includes the ability to withstand and recover from deliberate attacks, accidents, or naturally occurring threats or incidents" [1]. Resilience gained great importance after the catastrophic climate-related events that have occurred recently, which resulted in power system degradation. The events caused power loss for millions of customers and long outage periods. The global risk perception survey of 2015 states the top 10 risks facing society in terms of impact. Among them, failure of climate-change mitigation and adaptation currently stands first. Figure 1-1 shows the list of all the risks based on the economic, environmental, geopolitical, societal and technological categories [2].

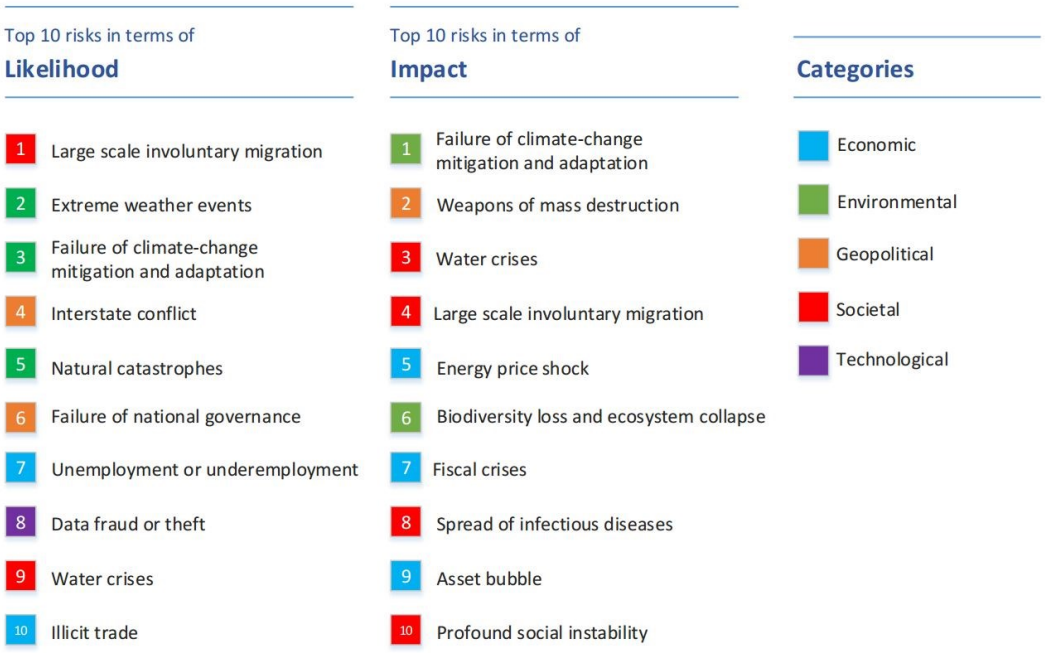

Figure 1-1 Top 10 risks in terms of likelihood and impact [2]

The contingencies that can arise in the power system, which can cause large power outages, are extreme weather and natural disasters, major generation failure, loss of transmission lines, and cyber-attacks [3].

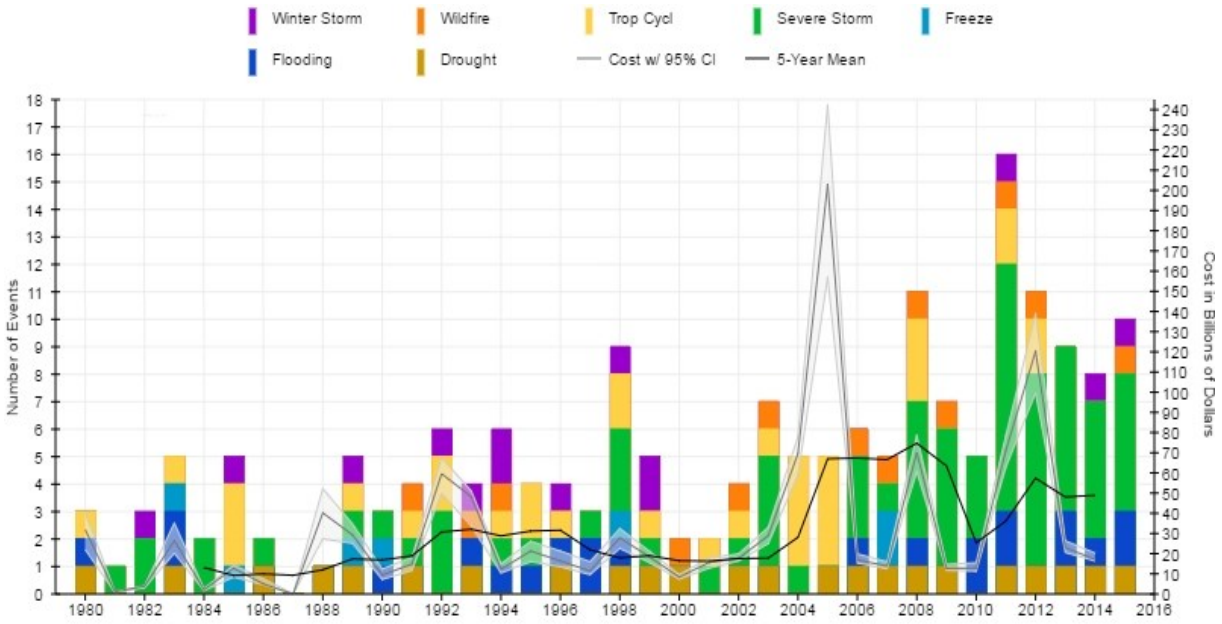

Figure 1-2 Billion dollars disaster events by year [4]

Figure 1-2 shows the billion dollar disaster events, defined as natural disaster events with losses exceeding one billion dollars within the U.S from 1980-2016 [4]. The last decade has seen blackouts around the world due to natural disasters such as the 2005 Hurricane Katrina, 2011 Japan Earthquake, and 2012 Hurricane Sandy [5]. In 2016, there have been eight weather and climate related disaster events including two flood events, and six severe storm events that cost more than one billion dollars in losses in the U.S. The destructive northwest windstorm on 17 November 2015 adversely affected the power network in and around the proposed region of the microgrid. The data acquired from the sponsor in Figure 1-3 shows the number of customers without power over the 10-day period from 17 Nov to 27 Nov 2015 after the windstorm. The graph shows that around 180,000 customers lost power immediately after the storm and it took

around 10 days to restore the power completely. If there had been a microgrid in place during such conditions, the outage time can be avoided by improving the resilience of the system.

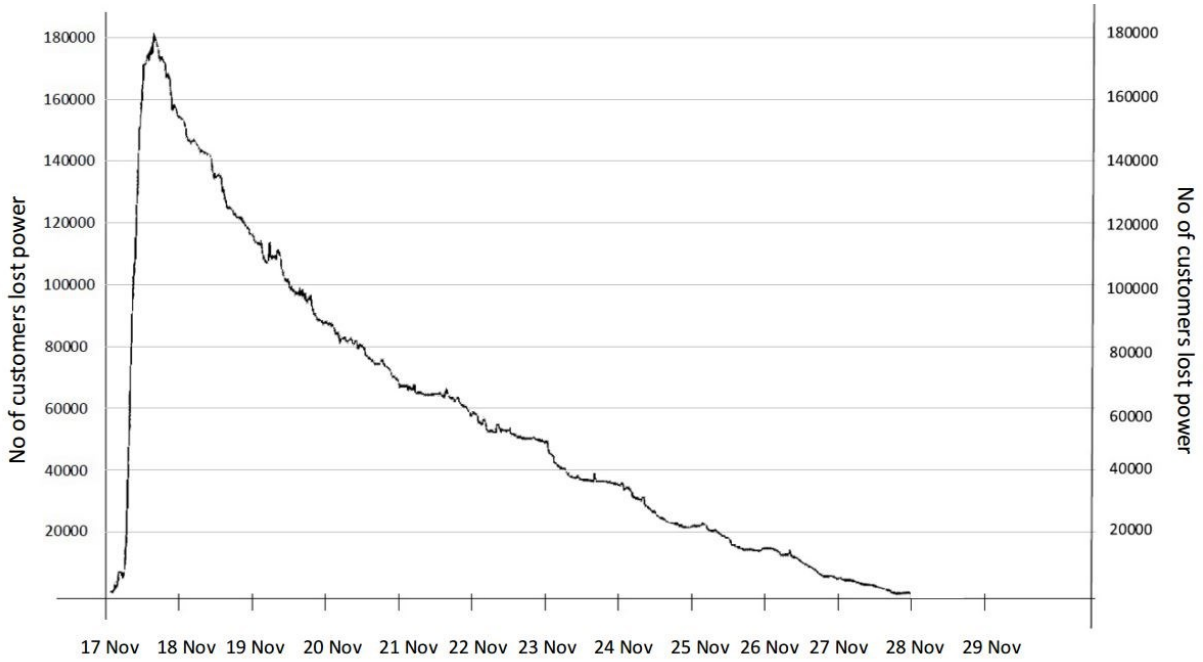

Figure 1-3 Number of customers lost power during the windstorm from 17 to 27 Nov 2015

Wide scale power outages can also be caused by cyber-attacks on the critical infrastructure. The penetration of internet technologies into the power system has created a platform for attackers to target the power networks. The futuristic concepts like Internet of Things (IoT) may turn the system more brittle if proper planning is not done. The other major reasons for large power outages can be failure of generation and misoperation of the protection devices whose failures are likely less to occur.

The current control and monitoring system lacks the inherent ability to analyze unexpected failures and take necessary remedial action to stop the propagation of the outage. Therefore, it is evident that a more resilient electric grid must become a high priority in reconfiguring and updating the nation's electric power distribution and transmission system [6].

1.2 PROPOSED SOLUTION

The existing power system network still depends to a significant extent on centralized control. Failures on such a large-scale system cannot be afforded, so decentralization of the power grid can make it more resilient [7]. In case of such a large event that can cause large-scale power outages, the operational flexibility and local generation capabilities of microgrids can be coordinated to provide local restoration capabilities by supplying the critical loads [8]. Microgrids have proven themselves capable of supplying load when the utility service is lost [9]. The microgrid disconnects from the main grid and supplies power to local loads using local generation resources, potentially including energy storage. Many projects across the world are aimed at developing microgrids, as they are seen as one of the most promising measures for enhancing future power-system resilience [10]. The advantages from forming a microgrid include reduction in power losses and increased reliability, and also include enabling the integration of green electricity sources [11]. Microgrid projects are moving towards commercial development due to an increased importance concerning resilient architecture. As it is difficult to abate the growing requirements for electricity, a collage of approaches, technologies, and solutions will meet the demand. After examining the electricity demand-growth problems, analysis indicates that microgrids will play a significant role in the future evolution of energy service provision [12].

The Department of Energy (DOE) Smart Grid R&D Program has launched a national effort on electric distribution grid resilience. This effort supports Executive Order 13653 “Preparing the United States for the impacts of Climate Change” and the goal of “building stronger and safer communities and infrastructure.” [13] The main objectives of this program are:

- Modernizing the electric distribution grid through the adaptation and integration of advanced technologies and new operational paradigms (microgrids and transactive controls)
- Supporting increasing demand for renewable energy integration and grid reliability and resiliency at state and local levels [13].

1.2.1 Microgrid Definition

The US Department of Energy (DOE) defines a microgrid as a group of interconnected loads and distributed energy resources within clearly defined electrical boundaries that acts as a single controllable entity with respect to the grid. A microgrid can connect and disconnect from the grid to enable it to operate in both grid-connected or islanded-mode [14] [15]. The value of microgrids to protect the nation's electrical grid from power outages is becoming increasingly important in the face of the increased frequency and intensity of events caused by severe weather [6]. The U.S. DOE Office of Electricity Delivery and Energy Reliability (OE) has designated the research and development (R&D) of next-generation microgrids systems a high priority. The DOE's OE has allocated funding for microgrid R&D to meet its 2020 goals. The goal states "To develop commercial-scale microgrid systems (capacity <10 MW) capable of reducing outage time of required loads by >98% at a cost comparable to nonintegrated baseline solutions (uninterrupted power supply [UPS] plus a diesel generator set), while reducing emissions by >20% and improving system energy efficiencies by >20%, by 2020." [6] [16]

A microgrid is characterized as the 'Building Blocks' of a smart grid and its organization is based on the control capabilities offered by increasing penetration of distributed generation, renewable sources, storage devices, switching capacitors and controllable loads [17].

1.2.2 Microgrid Demonstration Projects

In the recent years, the US has become a leader in microgrid demonstration and technology development. There are many microgrid demonstration projects taking place in the U.S. Figure 1-4 shows the demonstration projects overview as of 2011 [5] [18]. The American Recovery and Reinvestment Act (ARRA) of 2009 spurred investments in smart grid technology and programs at utilities across the country. The smart grid investment grant program and smart grid demonstration projects that it funded provided unprecedented opportunities to learn from smart grid implementation [19].

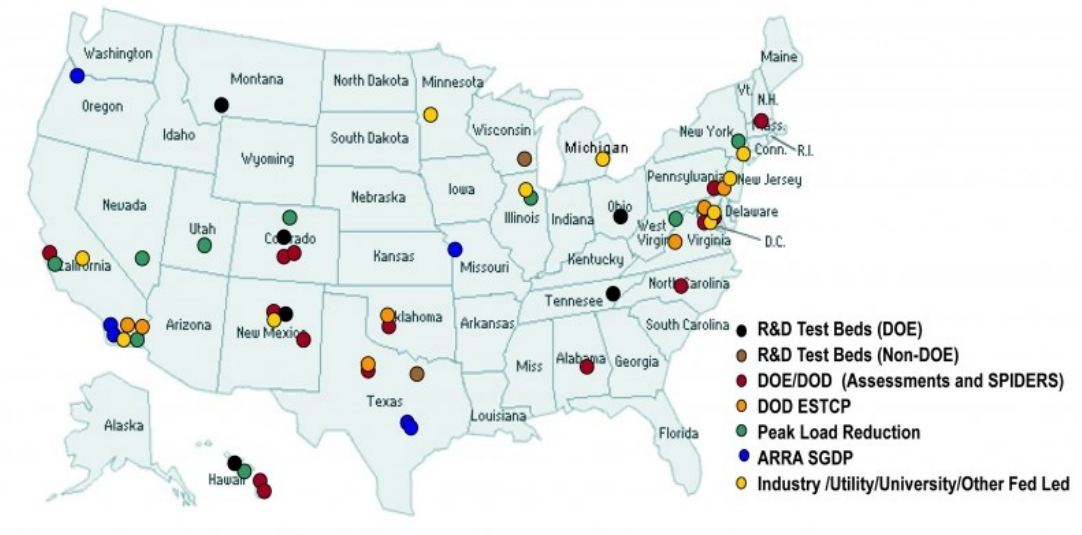

Figure 1-4 Current microgrid demonstration projects across the U.S. [18]

The Department of Defense's (DOD) flagship microgrid project was called Smart Power Infrastructure Demonstration for Energy, Reliability and Security (SPIDERS) and the Department of Energy's (DOE) gave grants to nine microgrid demonstration projects, generating significant activity in the space. Other efforts include the IEEE 1547 and IEEE 2030 series of standards, the Consortium for Electrical Reliability Technology Solutions (CERTS), and software tools like DER CAM [20], Grid Lab-D [21], Open DSS [22], Homer Energy [23]

and other recent developments have filled in the gaps in the microgrid sector [17]. The two main R&D and demonstration projects going on currently in the U.S are SPIDERS, co-run by DOE, DOD and Department of Homeland Security (DHS) and the Renewable and Distributed Systems Integration (RDSI) microgrid grants program, run by DOE. The DOE's RDSI projects are discussed in this section to gain understanding of their contribution [17].

A. Chevron Energy Solutions – CERTS microgrid demonstration (Santa Rita Jail, CA)

The overall goal of this project is to prove the commercial viability of a CERTS Microgrid, one that aims to reduce the cost of a microgrid by avoiding complicated control systems by incorporating off the shelf components. The project was able to disconnect from, and resynchronize to the grid, offset the peak-load period costs, and reduce the load on the distribution feeder during peak load. As part of the CERTS system, they used a simple controls protocol requiring only the voltage and frequency at each terminal to share real and reactive power between generation and storage [24].

B. SDG&E – Beach cities Microgrid (Borrego Springs, CA)

The project aimed to be a test bed and proving ground for GridWise^{TM} information-based technology to allow more power to be delivered using existing infrastructure and to increase the lifetime of existing infrastructure. The area of the microgrid included a distribution grid that is owned by the utility but some or all of the generation resources are owned by the customers in a 125 residential home area [24].

C. University of Hawaii – Transmission Congestion Relief (Maui, HI)

This project aimed at developing an aggregate model and monitoring system for the surrounding area to assist in increasing visibility into the system and allow for better-informed

decisions of adding more renewable energy resources to the system. This would improve overall service quality, system reliability, and reduce the operating cost of the system. The project coupled an advanced system model and smart meters to collect and analyze real world data to manage the high penetration from DG better [17] [24].

D. ATK Space Systems – Powering a Defense Company with Renewables (Promontory, UT)

This project aimed to integrate renewable DG into an intelligent automated energy distribution system for ATK Space Systems. By integrating heat recovery, wind turbines, and energy storage, the company projected they will reduce on-demand substation load by 15% of their 17MW peak load. To integrate these technologies into the existing system they planned to add load aggregation, monitoring, fault detection, diagnostics, remote monitoring, controls and black start systems [17] [24].

E. City of Fort Collins – Mixed Distribution Resources (Fort Collins, CO)

The Fort Collins project aimed to demonstrate successful renewable DG monitoring, aggregation, integration, and DR. Efforts were set towards reducing peak loading by 20% to 30% over two feeders. With over 3.5 MW of DER in 5 different locations aggregated from PV, micro-turbines, duel fuel CHP, reciprocating engines, backup generators, hybrid vehicles and fuel cells the city was able to meet its goal [24].

F. Illinois Institute of Technology – The Perfect Power Prototype (Chicago, IL)

The goal of this project was to develop a self-healing, learning and self-aware Smart Grid capable of reacting to and routing around faults as well as dispatch DG when needed. The system would respond to internal sensors, external power grid conditions, power prices and weather conditions [24].

G. Con Ed – Interoperability of DR Resources (New York, NY)

Due to the uniquely high load density of New York, NY and its high profile loads such as Wall Street and many buildings crucial to national and international trade, the utility aimed to support the grid with demand response and distributed generation resources. The project included developing and demonstrating methodologies to increase the grid's ability to provide demand response to costumers [24].

H. Allegheny Power – WV Super Circuit Demonstration the Reliability Benefits of Dynamic Feeder Reconfiguration (Morgantown, WV)

In order to demonstrate improved distribution system performance with the integration of distributed resources the project proposed the use of dynamic feeder reconfiguration across several feeders and a multi-agent grid management system for automated controls [24].

1.2.3 Microgrid Capability in Worldwide Market

Future microgrid systems present many opportunities and potential applications. The microgrids are likely to have exponential growth with a wide variety of applications and interconnections with utility grids [6]. The microgrids that are being installed today are equipped with early generation-automated functionalities for supplying power to the critical loads. In future, advanced microgrid systems will be in demand with the increase in Distributed Energy Resources (DER) and renewable energy integration combined with complex intelligent transmission and distribution network. Figure 1-5 shows the annual total microgrid capacity and implementation revenue in the worldwide market estimated from 2015-2024. Although the graph is only an estimate, the microgrid implementations may reach these targets.

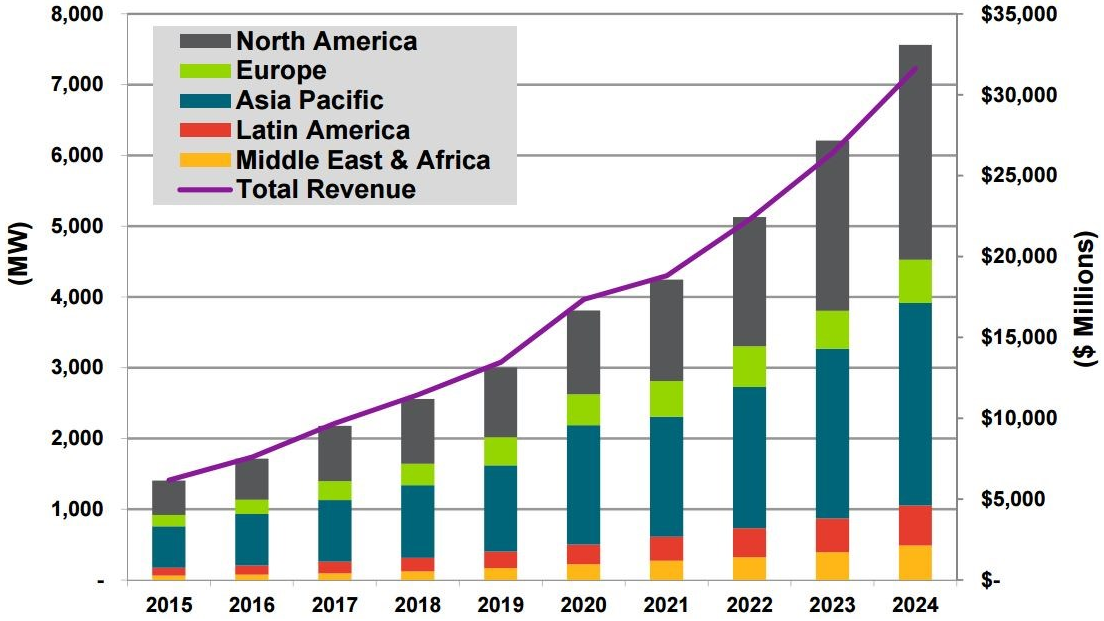

Figure 1-5 Annual total microgrid capacity and implementation revenue by region, world markets: 2015 – 2024 [25]

1.3 OBJECTIVES OF THIS THESIS

The main objective of the thesis is to perform a study for establishing a microgrid to supply high priority loads in a central business district of a moderate size city in the west part of the U.S. The microgrid uses hydroelectric generators located near to the critical loads as a main source of energy with a supplement supply by the photovoltaic installations. Implementation of the microgrid will require disconnection from the main grid, reconfiguration to pick up critical loads such as hospitals, a courthouse, a university campus and other facilities, while shedding non-critical loads. These transitions need to occur while maintaining the stability of the microgrid. The studies include:

a) Identifying the electrical boundaries of the microgrid and forming a unified model of the microgrid from data divided into different models in different simulation packages.

b) Analyzing the energy resource potential available to can supply electrical energy to the microgrid, this includes the analysis of hydro and solar energy potential in the region of the microgrid and estimating the amount of solar energy that is needed to supply most of the critical loads based on the capability to generate power.

c) Organizing the components of the microgrid, and analyzing the historic load consumption profiles and power generation profiles of the generators to estimate the requirements.

d) Modeling and simulation of the entire system together in a software package called Powerworld simulator [26]. This talk includes acquiring the data required from models in SynerGEE electric simulation software [27], and modeling every significant component of the microgrid.

e) Proposing a transition process from grid mode to the microgrid. Analyzing the results and drawing conclusions on viability of this microgrid. Optimizing power factor by capacitor sizing and identifying the locations to place them.

f) Performing forecast study based on the historic profiles and proposing ideas of day ahead and week ahead scheduling of the microgrid operation.

g) Steady-state and transient stability analysis of the microgrid model using the dynamic models suggested by WECC and Powerworld and including the real machine data.

h) Sizing an energy storage device such as a battery for the microgrid and identifying the locations to place the battery to improve the microgrid operating conditions.

i) Performing analysis such as time step simulation, contingency analysis, transient stability analysis and optimal power solution in Powerworld to identify the feasibility of the microgrid.

j) Proposing microgrid controller ideas for the optimal operation and control of the microgrid. This implementation will be done in the next phase of the sponsored project.

k) Exploring additional simulation software tools that would benefit the microgrid modeling including validating the Powerworld model with a Real Time Digital Simulator (RTDS) model.

The costs associated with failure to supply critical loads are significant. The ability to create a microgrid largely using existing generation assets with only the addition of control devices can result in significant savings during major events.

The results of the study and microgrid development can potentially be applied to other areas of the utility system or to other utilities in the region or nation. By locally supplying the power demand to customers, utilities can decrease system generation and recovery costs during outages. The application of microgrids can foster the application of clean energy very close the critical loads.

1.4 LITERATURE REVIEW

1.4.1 Microgrid Overview

Microgrids are a future power-system configuration providing clear economic and environmental benefits compared to routine expansion of our legacy modern power systems [28]. The microgrid is a subset or building block of a smart grid. According to the European technology platform for smart grids [29], a smart grid is an electricity network that can intelligently integrate the actions of all users connected to it – generators, consumers and those that assume both roles – in order to efficiently deliver sustainable, economic, and secure electricity monitoring, control, communication, and self-healing technologies. Microgrids can provide premium power through the ability to smoothly move from dispatched power mode

(while connected to the utility grid) to load tracking (while in island mode). The unique nature of the microgrid design and operation requires a fresh look into the fundamentals [30].

1.4.2 Benefits of Microgrid

Microgrids offer significant benefits for the customers and utility grid as a whole:

i. They improve reliability and resiliency by introducing the self-healing capability at the local distribution network level.
ii. They reduce the carbon footprint by reduction in the use of conventional sources of energy if they are based on renewable energy generation.
iii. They lead to lower cost of operation by reducing the transmission and distribution (T&D) cost.
iv. The presence of the generation close to the demand reduces the transmission and distribution line losses.
v. The utilization of renewable DGs and offering energy efficiency by responding to real time market prices [3].
vi. Microgrids can also provide additional benefits to the local utility by providing dispatchable power for use during peak power conditions and alleviating or postponing distribution system upgrades [31].

1.4.3 Microgrid Architecture

Microgrids are systems that have at least one distributed energy resource, associated loads, with the ability to form intentional islands in an electrical distribution system [31]. The initiation of a microgrid is usually caused by operation of an upstream switch or a breaker. The technologies that support the formation of a microgrid, the availability and cost of installation, will drive the practical implementation of the microgrids in future. Figure 1-6 shows the

microgrid components that contains the distributed generation, an interconnection switch, distributed storage, loads, and possible control systems [31].

Distributed generation (DG) is an approach that employs small-scale technologies to produce electricity close to the end users of power. DG technologies often consist of modular (and sometimes renewable-energy) generators, and they offer a number of potential benefits. In some cases, distributed generators can provide lower-cost electricity and higher power reliability and security with fewer environmental consequences than traditional power generators can [32]. The DGs usually have an output range of few kW to 10 MW.

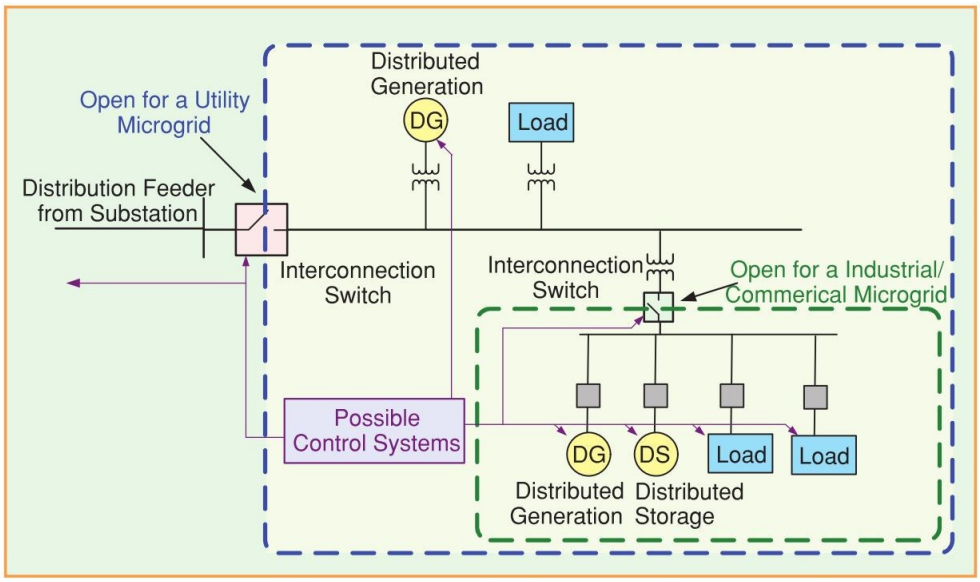

Figure 1-6 Microgrid and its components [31]

Distributed storage is used to supply the variation between total generation and total load. The capacity of storage is determined by the net power transfer in one direction over time. Storage applications can be categorized based on energy density requirements or on power density requirements [31]. Storage systems enhance the overall microgrid system by stabilizing the DGs to run at constant and stable output during load fluctuations, reducing emission and losses; by providing the ride-through capability and in some cases by permitting DG to operate

as a dispatchable unit. There are many different forms of storage technologies available and a few of them are discussed in Section 2.3.3.

The interconnection switch in Figure 1-6 is located at the point of common coupling (PCC) of the microgrid. The switch isolates the microgrid into an island if there is a severe disturbance or outage on the utility side. In order to accomplish this task, the switch needs to be monitored and controlled by special protective relaying equipment that can detect the abnormal situations on the utility side. The control equipment typically includes an islanding detection scheme, which helps ensure a successful islanding in case of a contingency [33]. To improve the applicability and functionality, the controls are designed to be technology neutral and can be used with a circuit breaker as well as faster semiconductor based static switches [31].

Microgrids can be distinguished from the distribution system based on use of distributed energy resources (DER) with their controllability, such that a microgrid appears to the upstream network as a controlled, coordinated unit [8]. The microgrid will have a central controller, which receives the measurements and inputs from all the components in the microgrid and sends control instructions to the controllable components. The two basic problems that need to be addressed in a microgrid are voltage control and frequency/load-generation balance. During grid-connected mode, when the microgrid is connected to the utility grid, voltage control is the key issue, and can be managed by central controller with the help of load tap changers and capacitors. It can also be addressed with a (P/V) droop control solution [34]. When the microgrid is isolated, which is in islanded mode, frequency control is the main concern, as the microgrid should have some buffer to ensure initial energy balance. Energy storage will also

help in this case; the generation and actively managed loads can contribute to balance the system locally using droop control strategy [8].

The microgrid frequency will not reach the nominal value by using the primary action of the droop controlled DER. The secondary control will dispatch controllable microsources to correct the frequency deviation [8]. This leads to the discussion of classes for different control strategies, one is the centralized control that controls through a master controller and the other is a decentralized (local) control that relies on local measurements to define new reference parameters. The centralized control makes decisions by acquiring the information from all the different entities and estimating the overall state of the microgrid. This also includes controllable load shedding techniques based on the critical load priorities. The advantage of local control is that it relies on local measurements, thus avoiding any communication dependencies leading to jitter or delay. The communication architecture within the microgrid needs to be well established with the demand control applications. It is advisable to combine the central and local control schemes where the fast and coordinated response is required.

In some cases, microgrid operation begins with a shutdown and a subsequent black start of the system using an automated start procedure. It is necessary to ensure that the microgrid is properly equipped with communication capability, automated switches, adequate protection equipment, and a central controller that acts as the brain of the microgrid. The sequence of events that triggers the black start of the microgrid starts with the microgrid status determination by both upstream and downstream devices checking for faults on either side, and deciding to switch to microgrid if there is no alternative. Then, the microgrid preparation starts with a signal to local controller to disconnect all the points of common coupling and non-critical loads. The DGs with black start capability can be initiated first and then the storage units are connected to

ensure the microgrid is operating at nominal frequency and voltage under a no-load condition. The other DGs can be synchronized while ensuring desirable conditions. There should be coordination between the non-controllable sources and loads to avoid large frequency variations. Once the utility grid restores, nominal frequency and voltage, resynchronization can be done.

1.4.4 IEEE 1547 Series Guidelines

The Institute of Electrical and Electronics Engineers (IEEE) Standard 1547 has been a foundation document for the interconnection of distributed energy resources (DER) with the electric power system or the grid. It is unique as the only American national standard addressing systems-level DER interconnected with the distribution grid [35]. Figure 1-7 shows the series of standards and amendments that came after the initial standard. The complete overview of the IEEE series of standards in the areas of fuel cells, photovoltaic (PV), dispersed generation, and energy storage is available in [36].

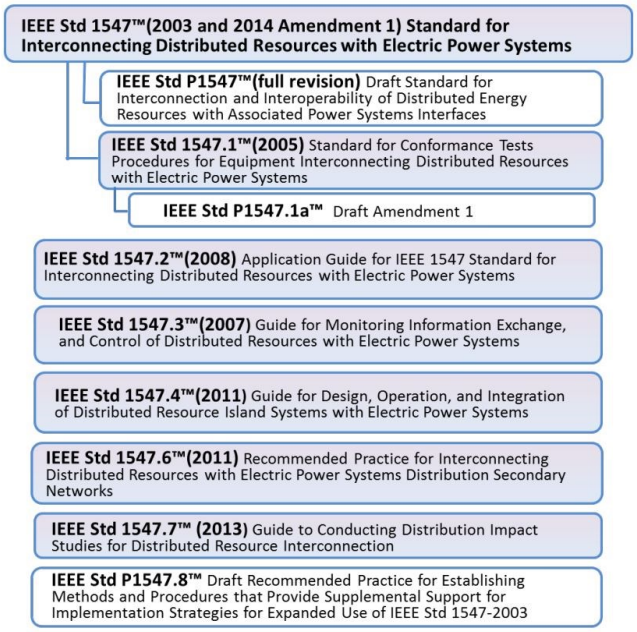

Figure 1-7 IEEE 1547 series interconnection standards

The 1547 – 2003 standard states that the DERs need to be disconnected from supplying the local loads if the power grid they are connected goes down. The reason for this statement is that it might cause a hazardous situation for any line crew inspecting the faulted lines, and they may be electrocuted if they are unaware of the DER status. As the DER is a small system when compared to the entire grid, it will have less inertia and could leads to poor power quality.

However, the 1547.4 – 2011 [37] standard covers intentional islands in electric power systems (EPSs) that contain DERs. The DER island, which is also referred to as a microgrid is the term used to describe intentional islands. This standard states that intentional islands or microgrids can be formed if there are proper controls associated with the microgrid by taking care of power quality, safety, and technologies like islanding detection, resynchronization etc. Thus, this standard discusses the guidelines for forming microgrids.

Since the 1547 guidelines [38] were published in 2003, there has been significant development of new interconnection lessons learned and best practices of implementation in real world. This led to revision of 1547 standard and approval in mid-2013 [15].

The amendments that support microgrids in the 1547-2003 standards are:

a) With the coordination between the microgrid and area EPS, the microgrid will participate to regulate the voltage by changes of real and reactive power. The microgrid will not cause the voltage to go out of ANSI C84.1-2011, Range A [39].
b) If any measured voltage falls in the ranges in Table 1-1 occur, the microgrid will cease to energize area EPS within the clearing time indicated. With mutual agreement between area EPS and microgrid, dynamic voltage and clearing time settings will be allowed.

c) If any frequency in the range of Table 1-1 occurs; the microgrid will cease to energize the area EPS within the clearing time. Dynamic frequency and clearing times are permitted under mutual agreement between microgrid and area EPS.

Table 1-1 Microgrid islanding transition requirements [40]

Voltage range (pu)	Clearing time (sec)	Clearing time (sec) adjustable up to and including	Frequency range (Hz)	Clearing time (sec)	Frequency (Hz)	Clearing time (sec) adjustable up to and including
Default settings			Default settings		Ranges of adjustability	
V<0.5	0.16	0.16	>62	0.16	60-64	10
0.45≤V<0.6	1	11	f>60.5	2	60-64	300
0.5≤V<0.8	2	21	<59.5	0.16 to 300	56-60	300
1.1≤V<1.2	1	13	f<57	0.16	56-60	10
V≥1.2	0.16	0.16				

The resynchronization of the microgrid to EPS can be performed by maintaining the following requirements [41]:

a) EPS and microgrid voltage magnitude is within the range B of Table 1 of ANSI/NEMA C84.1-2011, i.e. 0.95-1.05 per unit [39].
b) EPS and microgrid frequency between 59.3 Hz to 60.5 Hz.
c) EPS and microgrid conditions are maintained continuously for at least 5 minutes.

The IEEE 1547.4 – 2011 guidelines suggest important considerations that need to be considered while forming a microgrid, they are: [37]

i. Changes in power flow magnitude and direction
ii. Proper control of voltage, frequency and power quality
iii. How many point of common coupling (PCCs) exist
iv. Protection schemes and coordination modifications

v. Monitoring, information exchange and control (MIC)
vi. Load requirements of the area or local EPS that will be islanded
vii. Characteristics and functionality of the DRs
viii. Steady-state and transient conditions
ix. Interactions between electrical energy sources
x. Reserve margins, load shedding, and demand response
xi. Cold load pick up

A transition to island mode or microgrid mode can be a result of a scheduled event or unscheduled events. Scheduled transitions are intentional and the duration of the planned island properly managed. Unscheduled transitions are inadvertent events that are typically initiated by loss of the area EPS. The transition will be managed by an island interconnection device (IID), and protective relays. The microgrid needs to able to support the system voltage and frequency after the transition. It needs to be able to supply real and reactive power requirements of the loads within the island and serve the range of load operations by having a margin that is a function of the load factor. Voltage regulation equipment needs to be modified to meet the requirements of the microgrid. One of the generation resources can be operated outside the IEEE 1547 standards to assure the voltage and frequency stability in the microgrid. There should be proper monitoring to understand the status of the island. Adaptive relaying may be implemented [37].

When a microgrid is planned, the following information needs to be collected [37].

i. Site survey, location, size and configuration of capacitor banks, voltage regulation equipment, reactors, protective and sectionalizing equipment, and transformers.

ii. Load characteristics, generation characteristics including fuel source and black start capability

iii. Abnormal voltage and frequency ride-through capabilities, grounding of the system, impedances model, voltage regulation, protection scheme and automation scheme.

iv. Acceptable voltage, frequency and harmonic range (normal and transient), maximum acceptable rate of change of frequency, acceptable dynamic stability limits and imbalance level of voltage

v. Ratings and types of switching devices, protection equipment and settings, and provision for future expansion

1.4.5 IEEE 2030 Guidelines

The technology advancements and development of advanced Distributed Energy Resources (DER) grid operations and control functionalities are surpassing the requirements in current standards and codes for DER installations and interconnection with the distribution grid [35]. Interoperability is the capability of two or more networks, systems, devices, applications, or components to externally exchange and readily use information securely and effectively [42]. Smart grid interoperability provides organizations the ability to communicate effectively and transfer meaningful data, even though they may be using a variety of different information systems over widely different infrastructures, and sometimes across different geographical regions [43]. In addition to the IEEE 1547 standards, the smart grid interoperability and associate interfaces will come from IEEE standard 2030 [42]. Figure 1-8 shows the definition of interoperability (IEEE 2030) and graphically depicts the interoperability focus areas.

Interconnection and intra-facing frameworks and strategies with design definitions are addressed in this standard, providing guidance in expanding the current knowledge base. This

expanded knowledge base is needed as a key element in grid architectural designs and operation to promote a more reliable and flexible electric power system [36].

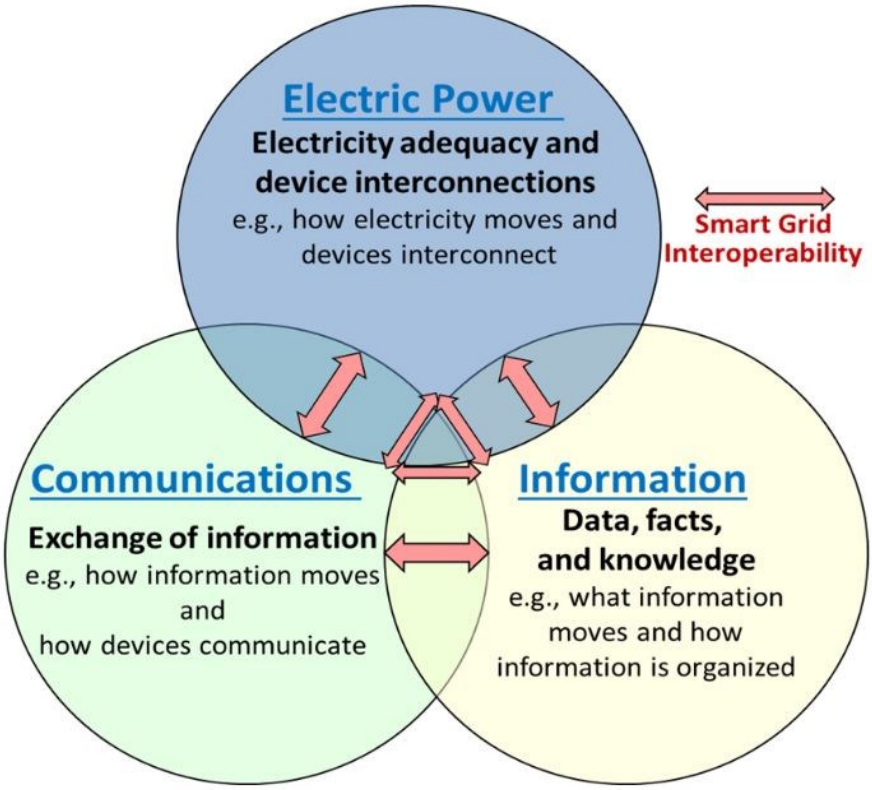

Figure 1-8 Smart grid interoperability: the integration of power communications, and information technologies [42]

Smart grid interoperability is usually associated with the following:

- Hardware/software components, systems, and platforms that enable machine-to-machine communication to take place.
- Data formats, where messages transferred by communication protocols need to have a well-defined syntax and encoding.
- Interoperability on the content level; a common understanding of the meaning of the content being exchanged [43].

Figure 1-9 shows the series of standards published under IEEE SCC21 (Standards Coordinating Committee on fuel cells, photovoltaics, dispersed generation, and energy storage) [36] or in development.

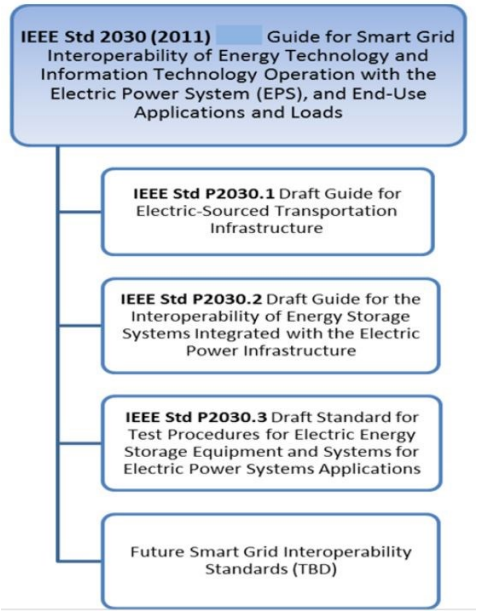

Figure 1-9 IEEE SCC21 2030 series of smart grid standards

1.5 ORGANIZATION OF THIS THESIS

Chapter-1 of this document introduced the problem statement and the proposed solution to overcome the problem. After defining the microgrid and its existence, the chapter described microgrid project implementations and potential future growth. Then, a literature review talked about the concepts for microgrids and discussed development in recent times along with the technologies involved, followed by discussion of relevant IEEE standards to increase the penetration of microgrids.

Chapter-2 contains the characteristics of the model of the proposed microgrid, the electrical boundaries for the microgrid along with energy resource models. The different

components that can build a microgrid are discussed in detail. The components include power generation resources, electrical loads, energy storage devices, and the microgrid controller.

Chapter-3 discusses the modeling of the microgrid, the simulation software tools used (Powerworld, SynerGEE electric, and Real Time Digital Simulator (RTDS)) to build the model and how the each component is modeled in those software packages. It includes the procedure involved in importing the data from the different programs and lists all the parameters used in the microgrid model.

Chapter-4 discusses the simulation results from the microgrid models and the analysis that is involved in operation and control of the microgrid. The ideas proposed to operate the microgrid are presented in this chapter along with the microgrid planning and control aspects.

Chapter-5 contains conclusions and future work, including proposed ideas that are useful for the implementation of the microgrid.

Appendix-A contains the example of a Powerworld auxiliary file and Appendix-B contains the calculations involved in generator capability-curve modeling. Appendix C presents a Java program for generating Powerworld auxiliary files.

CHAPTER 2. CHARACTERISTICS OF THE PROPOSED MICROGRID

This chapter discusses the study system considered for the modeling and it describes how the various components of the microgrid are modeled and how each contributes towards the final system model. A moderate sized city in western region of the US plans to establish a microgrid. The city is located near a river with two hydroelectric generation facilities supplying power to the regional power grid. This microgrid is unique since it will be predominantly supplied by hydro generation that is close to the critical loads within the microgrid. The model data was acquired from the local utility serving the region. The existing network has smart meters installed for part of the microgrid, which record the hourly load and generation metering information, and which is available for analysis. This data is very useful for understanding the behavior of the loads and generation over different seasons over the year. This study model the different components of microgrid based on the definition of electrical boundaries.

2.1 ELECTRICAL BOUNDARIES OF MICROGRID

Figure 2-1 shows a one-line diagram of the transmission network within the city and including the scope of the microgrid. Normally, a significant amount of power comes from the 500kV line shown in the Figure 2-1; which is stepped down to 230kV and further to 115kV at substation 10 and substation 9. The 115kV transmission network connects to various substations with circuit breakers at each substation, which can be operated remotely. It is important to define the electrical boundaries of the microgrid before modeling the system, as it needs to be isolated from rest of the power grid by opening breakers at the Points of Common Coupling (PCCs). Substations 1, 2, 3, and 4 are identified as boundaries in the system model, which are normally supplying most of the critical loads in microgrid from external generation.

Breakers B1, B7, B8, and B13 shown in Figure 2-1 will be opened when there is an external contingency requiring formation of a microgrid, with two hydro generators located at substation 2 and photovoltaic sources distributed all around the microgrid area.

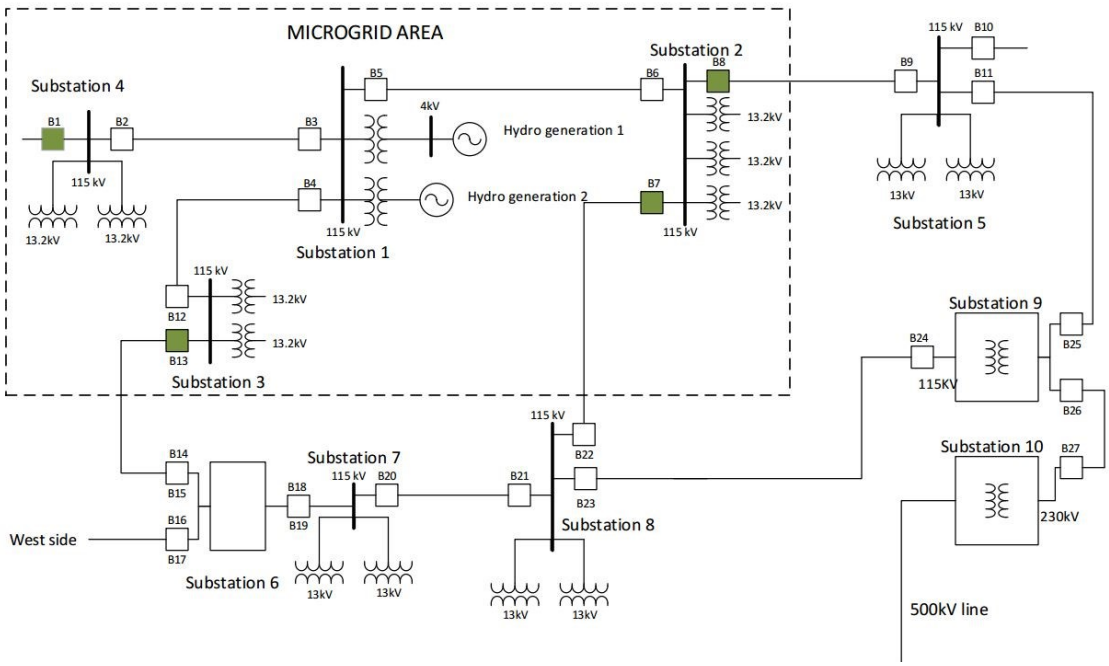

Figure 2-1 Transmission network around the area of microgrid (The microgrid boundary is marked)

2.2 ENERGY RESOURCE MODELS

Two important renewable energy resources in the region of microgrid are available for power generation in microgrid. They are hydroelectric energy and solar energy. The water flow in the river affects the generation from the hydro generators. In the same way, the seasonal and daily variation of solar irradiation in the region will have impact on the power generated through solar panels. The hydro and solar energy potentials of this region are first analyzed to determine the possibility of microgrid to supply critical loads in the area of interest. The critical loads in the area of interest are the city courthouse and jail, several hospitals, a university campus area

and the downtown business district. Details of these loads and priority of them will be discussed in section 4.2.

2.2.1 Hydro Energy Potential

The United States Geological Survey (USGS) database [44] provides data on the water flow of the river where the hydro generation facilities are located. Figure 2-2 shows the monthly average discharge of water measured in cubic meters per second averaged over a period from 1891-2016. Analyzing this data shows that the water flow is high enough to generate maximum generator nameplate generation only during few days in winter and spring. In summer and fall seasons, the river has less capacity to generate power, as the water flow is low. However, solar energy has some potential to supply more energy during that time.

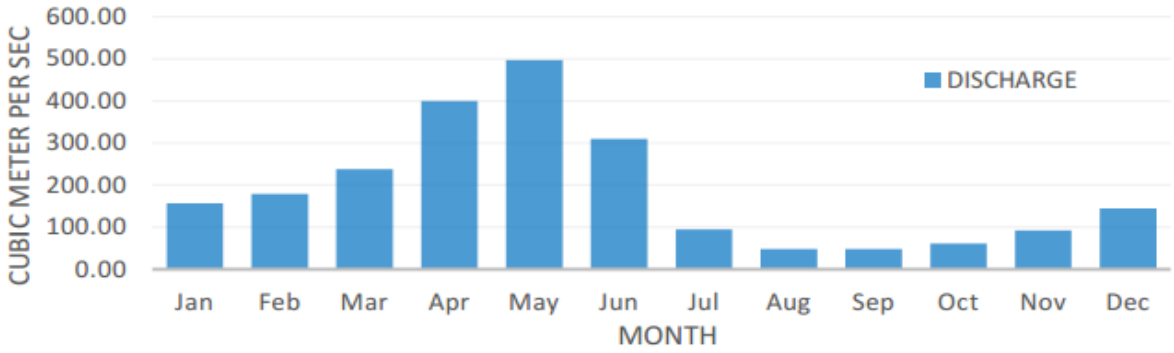

Figure 2-2 Monthly average river discharge from 1891 – 2016

2.2.2 Solar Energy Potential

The National Renewable Energy Laboratory (NREL) [45] has records of a solar radiation incident at sites across the United States using three different types of photovoltaic collectors. The three different types of photovoltaic collectors are flat plate collectors facing south at a fixed tilt, 1-axis tracking flat plate collectors that tilt along with a north south axis, and a 2- axis tracking flat plate collectors that also track east to west. The solar energy is measure in kWh per square meter of collector per day. Figure 2-3 shows the solar radiation data

averaged over a period of 30 years from 1961-1990. It is evident from the data that solar energy potential is high during summer and early fall seasons. Photovoltaic generation can compensate for the low water availability during these seasons, if there is sufficient installation of photovoltaic cells along with proper controls.

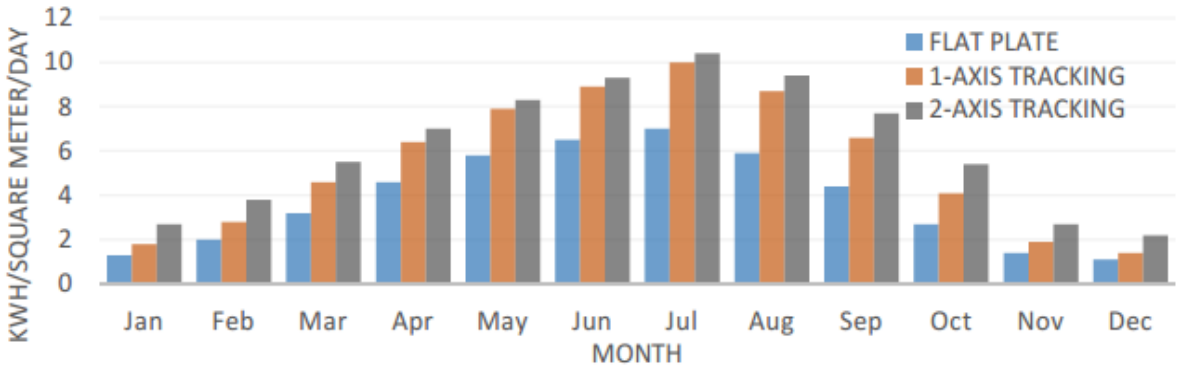

Figure 2-3 Solar radiation average in the city for 30 years

2.2.3 Solar Energy Estimation for Potential Sites

The National Renewable Energy Laboratory (NREL) developed a tool called the PVWatts Calculator, which is freely available [46]. The tool estimates the amount of solar energy that the rooftop of a building can supply if photovoltaic cells were installed all over it. The roof top area of building housing the critical loads in this study was estimated with the help of this tool to understand the potential solar energy generation. Figure 2-4 shows the estimated solar energy in kWH per year from the different critical loads in the microgrid. This is an estimation, not to be confused with the installed capacity. Analyzing the data shows that there is very good potential of solar energy (10.3 MW installed DC capacity) [47] during summer and fall from these buildings.

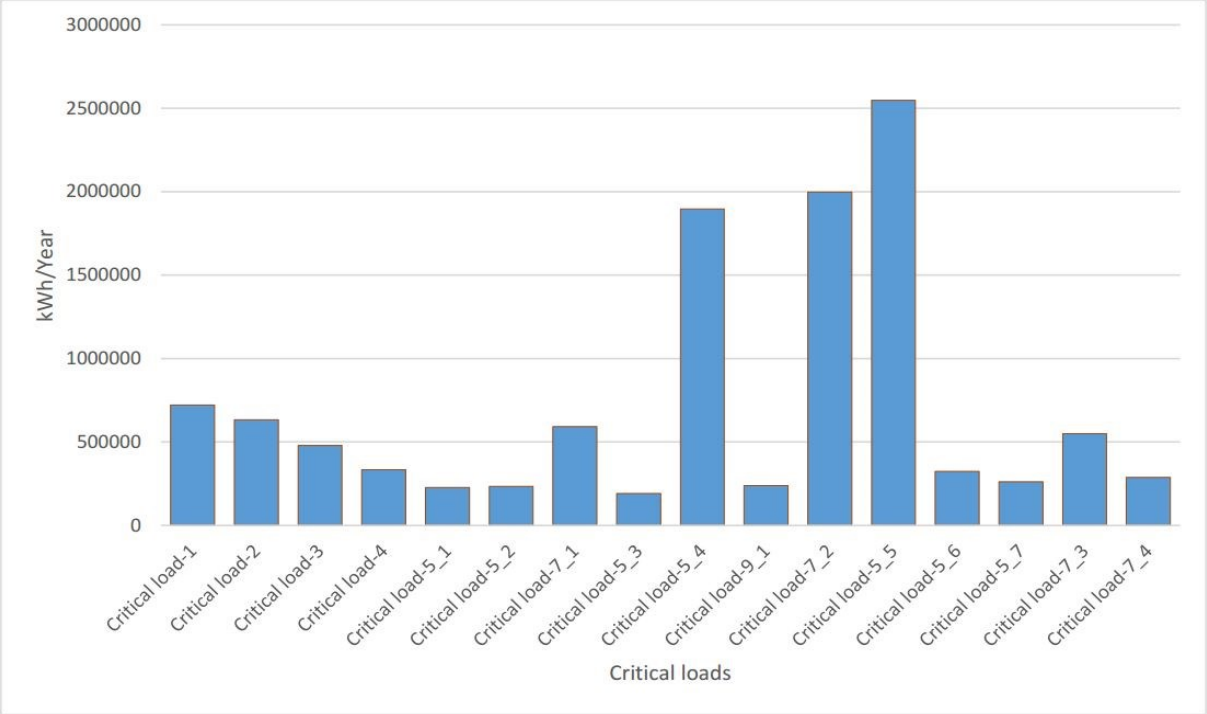

Figure 2-4 Photovoltaic energy generation estimation from critical load roof tops

2.3 COMPONENTS OF A MICROGRID

The microgrid contains mainly four main types of components as shown in the Figure 2-5. There are power generation sources, electricity consuming devices, energy storage devices, and a microgrid controller or controllers. Transmission or distribution lines and transformers interconnect the main components.

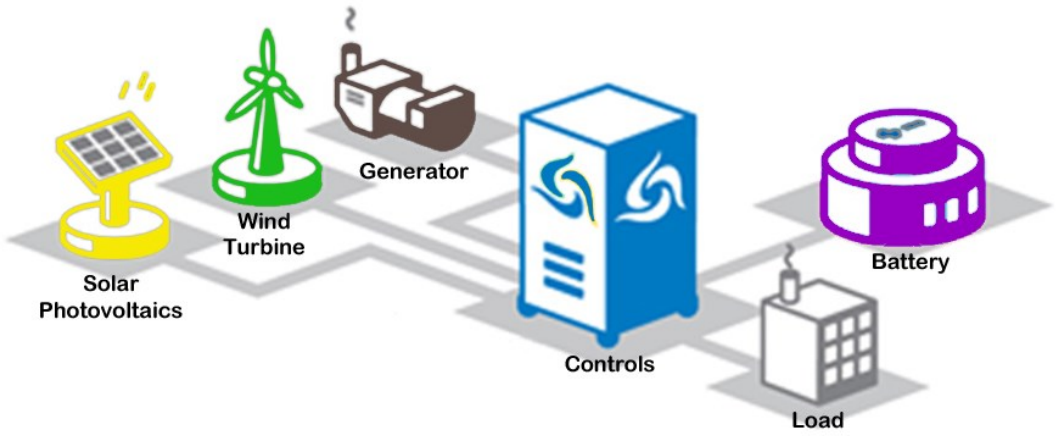

Figure 2-5 Typical microgrid components

2.3.1 Power Generation Resources

The most important components for operating the microgrid are the power generation resources. They can be any type of conventional and non-conventional generation source. In this study system, there are two hydro generators, which contribute the major proportion of the power supply. The two hydro generators are run-of-the-river plants that are located on a river flowing through the downtown of the city. The two generators have name plate ratings of 10MW and 15MW respectively under maximum water flow conditions in the river. These two hydro generators are synchronous machines having a static exciter, governor and along with a black start capability. However, one of the generators is an older machine and it needs a few enhancements in the governor controls. Figure 2-6 [48] shows generator systems and their associated controls for the hydroelectric power plants.

The Automatic Generation Controller (AGC) ensures that the frequency and voltage of the entire system is stable and real and reactive power flows are maintained. [49] This control system is associated with the generators, which is different from the microgrid controller that communicates with this. The two generators in the study system are driven by two different

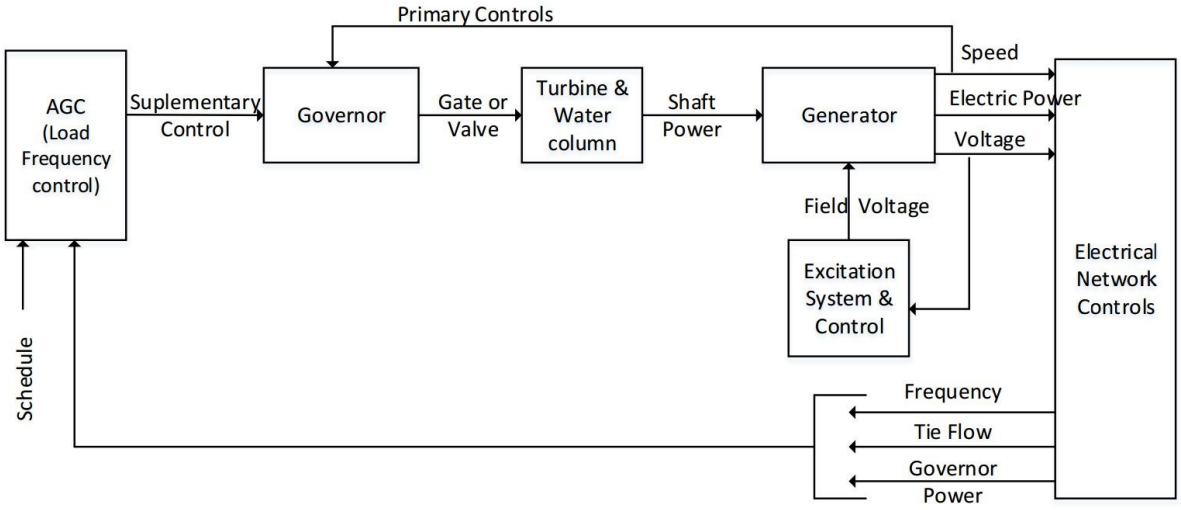

Figure 2-6 Generation controls block diagram

types of turbines, one is Francis turbine and the other one is a Kaplan turbine, which are chosen based on several other location-based constraints.

A. Analysis of Annual Generation Capability

The metering data from the two generators is acquired for three years (2013-2015). It is further analyzed to produce hourly averages of the generation for four different seasons. Typically, load profile analysis is done by taking two seasons (i.e.) summer and winter as they tend to have varying behavior of loads and generation in case of a large power system. In case of this microgrid, which rely more on hydro energy and partially on solar energy, the water flow in the river and solar intensity determine the capability to generate power. It is good to have analysis based on four different seasons. A tool called Energy Charting and Metrics (ECAM) [50] is utilized to analyze these generation profiles and compare them to the demand for the critical loads. The three-year average of hourly load profile of critical loads for the same period is entered in the tool.

The tool generates a 24-hour average of four different seasons with each hour averaged over the season. Figure 2-7 and Figure 2-8 show the real power average of generators 1 and 2 which are to be used in the microgrid. Their output is nearly constant over a given 24-hour period when supplying the entire power grid. The power generation of these generators reduces considerably during summer and in early fall, whereas they generates almost their maximum during spring and winter, potential can be observed in the plots. Figure 2-9 shows the generation profile of solar energy potential for 24-hour period in four different seasons based on NREL data. The solar energy is available only some parts of the day, and it varies with the season that can be observed in the Figure 2-10 shows the combined generation profile of the averaged output of two hydro generators over the last three years plus the solar energy potential.

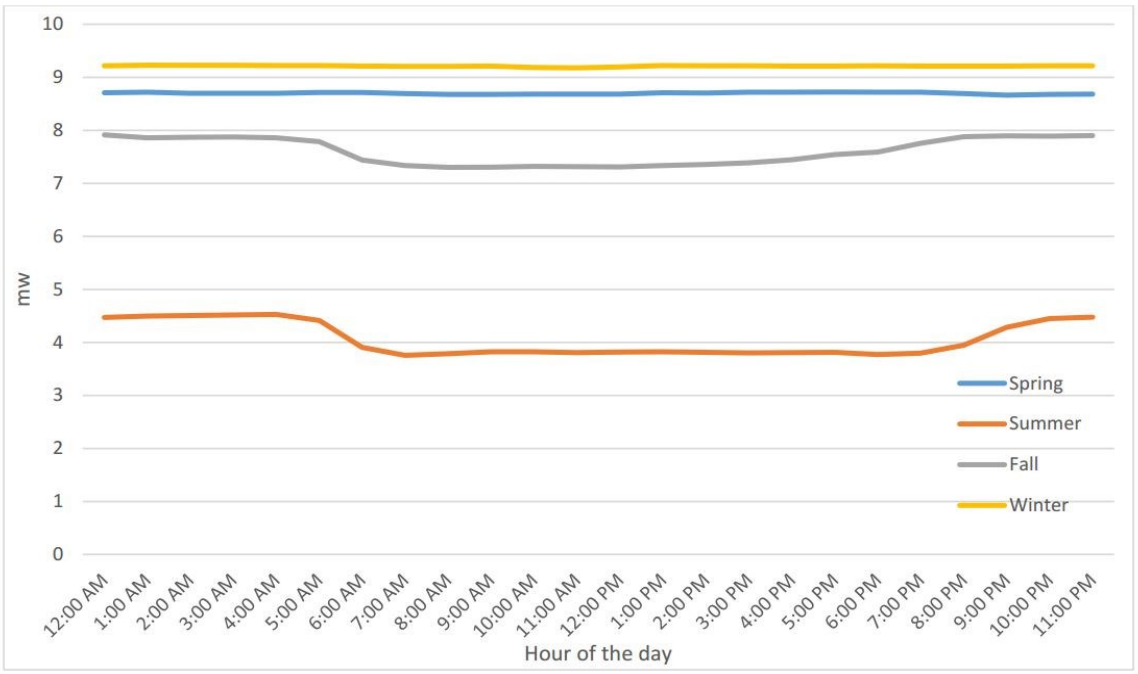

Figure 2-7 Average generation output profile of hydro generator-1 over 24-hour period in 4 seasons

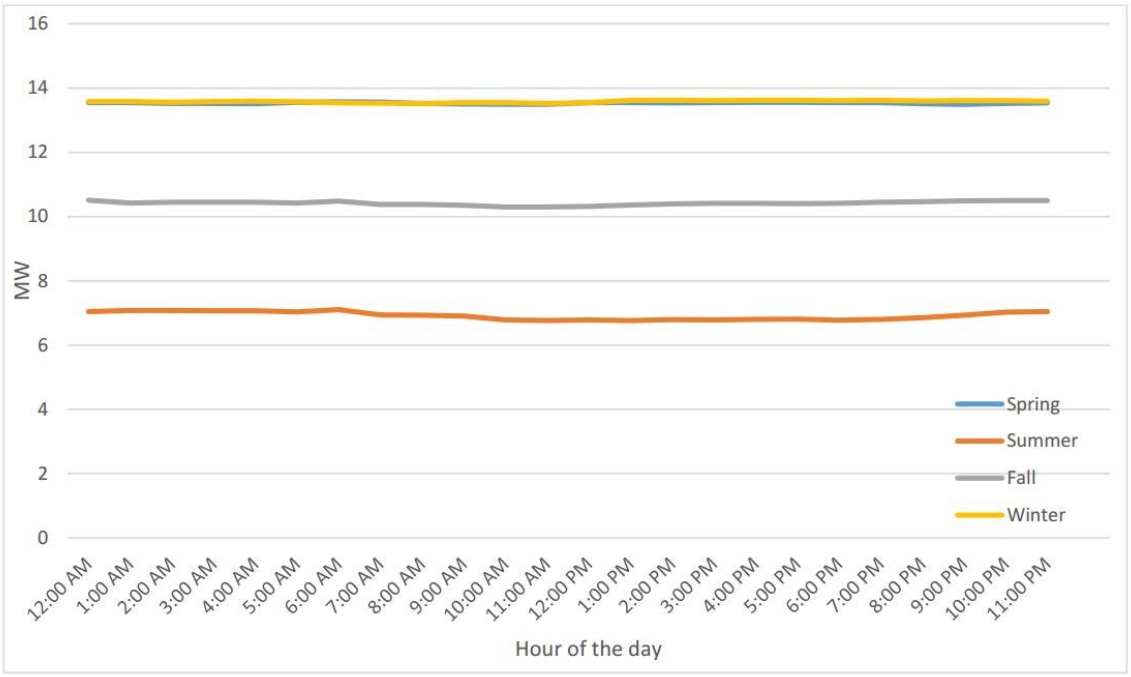

Figure 2-8 Average generation output profile of hydro generator-2 over 24-hour period in 4 seasons

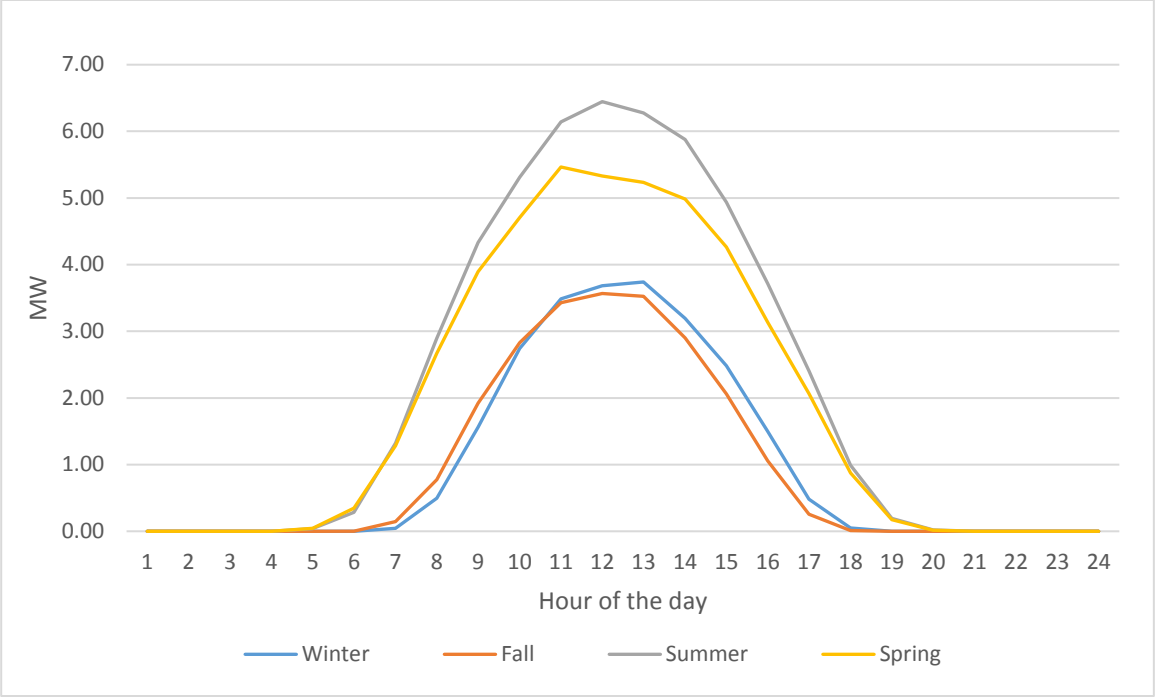

Figure 2-9 Average generation output profile of solar energy over 24-hour period in 4 seasons

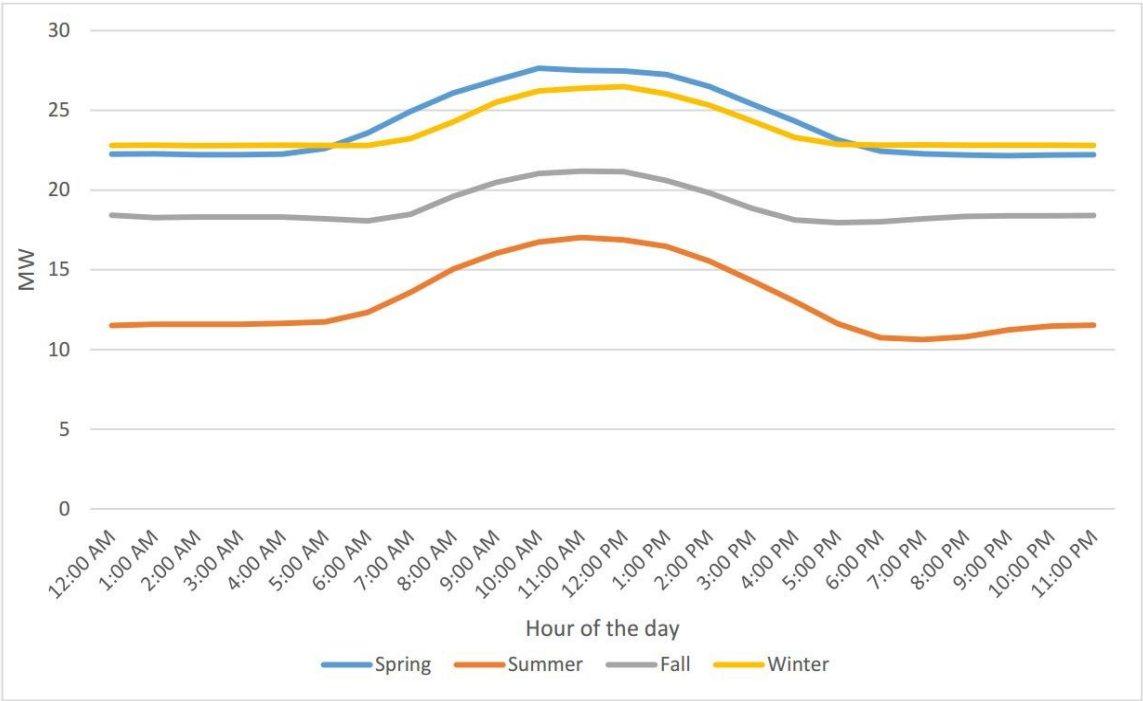

Figure 2-10 Combined average generation output profile over 24-hour period in 4 seasons

2.3.2 Electrical Loads

The electricity consuming devices in a microgrid are typically the electrical loads. There are many different types of loads based on the application but they can be aggregated by lumping them at interconnection point. The utility does not have detailed knowledge of what constitutes each customer load. However, they do have records from metered data over time. This study will characterize loads based on extrapolations from past metered-data.

The generation capability is limited within microgrid due to weak sources when compared with the power grid. Therefore, it is important to identify the loads that can be supplied within the microgrid based on the available generation resources. There should also be a distinction between the critical and non-critical loads. The non-critical loads will be shed during the microgrid operation to stay with generator capability. There are 9 critical loads identified, those having ability to disconnect based on criteria from the sponsor. The set of critical loads in this study system contain hospitals, a university, government buildings and a few other important loads. The metering data acquired from utility for the past three years was used to model each critical load. Energy Charting and Metrics (ECAM) tool is utilized to analyze the load profiles of critical loads based on data from a three-year average of hourly load profile of critical loads. The tool generates an hourly average of four different seasons with each hour averaged over the respective season. Figures 2-11 to 2-19 shows the load profile of 9 critical loads within the microgrid study system. It can be interpreted from the data that the load varies with the time of day and the peak maximum demand is during the late afternoon hours. This behavior varies for each critical load based on different usage and applications. The demand for power is more during summer, then followed by spring, and then fall and winter for these particular critical loads. Most of the critical loads follow similar behavior.

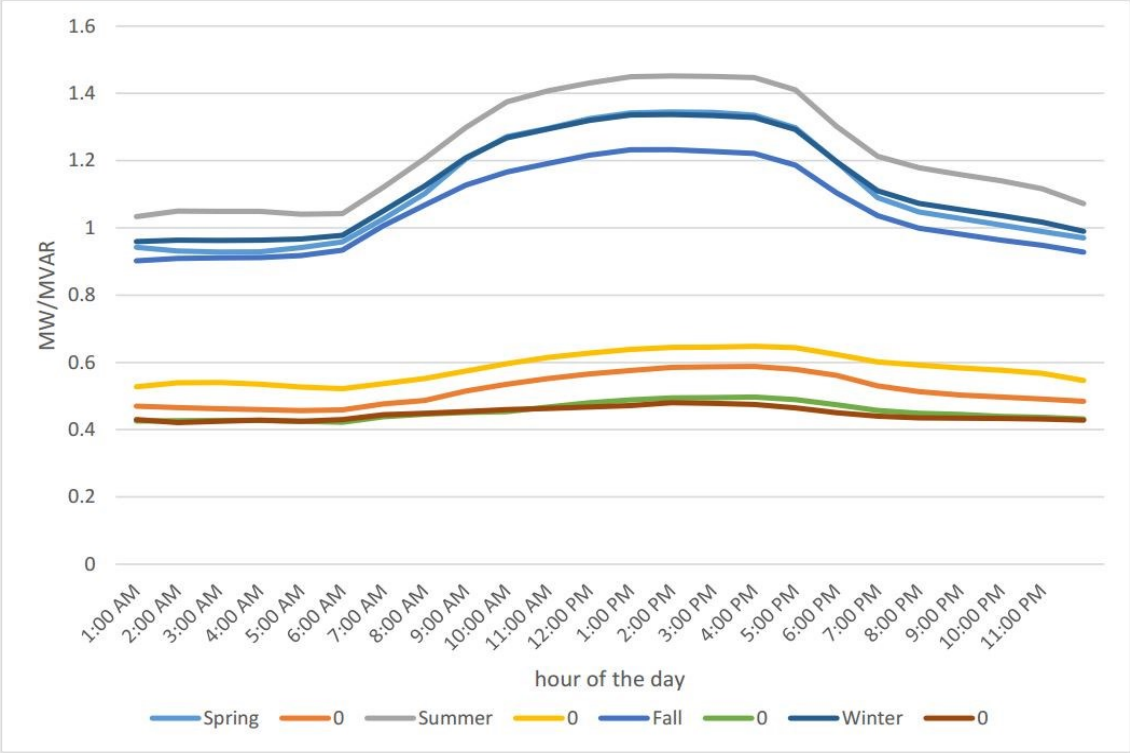

Figure 2-11 Critical load-1 profile averaged over a 24-hour period in 4 seasons

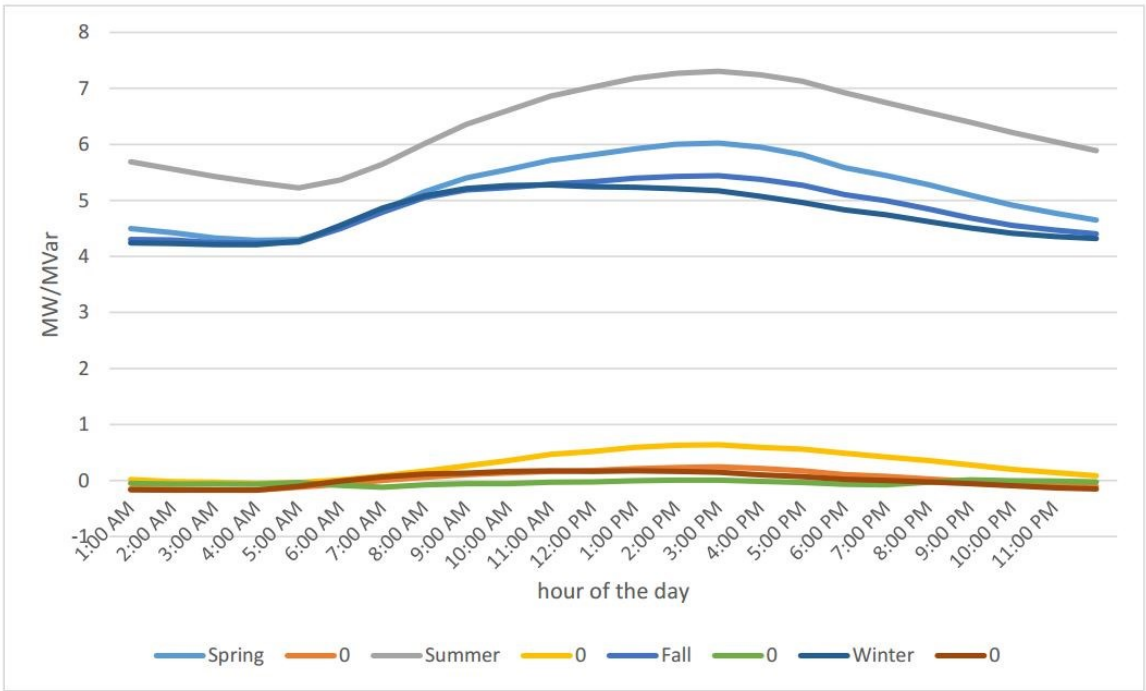

Figure 2-12 Critical load-2 profile averaged over a 24-hour period in 4 seasons

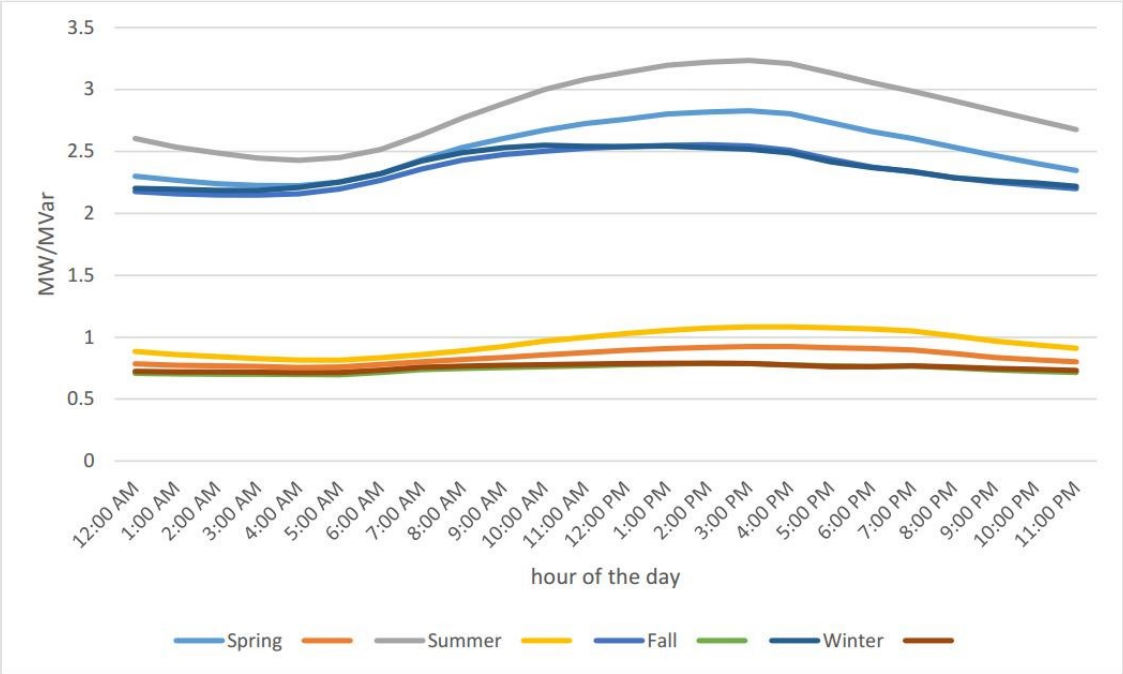

Figure 2-13 Critical load-3 profile averaged over a 24-hour period in 4 seasons

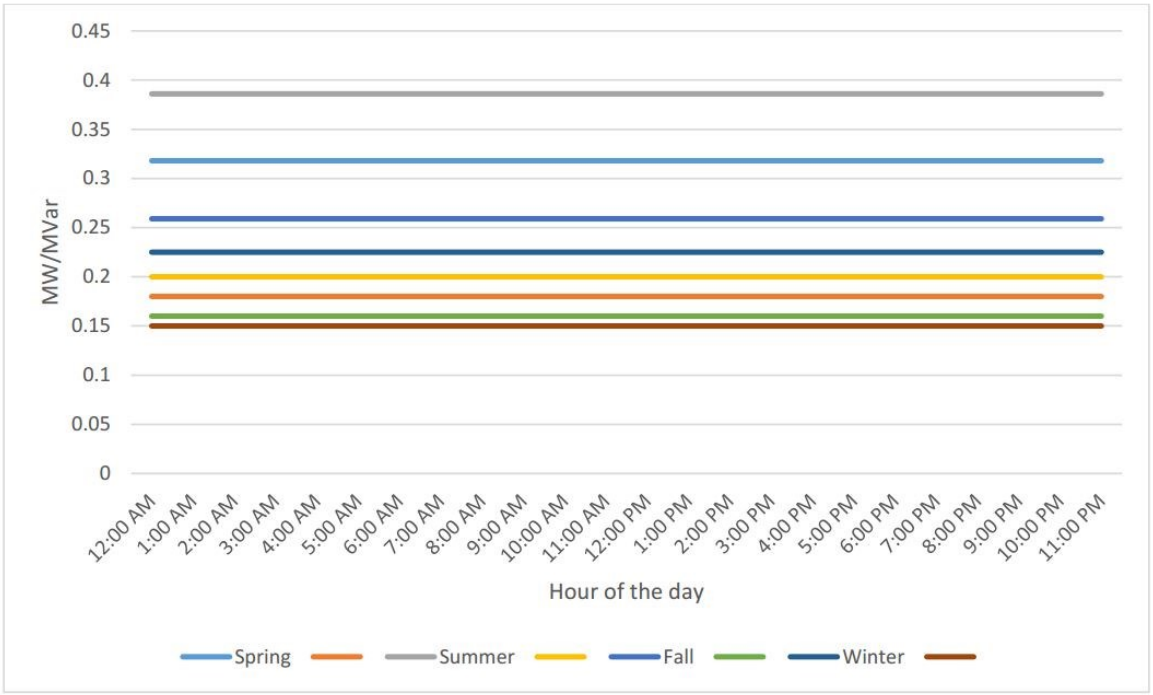

Figure 2-14 Critical load-4 profile averaged over a 24-hour period in 4 seasons

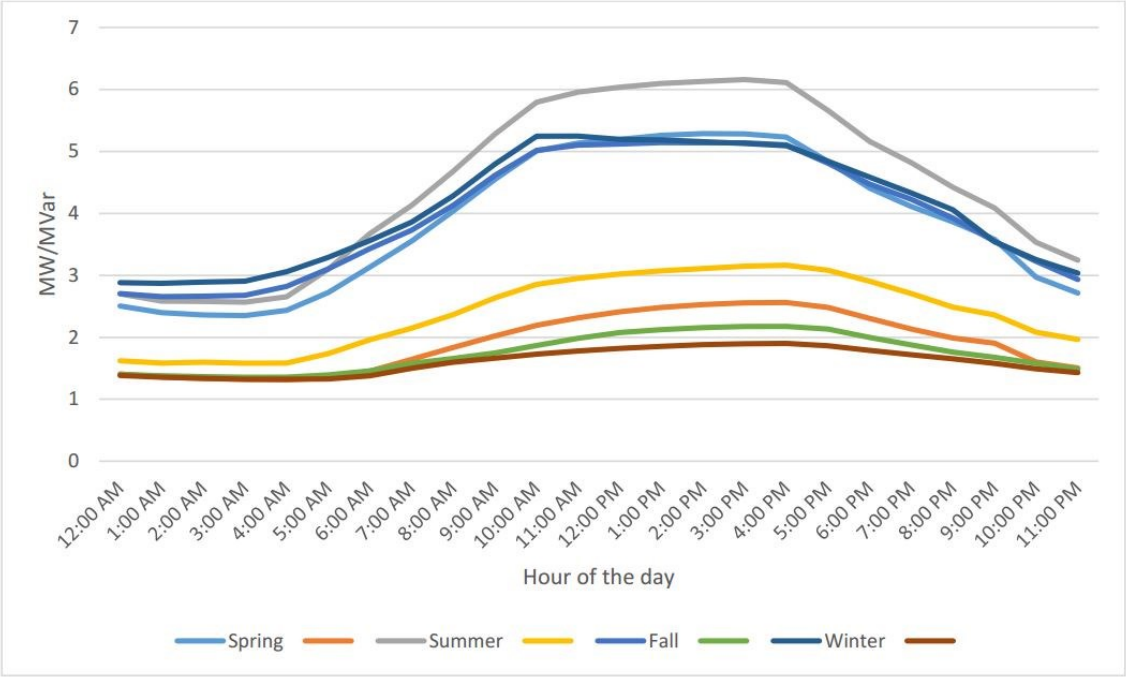

Figure 2-15 Critical load-5 profile averaged over a 24-hour period in 4 seasons

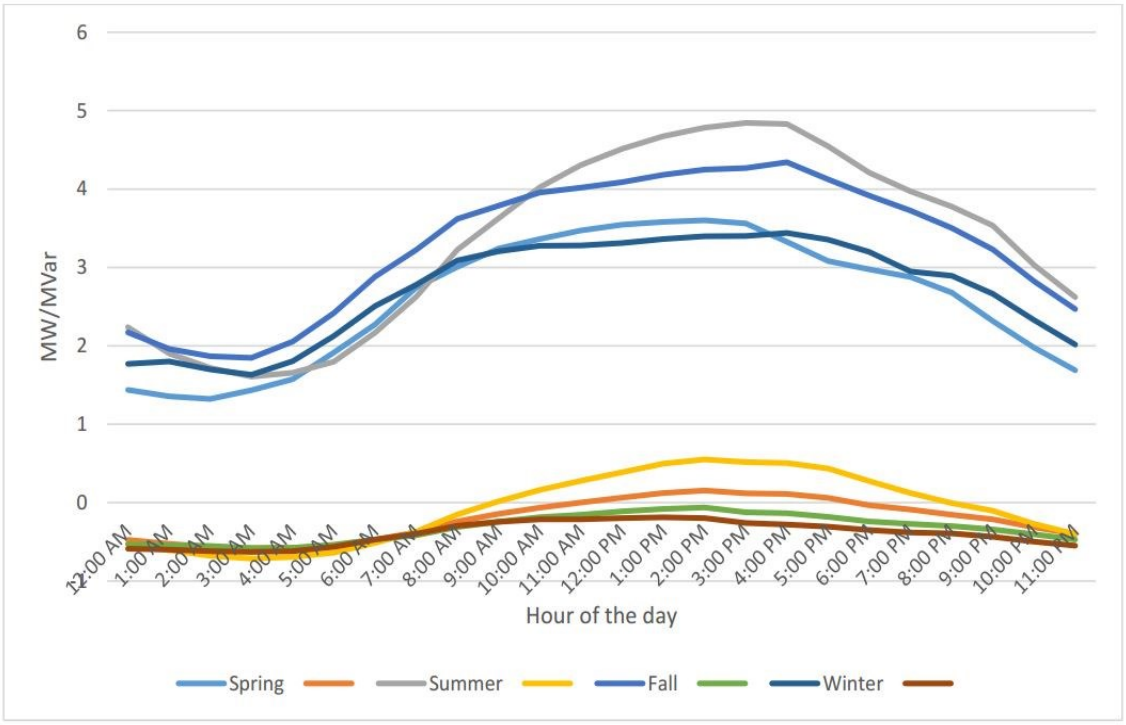

Figure 2-16 Critical load-6 profile averaged over a 24-hour period in 4 seasons

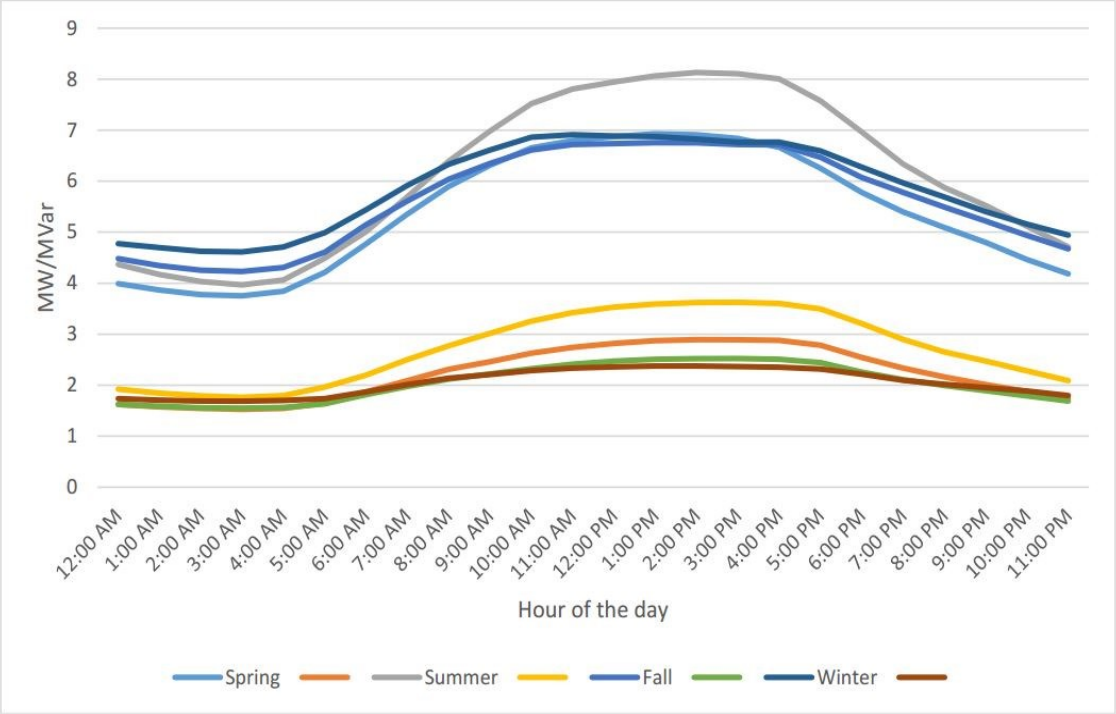

Figure 2-17 Critical load-7 profile averaged over a 24-hour period in 4 seasons

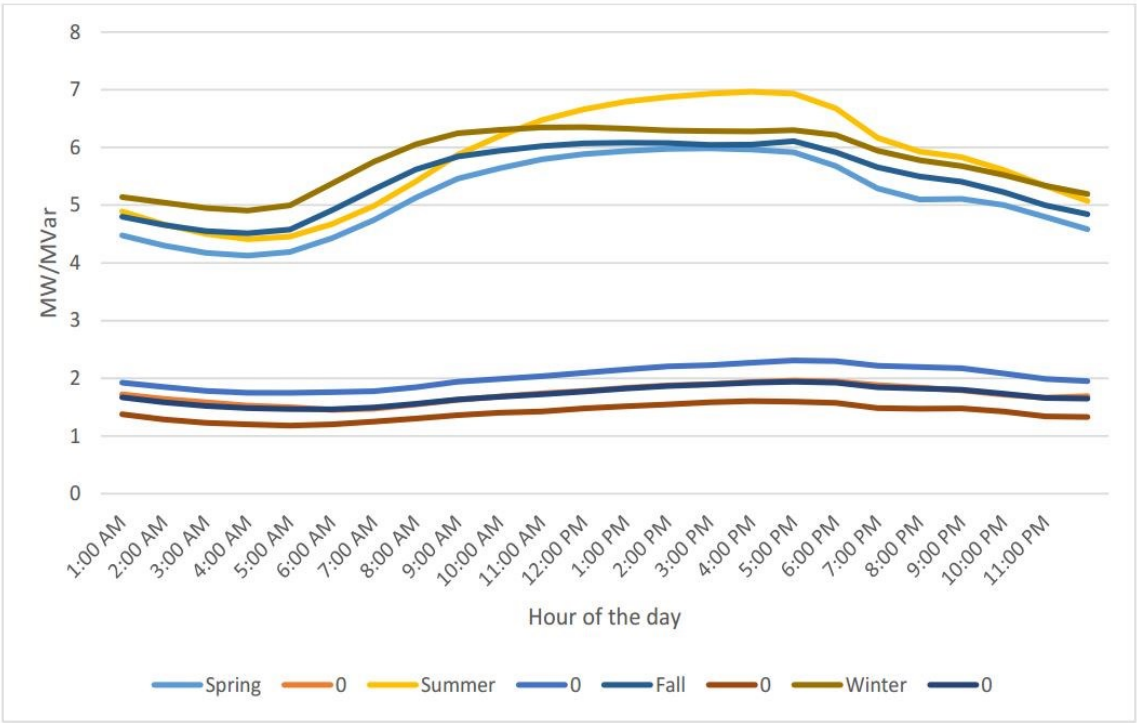

Figure 2-18 Critical load-8 profile averaged over a 24-hour period in 4 seasons

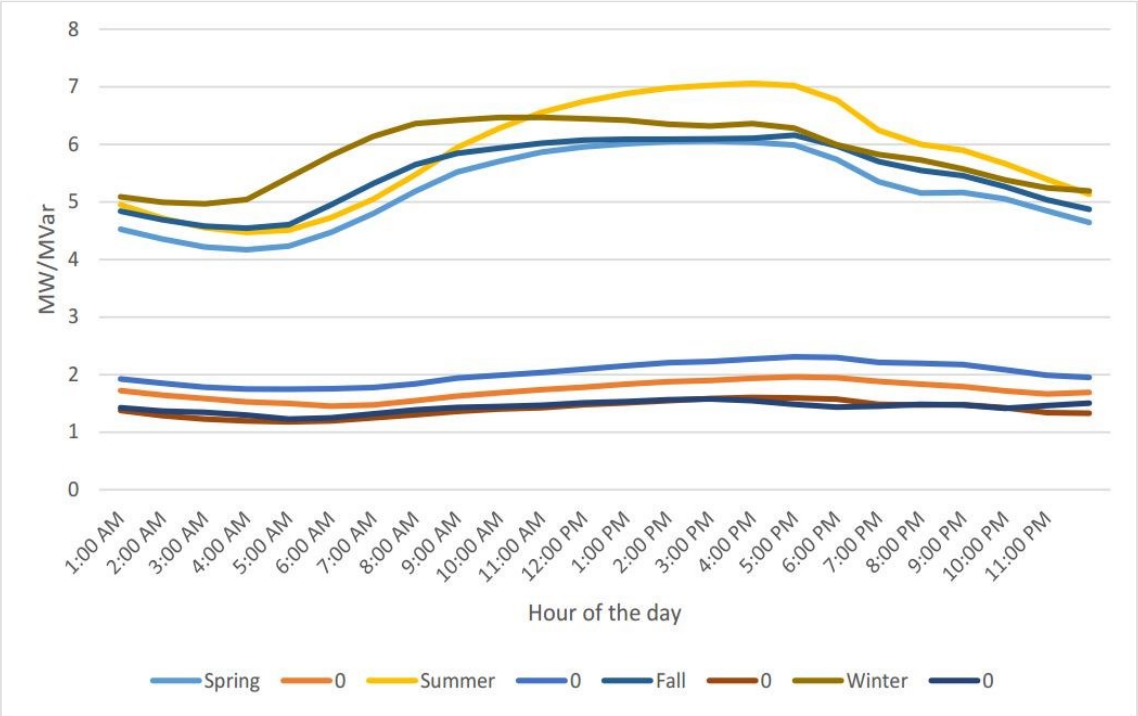

Figure 2-19 Critical load-9 profile averaged over a 24-hour period in 4 seasons

The loads profiles are loaded into Powerworld auxiliary files to represent the varying conditions. The auxiliary file changes the model parameters for different scenarios as will be discussed in Chapter-4. The system planning is done by considering the worst-case situations in a power system over the course of the year. In order to accommodate that analysis, the peak high and low values of each critical load and each of the generators is recorded along with these 24-hour profiles. There are eight different load and generation values used in four different seasons, each having a high and a low value.

2.3.3 Energy Storage Systems

Energy storage can play a vital part in microgrids, especially ones that are generation limited. Energy storage systems enhance flexibility in power generation, delivery, and consumption. It provides utility grids with several benefits and large cost savings [3]. The presence of energy storage system will enable microgrid to regulate its voltage and frequency.

There are currently many options in terms of storage media, each with unique characteristics. Figure 2-20 shows the different energy storage technologies available in the market as of 2011 and their position in terms of discharge time at rated power, system power ratings, and potential application [51].

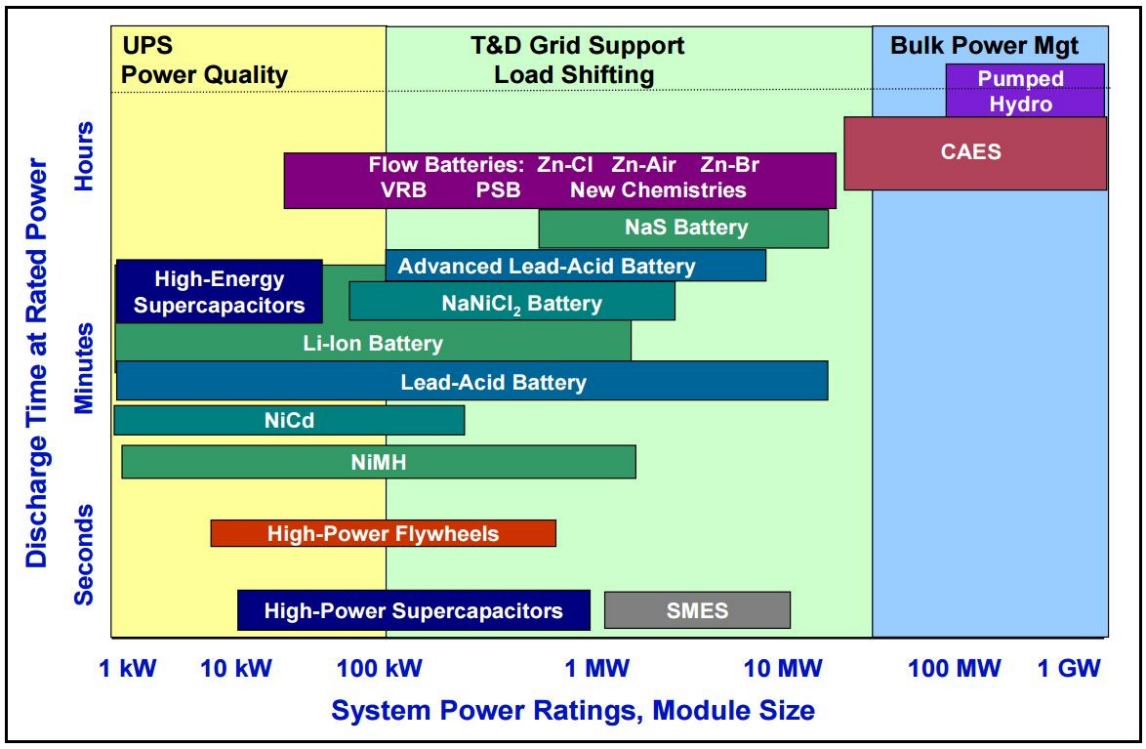

Figure 2-20 Positioning of energy storage technologies in 2011 [51]

Figure 2-21 shows the worldwide installed storage capacity as in 2011, it is interesting to know that 99% of the existing energy storage installations are of pumped hydro facilities. However, there are many new installations of battery taken place in the state of California in the US recently. The technological advancements and increased integration of distribution energy resources are driving the utilities and researchers to install new storage.

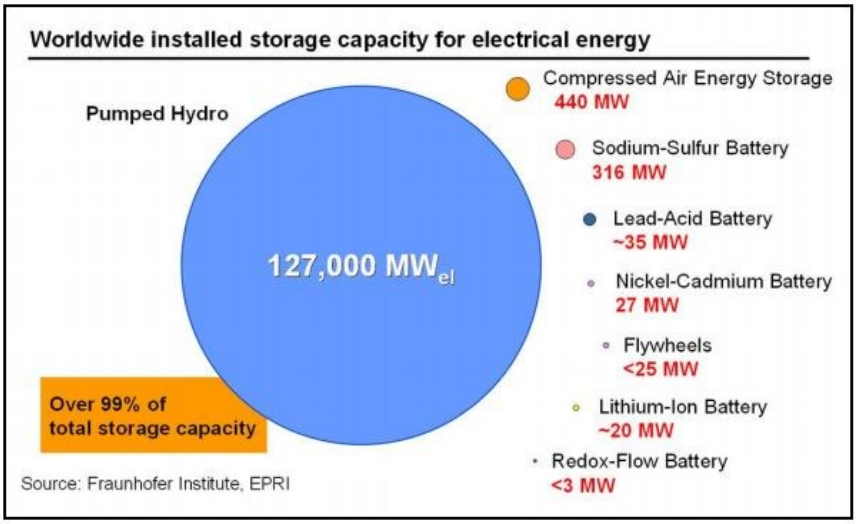

Figure 2-21 Worldwide installed storage capacity for power by technology in 2011 [51]

Table 2-1 summarizes the capital costs, operation and maintenance (O&M) costs, efficiency, and few other parameters such as Technical Readiness Level (TRL), Manufacturing Readiness Level (MRL) [52]. TRL -1 represents a technology still at basic level, while TRL-9 indicates the system is ready for deployment. The same applies with MRL as well [52]. The costs estimated below are according to data acquired in 2011 and the data in parenthesis represents the estimated cost in 2020. Chemical storage in the form of batteries is the most popular and frequently used method of energy storage. There are different chemistries of batteries available, among which, flow batteries and normal cell batteries are the most commonly applied ones. Other technologies such as flywheels and compressed air energy storage (CAES) are highly efficient but they are currently expensive and occupy a large volume for installation in the case of CAES. Therefore, they are not studied for this microgrid application.

Table 2-1 Capital costs for different battery technologies [52].
Note: Values are for 2011 technologies and the estimate for 2020 is in parenthesis

Parameter	Na-S Battery	Li-ion Battery	Pumped Hydro	Combustion Turbine	Demand Response	CAES	Flywheel	Redox Flow Battery
Technology readiness level	7	7	9	9	6	8	7	6
Manufacturing readiness level	6	6	7	10	2	7	5	5
Battery Capital cost ($/kWh)	415 (290)	1000 (510)	10			3	148 (115)	215 (131)
System Capital cost ($/kW)			1750 (1890)	1009 (990)	620	1000 (850)	1277 (610)	1111 (775)
Power conversion system($/kW)	220 (150)	220 (150)						220 (150)
Balance of plant ($/kW)	85 (50)	85 (50)					85(50)	85(50)
O&M fixed ($/kW-year)	3	3	4.6	10.24		7	18	39.5(5)
O&M variable (cents/kWh)	0.7	0.7	0.4	0.9		0.3	0.1	0.1
Round-trip efficiency	0.78	0.8	0.81	0.315		0.5	0.85	0.75

The storage method selection for a microgrid application depends on many different factors. Some of those factors that can be used for optimization are [53].

a) Reliability – the ability of the system to meet the load at all times over several years
b) Efficiency – turnaround efficiency of the storage device itself and the ability to minimize overall system losses
c) Technical maturity – the commercial availability at the time of proposed installation and proven reliability of the technologies used
d) Life span – the estimated length of the time that the system will be able to operate

e) Environmental impact – the impact that each component and overall system will have on the surroundings from manufacture to disposal.

f) Space considerations – it is difficult for the utility to find a right place to install storage devices [54]

Looking at different technologies available at the time of this writing, the Sodium Sulfur (Na-S) batteries have advantages of high operating life, high output capacity, faster response time and compact size. They work well over a pattern of daily discharge and charge. Another factor that needs to be considered while choosing and sizing the battery is Depth of Discharge (DOD). It is advantageous to size the battery more in order to reduce the DOD requirements that improves the battery life [52]. Na-S batteries have an estimated lifespan of 2500 cycles for a DOD of 100%, 4500 cycles for a DOD of 90% and 6500 cycles for a DOD of 65%. Disadvantages of this battery are the reduction in the efficiency while maintaining the temperature at 300°C and cost. The identification of location and optimal sizing of this battery will be discussed in Chapter-4 in detail.

Having a battery in the microgrid will help to supply additional critical-loads during peak hours by storing the surplus energy generated during load off peak hours. In addition to that, the energy storage also can provide many advantages in grid-connected mode. A few of the advantages are, savings in terms of power bought during the peak hours, improving power quality in case where variable renewables are connected to the grid and providing emergency power to critical loads.

2.3.4 Microgrid Controller

The microgrid controller is the most important component of a microgrid; it controls every component of the microgrid by making real time decisions based on the data acquired

and allows the microgrid to operate separately from the microgrid. The growing acceptance and degree of proliferation of the microgrid in the utility power industry is determined by the growth of microgrid controller capabilities and the operational features [55]. The microgrid controller receives the data acquired from different agents in the microgrid through the Supervisory Control and Data Acquisition (SCADA) system. The controller makes the decisions of load shedding, generator shedding, frequency control, and voltage balance. It also takes care of islanding detection and grid resynchronization. The controller must be designed in such a way that it can handle any abnormalities that might occur either in the grid connected mode or the islanded mode where it operates in tandem with the utility operating center. The microgrid controller model proposed for this microgrid is discussed in detail in Chapter-4.

CHAPTER 3. MODELING OF THE MICROGRID

A validated model of the microgrid needs to be developed in prior to performing analysis. At the start of the project, the generation, transmission and distribution systems in the microgrid footprint were modeled in different simulation packages. The generators and transmission lines were modeled in Powerworld as part of the larger WECC transmission model. The distribution network supplying part of the critical loads was implemented in a separate, disconnected Powerworld model. The remainder of the distribution network was modeled in SynerGEE. A model representing the microgrid as a single system was implemented in Powerworld by acquiring the data from these three different models.

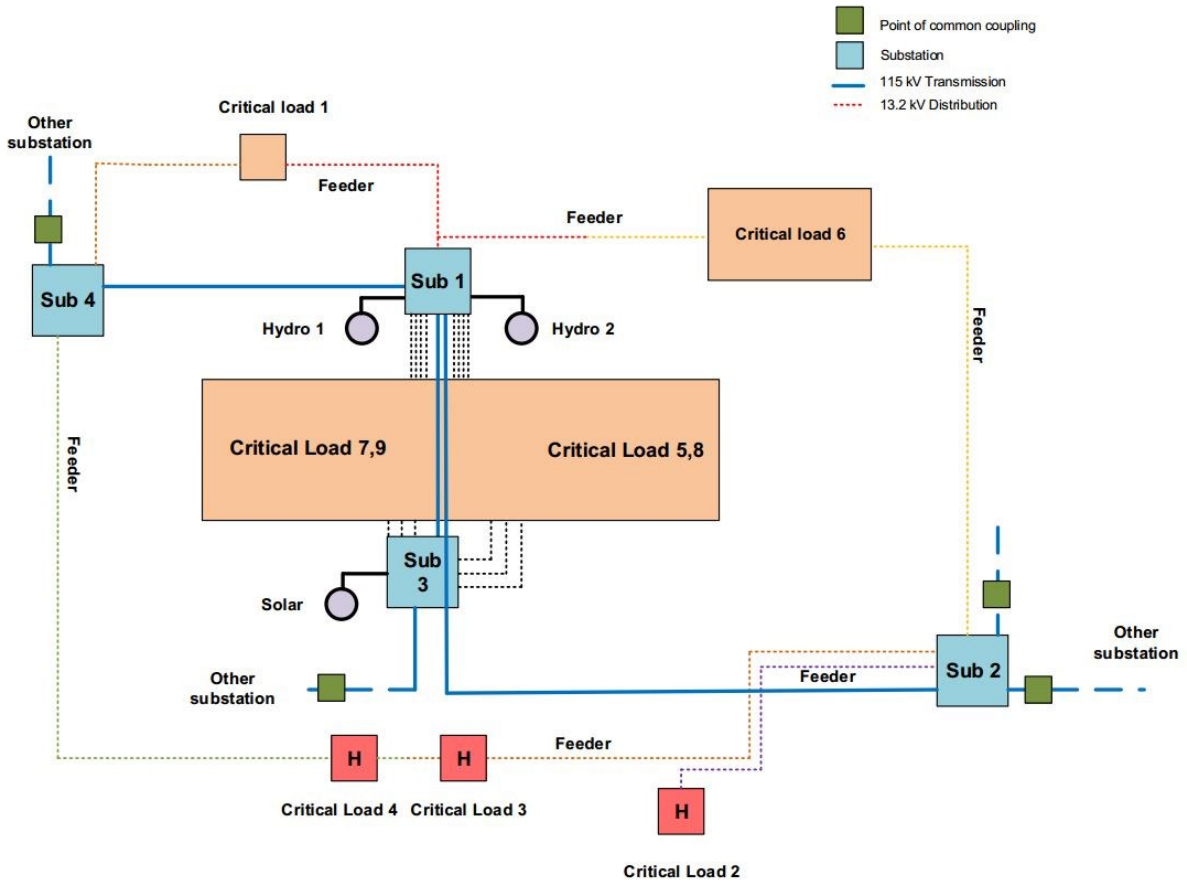

Figure 3-1 SynerGEE Electric simulation software overview

Figure 3-1 shows the block diagram representing the electrical boundaries of the microgrid shown as Point of Common Coupling (PCC). It also shows the generation resources, critical loads, power lines, substations. Further information about the model is discussed in section 3.3. The model contains an 115kV transmission network and a 13.2kV distribution network. The 13.2kV distribution network feeds the critical loads through different feeders, which connects to critical load by stepping down the voltage to 480V through distribution transformers.

3.1 SIMULATION SOFTWARE USED TO COLLECT MODEL DATA

There are three different simulation software packages used in this model are described in the following sections

3.1.1 Powerworld Simulator

The Powerworld simulator is an interactive power-system simulation package designed to simulate steady-state and dynamic high-voltage power system operation ranging from steady-state to several days. The software contains a highly effective power-flow analysis package capable of efficiently solving systems of up to 250,000 buses [26]. It has many features that are very useful in terms of planning. Its features include interactive animated diagrams, contingency analysis, geographic information systems (GIS), time step simulation, contoured displays and transient stability analysis.

3.1.2 SynerGEE Electric

The SynerGEE electric electrical simulation software package models and analyzes power distribution systems in a spatial environment in full detail from the substation to the customer. SynerGEE provides the flexibility to model power distribution systems over a 10-year period down to the second on radial, looped, and mesh network systems on multiple

voltages and configurations [27]. It has many features that are mainly useful for distribution planning including distributed generation and PV modeling, modeling of storage and battery control schemes, transformer load management, weather modeling, motor and flicker analysis, fault location and fault sequence analysis, arc flash hazard analysis, volt/ VAR optimization, and power quality and harmonic analysis. The SynerGEE version used cannot model non-radial systems, which is the reason a portion of the distribution network in study system is modeled in Powerworld.

3.1.3 Real Time Digital Simulator (RTDS)

The Real Time Digital Simulator (RTDS) consists of custom hardware and software, specially designed to perform real time ElectroMagnetic Transient (EMT) simulations. It operates continuously in real time with time steps down to 50μs while providing accurate results over a frequency range from DC to 3 kHz. This range provides a greater depth of analysis than traditional stability or load flow programs, which study phenomenon within a very limited frequency range. The RTDS simulator's digital parallel processing hardware is capable of simulating complex networks with hardware in the loop using a typical time step of 50μs. RTDS technologies proprietary software, designed specifically for interfacing to the RTDS simulator hardware, is called RSCAD [56].

3.2 ACQUIRING DATA FROM SYNERGEE FOR IMPORT TO POWERWORLD

Sponsor had the entire distribution system currently modeled in SynerGEE Electric simulation software. As the microgrid model was to be developed in the Powerworld simulator, the model data needed to be transferred to Powerworld. Figure 3-2 shows the screen shot of SynerGEE Electric with a sample model. The colored solid lines represent the overhead feeders and colored dotted lines represent underground cables. Each feeder will have a starting node

and the entire feeder is divided into several sections having section IDs, which are joined together at nodes represented by node IDs. This sample model has many devices such as smart switches, capacitor banks, voltage regulators, and loads with smart meters. The loads are modeled on three different phases of a feeder. This software also has a Geographical Information Systems (GIS) capability that maps the circuit diagram to physical locations. The capability also aids in determining the feeders supplying the critical loads.

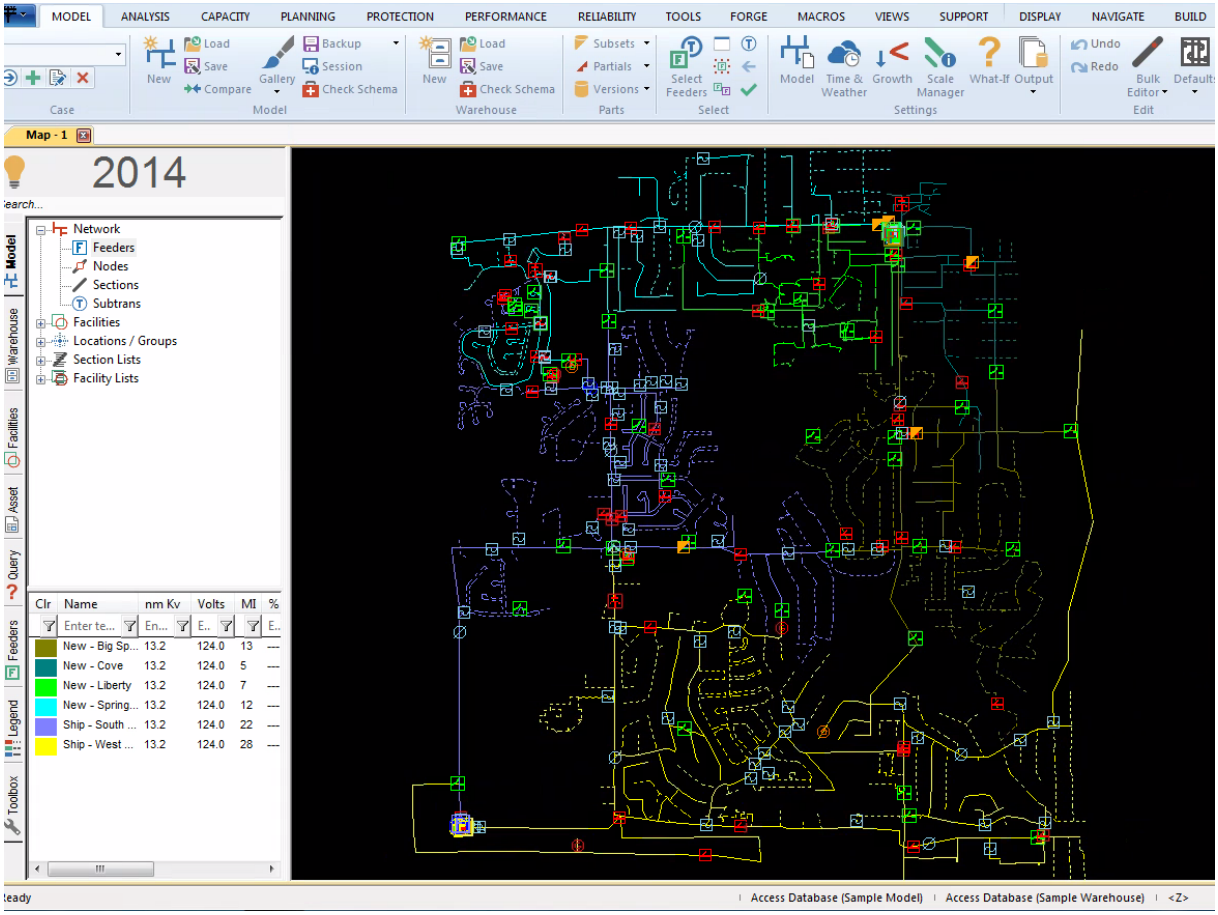

Figure 3-2 Sample feeder in SynerGEE

The critical loads that are supplied in microgrid are mostly situated at the end of feeders in the model. Feeder sections typically contain two mid-line breakers and an air switch in series with critical loads. The switches will not be much of a help in load shedding for microgrid

operation as they need to be remain as normally closed in order to supply critical loads. There are many non-critical lateral loads along the feeders supplying the critical loads. Some are connected through fuses and others have smart switches (remotely operated) to isolate them. The laterals loads need to be disconnected in case of a microgrid operation to stay within generator capabilities. The lateral loads are aggregated and modeled in Powerworld simulator with a circuit breaker to isolate them. The model includes lateral loads to study the impact of additional load including how they influence the frequency balance in case of excessive generation. Figure 3-3 shows an example of the configuration of the feeder sections in SynerGEE and an equivalent bus based model in Powerworld.

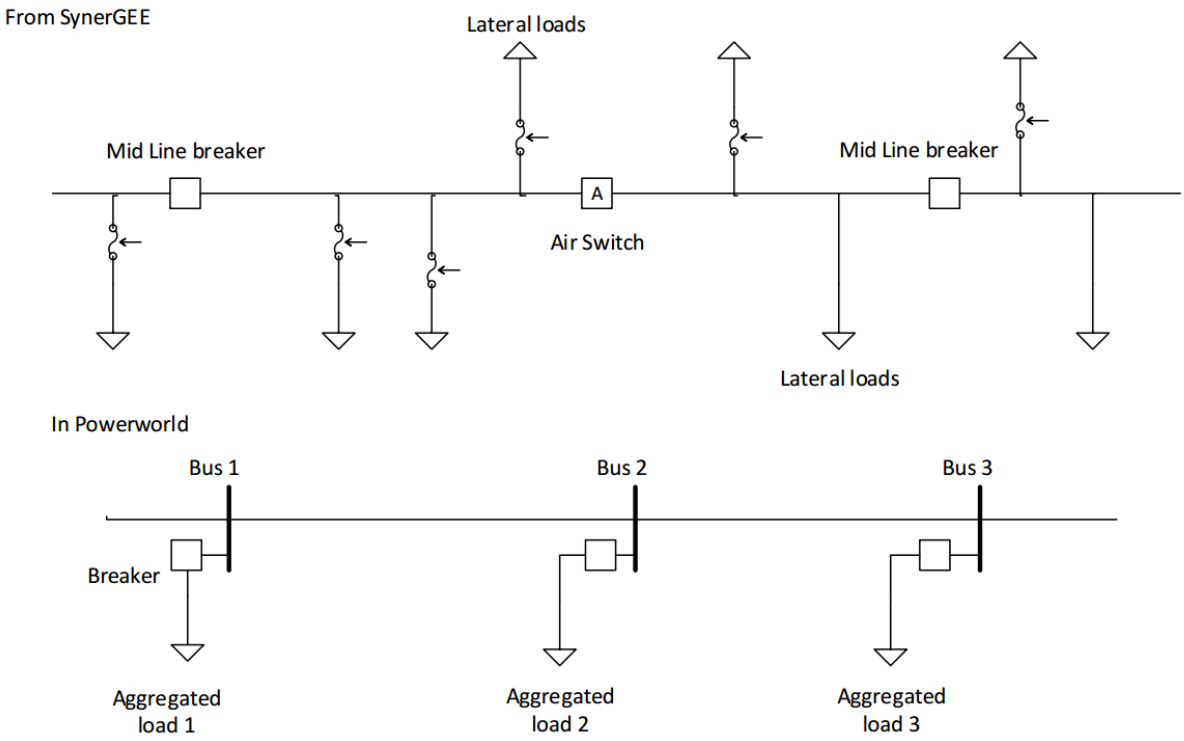

Figure 3-3 Modeling in Powerworld from SynerGEE data

The line parameters include resistance, reactance, capacitance, and line-loading limits are recorded and aggregated to model in Powerworld.

3.3 MODELING IN POWERWORLD

The data acquired from the three different models implemented in the different software packages is organized to build the microgrid model in Powerworld. Figure 3-4 shows the final Powerworld model. The model defines the electrical boundaries and identifies the four substations that are close to the critical loads. The microgrid model contains 115kV transmission lines interconnecting the four substations and 13.2kV distribution lines that are supplying the critical loads. More information about the modeling strategy is discussed below.

3.3.1 Line Parameters

The line parameters, such as positive sequence resistance and reactance and zero sequence resistance and reactance, were collected from three different models as discussed earlier. The resistance and reactance are expressed in per unit in terms of common base values (S_{base}=100MVA and V_{base}=13.2kV). Base conversion is done for the distribution parameters acquired from the partial distribution network Powerworld model.

Table 3-1 Line limits of the conductors

Three phase MVA					
Lines	Feeder section	Summer continuous (A)	Summer emergency (B)	Winter continuous (C)	Winter emergency (D)
Distribution lines	Section-1	10.3	10.3	12.5	12.5
	Section-2	11.0	11.0	12.5	12.5
	Section-3	10.3	10.3	15.3	15.3
	Section-4	3.7	3.7	4.2	4.2
	Section-5	2.8	2.8	3.2	3.2
	Section-6	3.7	3.7	4.2	4.2
	Section-7	11.0	11.0	12.5	12.5
Transmission lines	Section-1	119.7	119.7	176.5	136.4
	Section-2	189.2	189.2	189.2	189.2
	Section-3	159.4	159.4	180.7	164.9

Table 3-2 Positive sequence and negative sequence line parameters of the microgrid

	Per unit values	**TL1**	**TL2**	**TL3**	**DL1**	**DL2**	**DL3**	**DL4**	**DL5**	**DL6**	**DL7**
Positive sequence	Series Resistance (R)	0.00017	0.00016	0.00189	0.94394	0.5308	0.703791	0.626199	0.21873	3.7123	0.629478
	Series Reactance (X)	0.00142	0.00126	0.00799	0.56205	0.14944	0.990639	0.83715	0.46565	1.9759	0.246408
	Shunt Charging (B)	0.00612	0.00773	0.00931	NA	NA	NA	NA	NA	NA	NA
Zero sequence	Series Resistance (R)	0.000425	0.0004	0.004725	1.00641	0.15408	1.345629	1.1733	0.54576	3.9983	0.633648
	Series Reactance (X)	0.00355	0.00315	0.019975	0.73978	0.48084	2.911599	2.50797	1.46352	2.9122	0.246628
	Shunt Charging (B)	0.00612	0.00773	0.00931	NA	NA	NA	NA	NA	NA	NA

Table 3-3 Line types and their locations

	Line type	From end	To end		Line type	From end	To end
TL1	Transmission line	Sub-1	Sub-4	**DL3**	Distribution line	Sub-4	Critical load-3
TL2	Transmission line	Sub-1	Sub-2	**DL4**	Distribution line	Critical load-3	Sub-2
TL3	Transmission line	Sub-1	Sub-3	**DL5**	Distribution line	Sub-2	Critical load-2
DL1	Distribution line	Sub-1	Critical load-1	**DL6**	Distribution line	Sub-2	Critical load-6
DL2	Distribution line			**DL7**	Distribution line	Critical load-6	Sub-1

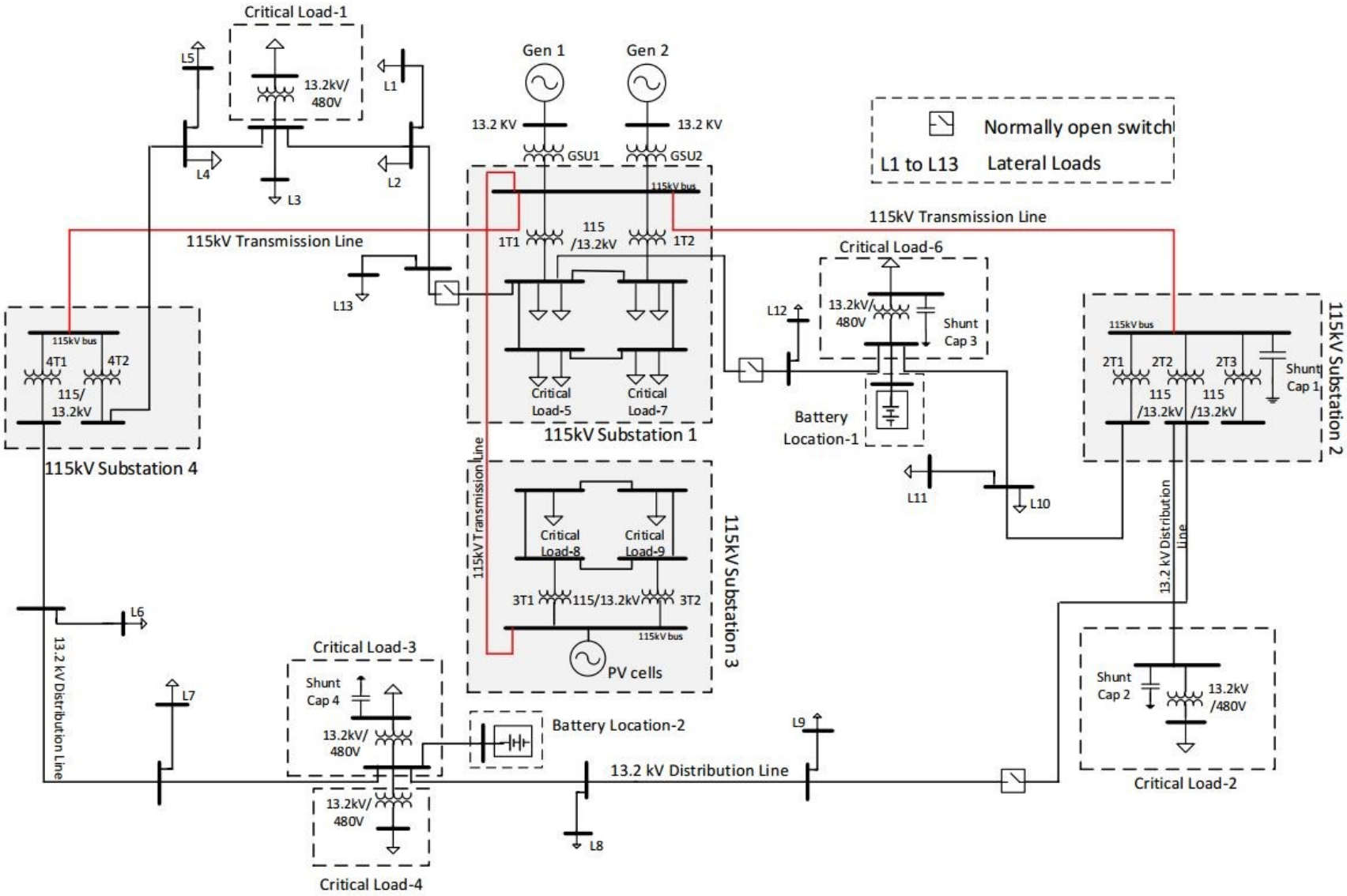

Figure 3-4 Final Powerworld model

The line limit is the ability of the conductor to carry the current. Powerworld has the ability to define eight different line limits (A through H) corresponding to four different seasons. Each season has a continuous rating (normal conditions) and emergency rating (contingency conditions). The line limits are expressed as three phase MVA limits. Table 3-1 shows the limits for summer and winter. The lowest ratings from these two seasons are used for the other two seasons. Table 3-2 and Table 3-3 shows the line parameters of transmission lines (115kV) and distribution lines (13.2kV) involved in the model. The distribution lines in the model has negligible shunt charging effect, therefore they are neglected.

3.3.2 Generator Modeling

The system includes two hydroelectric generators along with another generator representing the solar generation. Generator-2 (15MW) has better generation controls installed onsite than is the case for generator-1, so generator-2 is connected to the slack bus (swing machine) in this model. The generators are set with the maximum and minimum real and reactive power limits. The generator machine, governor and exciter models are included for the transient stability studies on this system. The generator-2 machine parameters are available from the tests conducted by utility in the machine, whereas generator-1 data is not available and approximations are made while loading the generator-1 parameters.

A. Machine model

Once the key information about the generators is gathered, two hydro generators were configured with ‘GENTPJ’ dynamic machine model with Gen-2 implemented using the parameters of the real machine. The Gen-1 parameters were not known, so the model parameters were chosen to be close to a real system. Figure 3-5 shows the block diagram of the

GENTPJ machine model [26]. More information about these models is provided in reference [57]. The reference [58] suggest using 'GENTPJ' machine models for stability studies.

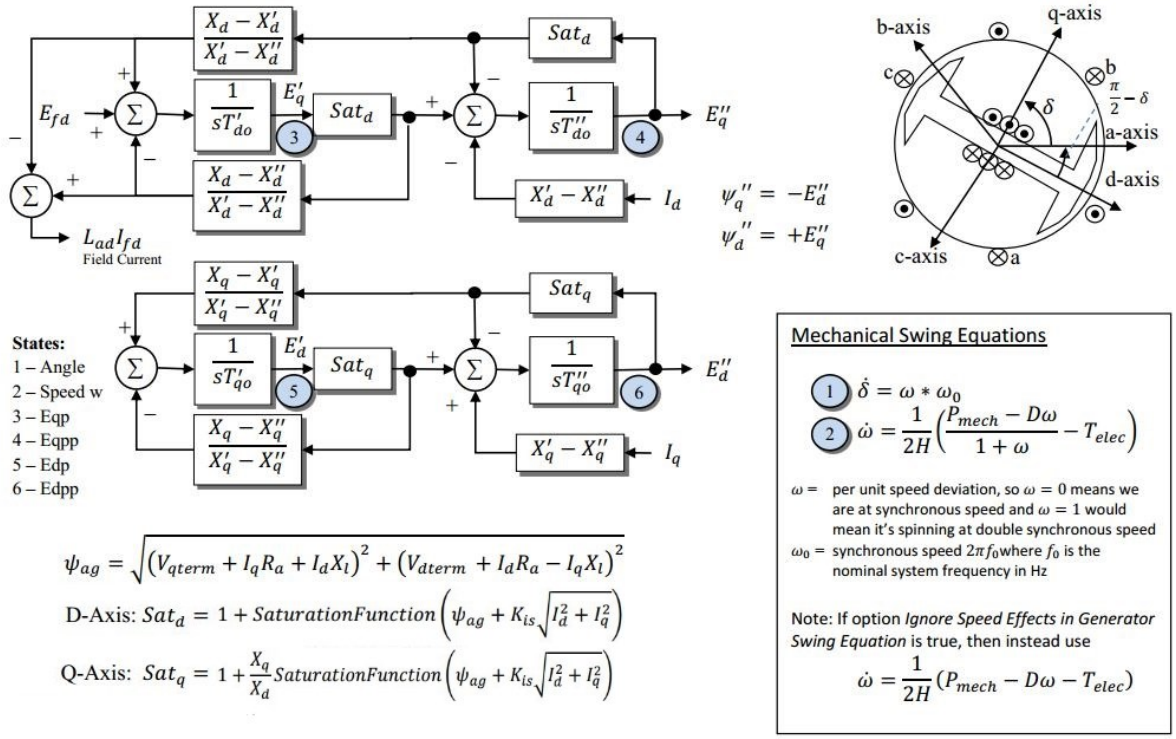

Figure 3-5 Block diagram of GENTPJ machine model [26]

Table 3.2 shows the parameters entered into the Powerworld model for the GENTPJ machine models of Gen-1 and Gen-2.

Table 3-4 GENTPJ machine parameters used to model Generator-1 and 2

Parameter	Description	Generator-1	Generator-2
T_{do}'	Transient d-axis time constant	5	5
T_{do}''	Subtransient d-axis time constant	0.035	0.03
T_{qo}'	Transient q-axis time constant	0	0
T_{qo}''	Subtransient q-axis time constant	0.05	0.05
H	Inertia constant	1.5	1.75
D	Turbine damping factor	0	0
X_d	Synchronous reactance	1	0.9
X_q	Q-axis synchronous reactance	0.4762	0.6

X_d'	Transient reactance	0.2	0.293
X_q'	Q-axis transient reactance	0.4762	0.6
X_d''	Subtransient d-axis reactance	0.1714	0.268
X_q''	Subtransient q-axis reactance	0.18	0.268
X_l	Stator leakage reactance	0.1429	0.23
S_1	Saturation factor	0.1	0.2
S_{12}	Saturation factor	0.2	0.55
R_a	Stator resistance	0	0
R_{comp}	Excitation compensation resistance	0	0
X_{comp}	Excitation compensation reactance	0	-0.06
Accel	Model acceleration factor	0.4	0.5
K_{is}	Current saturation factor	0.02	0.06

The parameters for generator-2 were acquired from the sponsor from a generator study completed on this machine as a part of routine WECC testing. Gen-1 did not have any study done since none was required for WECC due to its lower MVA rating, so typical parameters are assumed close to ones as shown in the Table 3-4.

B. Exciter model

The exciter provides DC excitation current that in turn will produce the magnetic field within the generator. The exciters of two generators in the study system are static exciters. The static exciters each have an AC/DC converter that supplies DC field current. The study system used the exciter EXST4B (IEEE Type ST4B) excitation system model. Figure 3-5 shows the block diagram of the model.

Table 3-5 shows the parameters entered into the Powerworld model for the EXST4B exciter models of Gen-1 and Gen-2. The same models are used for both the machines.

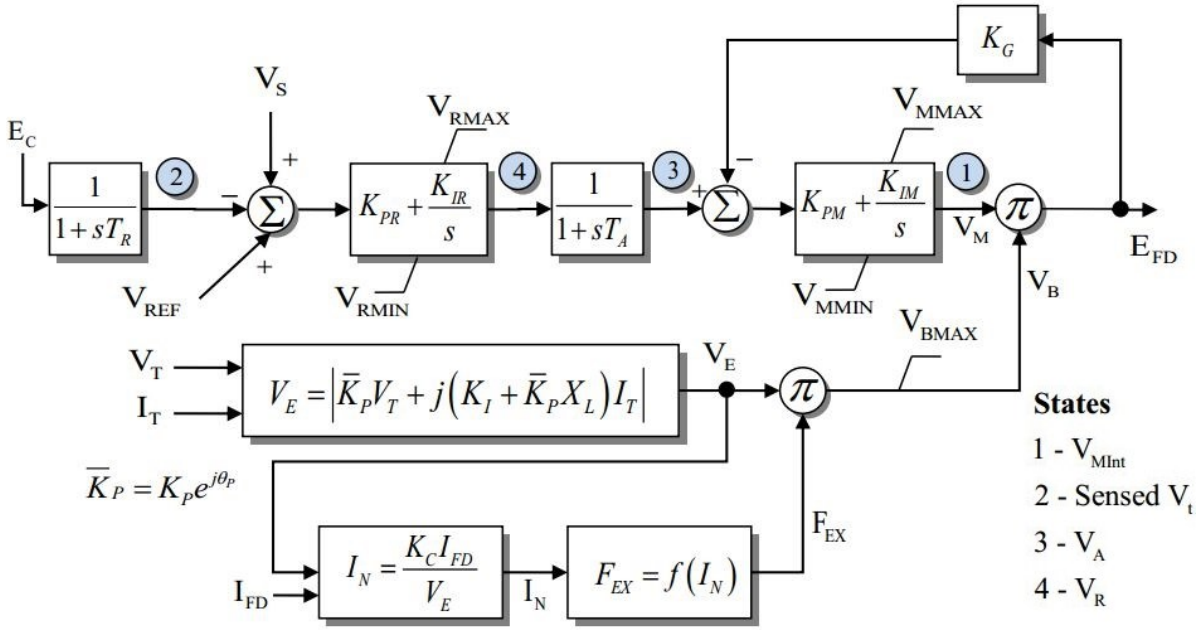

Figure 3-6 Block diagram of EXST4B exciter model [26]

Table 3-5 EXST4B exciter parameters used to model Generator-1 and 2

Parameter	Description	Values	Parameter	Description	Values
T_r	Voltage transducer time constant	0	V_{mMax}	FVR max signal	1
K_{pr}	AVR Proportional gain	16	V_{mMin}	FVR min signal	-0.87
K_{ir}	AVR integral gain	16	K_g	FVR feedback gain	0
T_a	AVR filter time constant	0.02	K_p	PPT secondary voltage factor	3.43
V_{rmax}	AVR max signal	1	ThetaPDeg	Potential source phase angle	0
V_{rmin}	AVR min signal	-0.87	K_i	Current source gain	0
K_{pm}	FVR proportional gain	1	K_c	Rectifier regulation factor	0.15
K_{im}	FVR integral gain	0	X_l	Potential source leakage reactance	0
			V_{bMax}	PPT voltage limit	99

C. Governor model

The governor controls the speed of the machine and thus maintains the output frequency. Any frequency changes are fed back to the governor, which takes corrective actions to bring the frequency to the normal state. Since the sponsor does not have good governor models, the HYGOV model is chosen to represent the governors in the study system. Figure 3-7 below shows the block diagram of the model.

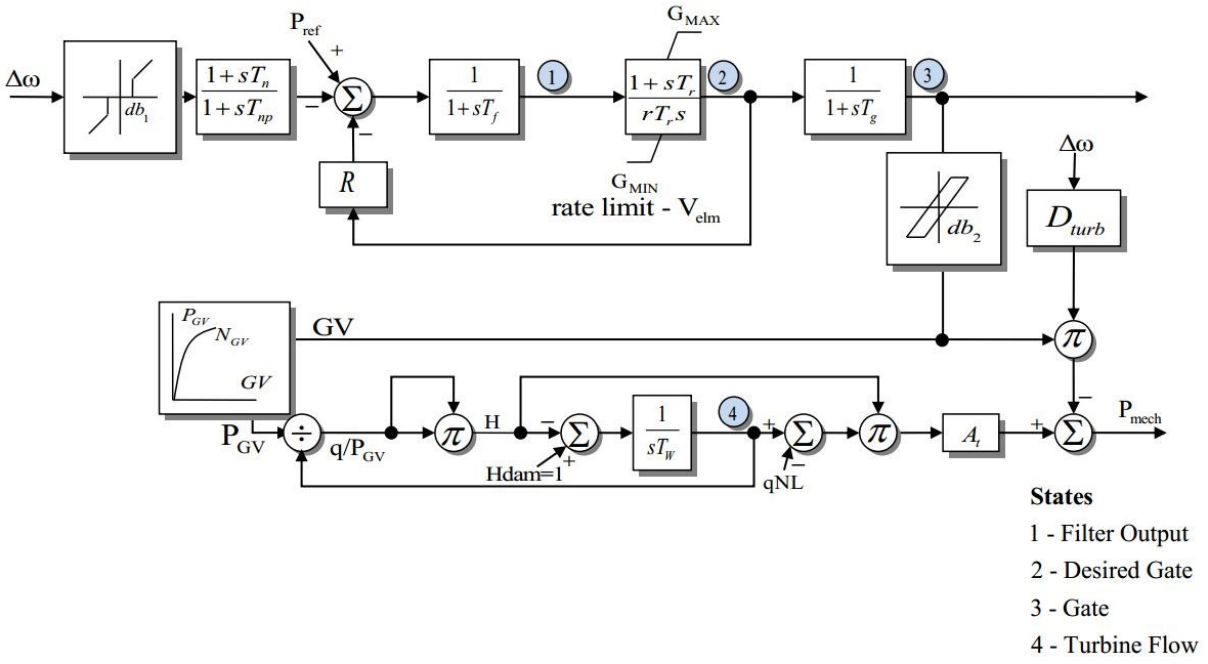

Figure 3-7 Block diagram of HYGOV governor model [26]

Table 3-6 shows the model parameters used for the HYGOV model in Powerworld. Reference [48] talks about determining the parameters used in the HYGOV governor model.

Table 3-6 HYGOV machine parameters used to model Generator-1 and 2

Parameter	Description	Values	Parameter	Description	Values
R_{perm}	Permanent droop (R), p.u.	0.04	G_{v1}	Nonlinear gain point 1, p.u. gv	0
R_{temp}	Temporary droop (r), p.u.	0.3	P_{gv1}	Nonlinear gain point 1, p.u. power	0
T_r	Washout time constant, s	5	G_{v2}	Nonlinear gain point 2, p.u. gv	0
T_f	Filter time constant, s	0.05	P_{gv2}	Nonlinear gain point 2, p.u. power	0
T_g	Gate servo time constant, s	0.5	G_{v3}	Nonlinear gain point 3, p.u. gv	0
V_{elm}	Maximum gate velocity, p.u./s	0.2	P_{gv3}	Nonlinear gain point 3, p.u. power	0
G_{max}	Maximum gate opening, p.u. of mwcap	1	G_{v4}	Nonlinear gain point 4, p.u. gv	0
G_{min}	Minimum gate opening, p.u. of mwcap	0	P_{gv4}	Nonlinear gain point 4, p.u. power	0
T_w	Water inertia time constant, s	1	G_{v5}	Nonlinear gain point 5, p.u. gv	0
A_t	Turbine gain, p.u.	1.2	P_{gv5}	Nonlinear gain point 5, p.u. power	0
D_{turb}	Turbine damping factor, p.u.	0.5	H_{dam}	Head available at dam, p.u.	1
Q_{nl}	No-load flow at nominal head, p.u.	0.05	B_{gv0}	Kaplan blade servo point 0, p.u.	0
T_{tur}	Not used	0.5	B_{gv1}	Kaplan blade servo point 1, p.u.	0
T_n	Lead time constant, s	0	B_{gv2}	Kaplan blade servo point 2, p.u.	0
T_{np}	Lag time constant, s	0	B_{gv3}	Kaplan blade servo point 3, p.u.	0
db_1	Intentional deadband width, Hz	0	B_{gv4}	Kaplan blade servo point 4, p.u.	0
E_{ps}	Intentional deadband hysteresis, Hz	0	B_{gv5}	Kaplan blade servo point 5, p.u.	0
db_2	Unintentional deadband, MW	0	B_{max}	Maximum blade adjustment factor	0
G_{vo}	Nonlinear gain point 0, p.u. gv	0	T_{blade}	Blade servo time constant, s	100
P_{gv0}	Nonlinear gain point 0, p.u. power	0	T_{rate}	NA	0

a) Frequency Droop Control

Droop is defined as a decrease in the generator speed setting at the load increases [34]. Droop is expressed as a percentage of the original speed setting from no load to full load. The normal recommended percent of droop is 3% to 5%. A minimum of 2.5% is required to maintain stability in a speed-droop governor [34].

$$\%\text{Droop} = \frac{No\ load\ Speed - Full\ load\ Rated\ Speed}{Full\ Load\ Rated\ Speed} * 100 \quad (3.1)$$

There will be an overshoot in the speed managed by governor if the droop settings are not set. The speed setting of the governor will be reduced if the load increases, thus correcting the speed to a lower speed setting. The droop setting will avoid speed overshoot.

There are two main modes of operation of a machine, one is isochronous mode and other is droop mode. In isochronous mode, the speed of the machine returns to original speed after a change in load has been applied. In droop mode of operation, the speed decreases by a set percentage (3-5%) after a load has been applied. If the original speed is desired, operator needs to raise the speed setting after the load is applied to return to original speed. Figure 3-8 shows the difference between droop and isochronous modes of operation.

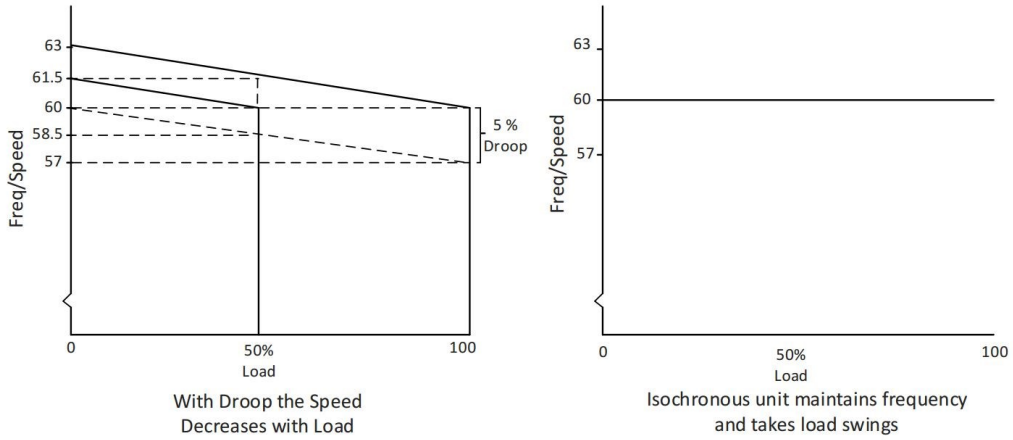

Figure 3-8 Comparison of droop and isochronous mode of operation [34]

The microgrid in this study has two generators with two exciters and governors. Unless the two governors have isochronous load sharing capabilities, it is not advisable for both the machines to run in isochronous mode. If they are running in isochronous mode, there will be two different speed settings; both tend to reach to an average speed. In this process, the machine with the higher-speed setting will take the entire load until it reaches its power limit and the other machine will be motored (driven by other machine). If two machines have the same droop setting, they will share load proportionally. If they have different droop setting, the load sharing will not be proportionate, and the operator needs to adjust the speed set point differently for each machine to make them carry their proportional share of load. In another case, one generator can run in droop mode and with other one operated in isochronous mode (swing machine). The droop machine will run at speed/ frequency of isochronous machine. The droop machine is set to generate a set of amount of power, whereas isochronous machine will change its output to follow variations in the load demand by maintaining the constant frequency. The maximum load on this type of system is limited to sum of the combined output of two machines, if the load increases above that, it will lead to frequency drop. The machine with the higher power capability is chosen to run in isochronous mode.

D. Generator capability curve

Generators operating ranges are designed to meet the temperature limitations at their ratings [59]. These limitations will lead to real and reactive power limits of generator. The reactive power output of a synchronous generator is constrained by several factors such as armature current limit, field current limit, and end region heating limit [60]. These limits are modeled as different circles in the active and reactive power output plane. The intersection of these circles form a curve which is called as generator capability curve as shown in Figure 3-9

[59]. The curve is usually constructed with the abscissa as kW and the ordinate as leading or lagging reactive kVAR with reference to the generator real power. Lagging reactive power is plotted as a positive value and referred to as overexcited condition. Leading reactive kVAR is plotted as a negative value that is referred as under excited condition [59].

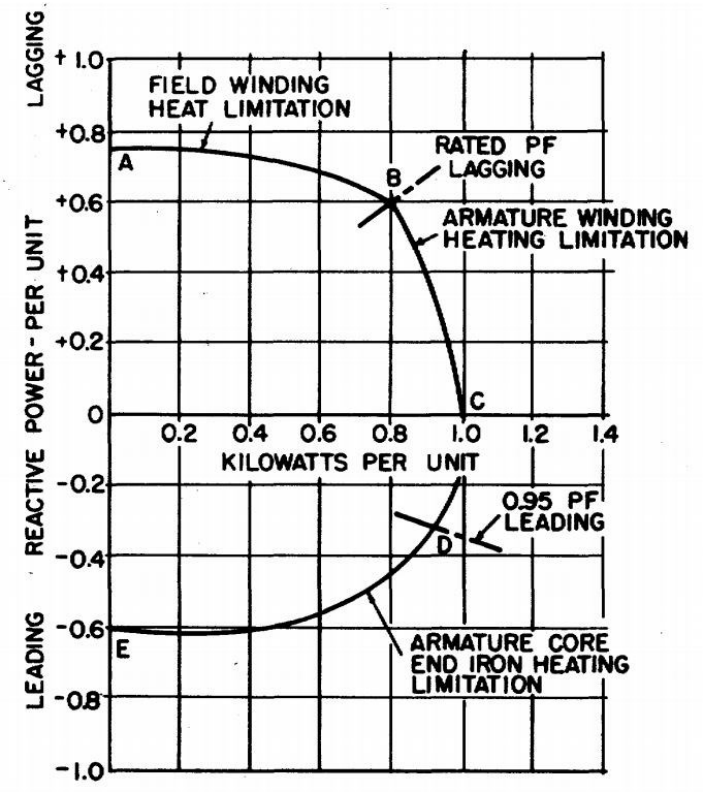

Figure 3-9 Generator capability curve of a synchronous machine [59]

The upper portion of the curve is from the field current limit, the right portion of the curve is from the armature current limit, and the lower portion of the curve is the circle from the end-region heating limit [60]. The generator parameters for the two machines in the study system are acquired and the generator capability curves are created. More information about the calculations is included in the Appendix-B. This capability curve is loaded into the Powerworld model using auxiliary files, which later helps in determining size of the capacitors to bring voltage to nominal value.

3.3.3 Transformer Modeling

There are three different types of transformers modeled in this system. First, the generator step up transformers represented as GSU1 and GSU2 in Figure 3-4. These transformers step up the voltage from 13.2kV to 115kV at substation 1. The next class of transformers are the step down transformers at the four transmission substations, which step down the voltage from 115kV to 13.2kV. They are labeled as 1T1, 1T2, 2T1, 2T2, 2T3, 3T1, 3T2, 4T1 and 4T2 at the four different substations. The last type of transformers are distribution transformers at the critical loads stepping down the voltage from 13.2kV to 480V. They are modeled at each critical load. The positive sequence and zero sequence parameters of the transformers were acquired and modeled appropriately. Some of the transformers have taps to change the tap positions to alter the voltage based on the requirement.

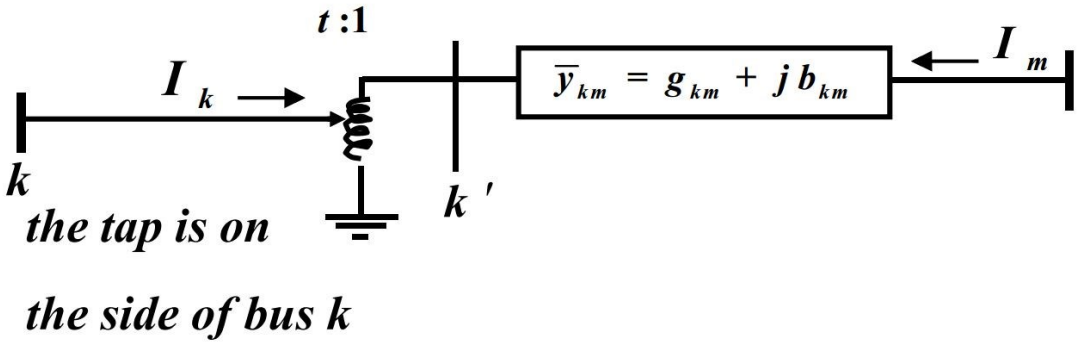

Figure 3-10 Transformer tap ratio on primary side [26]

The transformers at substation 1 and 3 has load tap changers (LTC) that can be switched on load and transformers at substation 2 and 4 has no load tap changers (NLTC) which needs the transformer to be taken out of service to change the tap, which is not advisable in a microgrid operation. The transformers at substation 1 and 3 are utilized to change the taps. For off nominal condition, the tap ratio is the ratio of the per unit step changes of voltage in primary side to secondary side. Figure 3-10 shows the tap ratio on primary side ('t'). Table 3-7 shows the tap

ratios settings of the transformers at substation 1 and substation 3. Only these four transformers are available to change the taps on load.

Table 3-7 Transformer tap ratios at substation 1 and substation 3

Substation-1			**Substation-3**		
0.86387	0.92762	0.9936	0.87077	0.92912	0.99593
0.87446	0.93319	1.00038	0.87574	0.93484	1.00251
0.87941	0.93883	1.00686	0.88082	0.94064	1.00917
0.88472	0.94454	1.01344	0.88591	0.94644	1.01585
0.88979	0.95067	1.02009	0.89111	0.95238	1.0227
0.89492	0.95652	1.02724	0.89637	0.9584	1.02956
0.9001	0.96245	1.03408	0.90164	0.96442	1.03659
0.90566	0.96845	1.04101	0.90703	0.97059	1.04373
0.91097	0.97489	1.04803	0.91248	0.97676	1.05087
0.91635	0.98105	1.05558	0.91794	0.98309	1.0582
0.92179	0.98728	1.0628	0.92353	0.98951	

3.3.4 Load Modeling

The critical loads are modeled in the system and numbered from one through nine based on the priority of that load (1 represents highest priority and 9 represents least priority) as shown in the Figure 3-4. The critical loads 5, 7, 8 and 9 are an aggregation of several critical and non-critical loads in that area. The reason that these are aggregated can be better understood from the Figure 3-11. In this region, each load is supplied by at least three of four feeders in order to provide reliability in case of emergency. So, the load will be redistributed on to another feeder even if a feeder is taken out of service. Options such as demand response can help to reduce power drawn by the non-critical loads by avoiding to supply them in microgrid operation. As discussed in Chapter-3, the loads vary with respect to time in a day and according to season. Therefore, these are modeled in Powerworld using Auxiliary files. The loads are considered as constant power loads while modeling in Powerworld.

The Auxiliary file is a text file in which the Powerworld simulator data can be stored and edited. There are many automation options available using auxiliary files in Powerworld. These are very useful to model the varying nature of the data, where new data can be loaded instantaneously. Example of an auxiliary file is shown in Appendix-A.

The lateral loads (L1 to L13) are aggregated as discussed earlier and model as shown in Figure 3-4. Each lateral load in the model has a breaker that is in normally open state.

Figure 3-4 shows a meshed network; there are disadvantages of operating microgrid in this configuration. There are problems are with protection coordination due to bi-directional power flow in this case. In order to avoid these problems, the critical loads are supplied radially by identifying breakers to leave normally open.

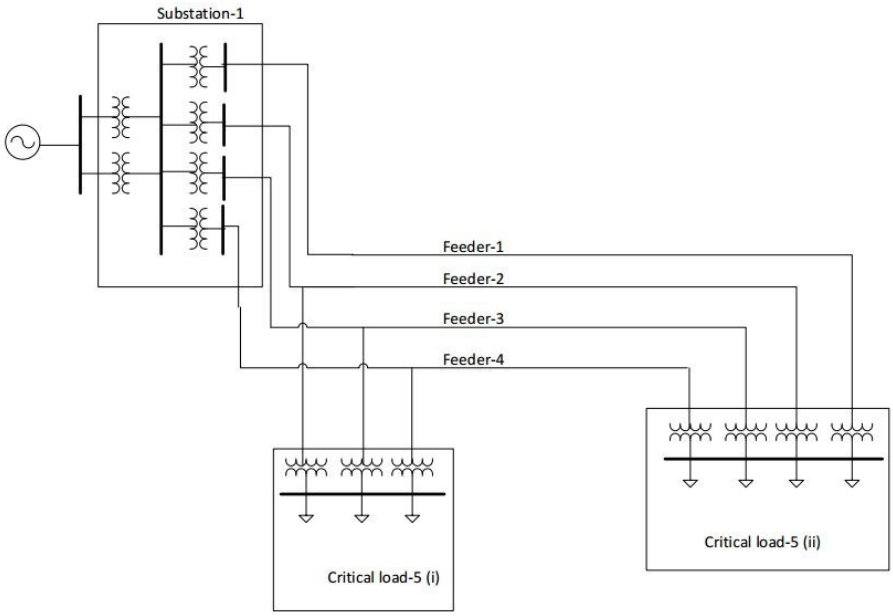

Figure 3-11 The feeder configuration for critical load-5

3.3.5 Capacitor Modeling

Shunt capacitors are used to supply reactive power at set location in the microgrid. They help to maintain the voltage within the microgrid, in this case in order to improve the steady-

state voltage within the system. The capacitors need to be properly sized as well as properly placed in ideal locations. The standard capacitor values available according to the sponsor are 300kVar banks, the capacitors modeled can vary in steps of 300kVar. The capacitors are modeled at four different locations in the microgrid after identifying the buses that are mostly affected by under voltages under loading scenarios. The locations are Substation-2, Critical load-2, Critical load-6 and Critical load-3. The capacitor values vary with respect to variations in load and generation. Therefore, they are modeled using auxiliary files.

3.3.6 Battery Modeling

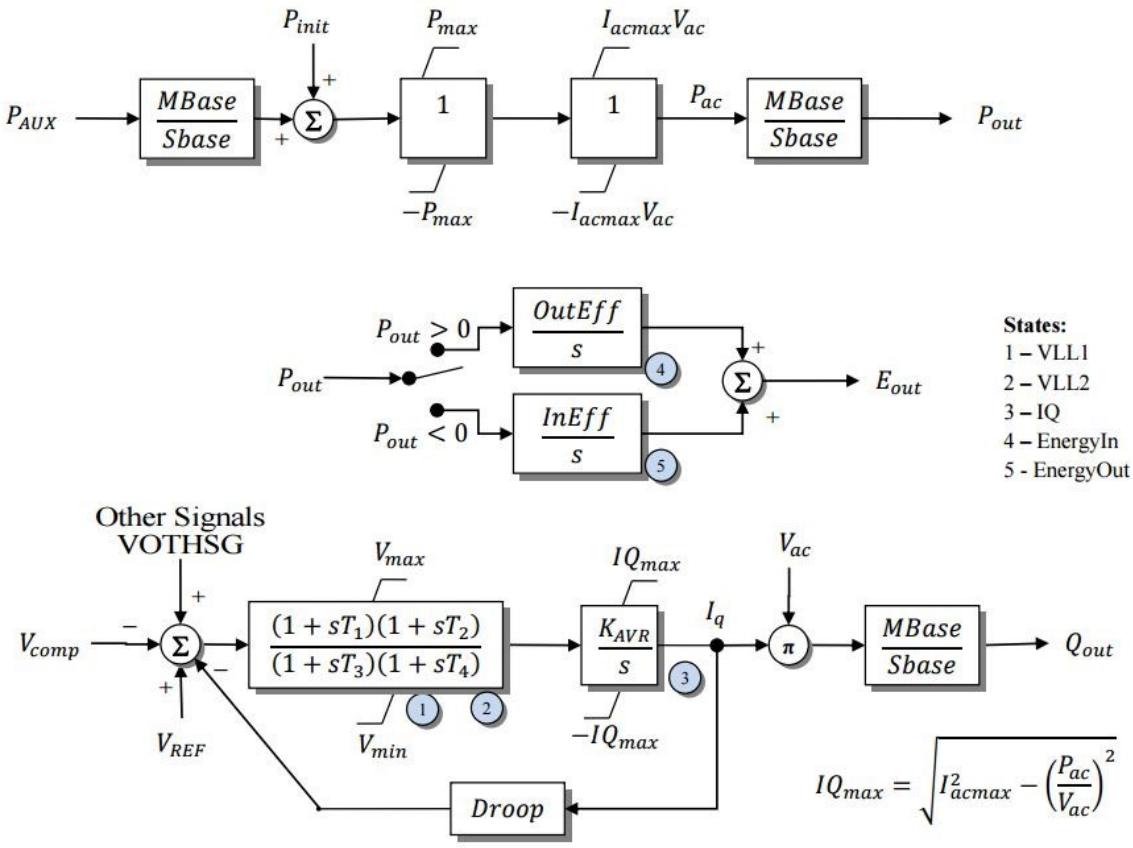

Figure 3-12 Block diagram of CBEST battery model [26]

As the utility scale, energy storage is moving from a proof of concept state to an application state (TRL level 7). Powerworld has only one battery model available for modeling,

(i.e.) the CBEST model and this is primary geared towards stability studies. Figure 3-12 shows the block diagram of the CBEST model [26]. There are two ideal locations identified for installation of batteries in the microgrid, as will be discussed in detail in Chapter-4. The batteries are modeled at Critical load-6 bus and Critical load – 3 bus in order to perform some comparative study to identify an ideal location for its placement.

A. Plant controller model for Battery

The Powerworld also has a plant controller model, which is used to replicate the converter used for battery in stability studies. Figure 3-13 shows the block diagram of the plant controller model REPC_A included in the microgrid [26].

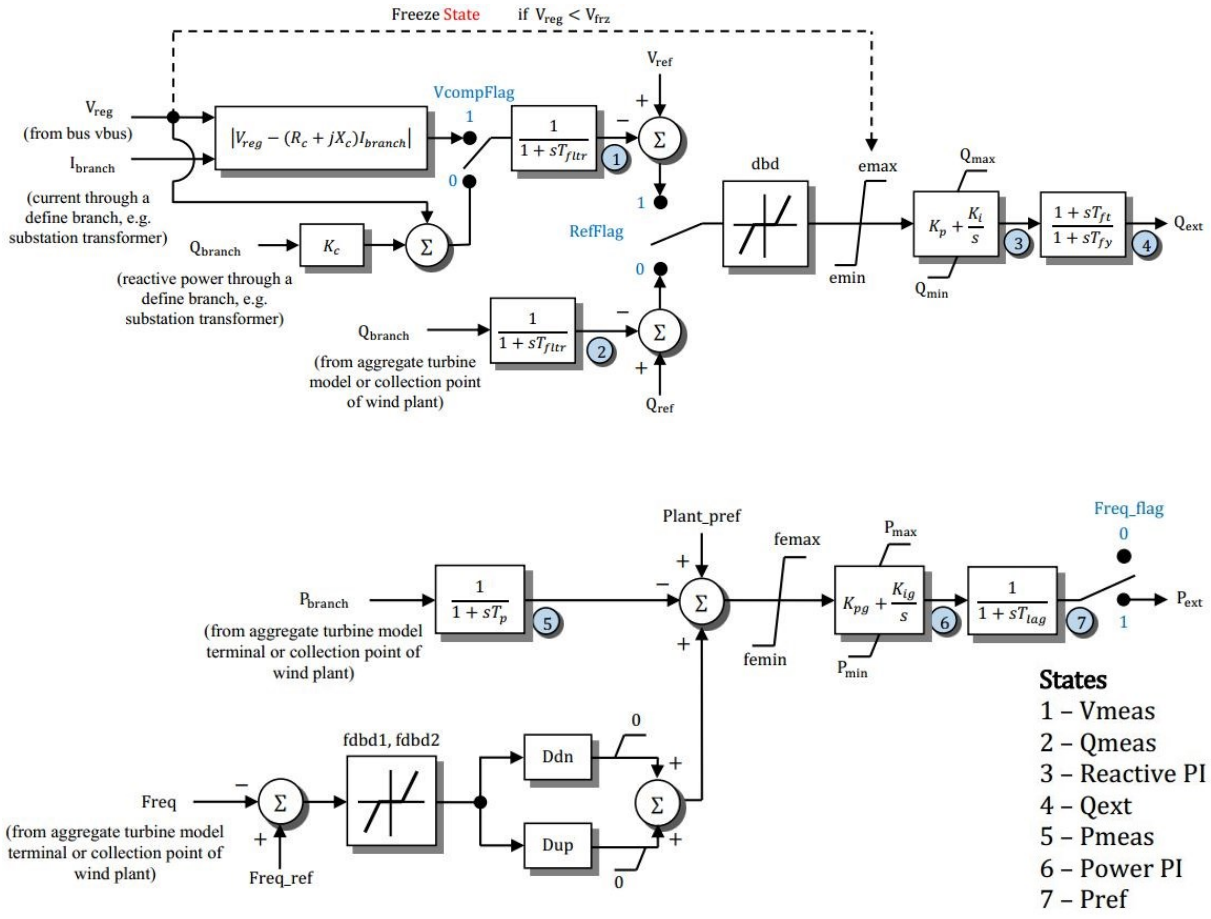

Figure 3-13 Block diagram of REPC_A plant controller model [26]

3.3.7 Photovoltaic Cell Model

The solar generation is modeled as an aggregated generator supplying to the grid at substation-3 in the microgrid. Figure 3-14 shows the block diagram of the model included for transient stability studies. The distributed PV system model PVD1 is used.

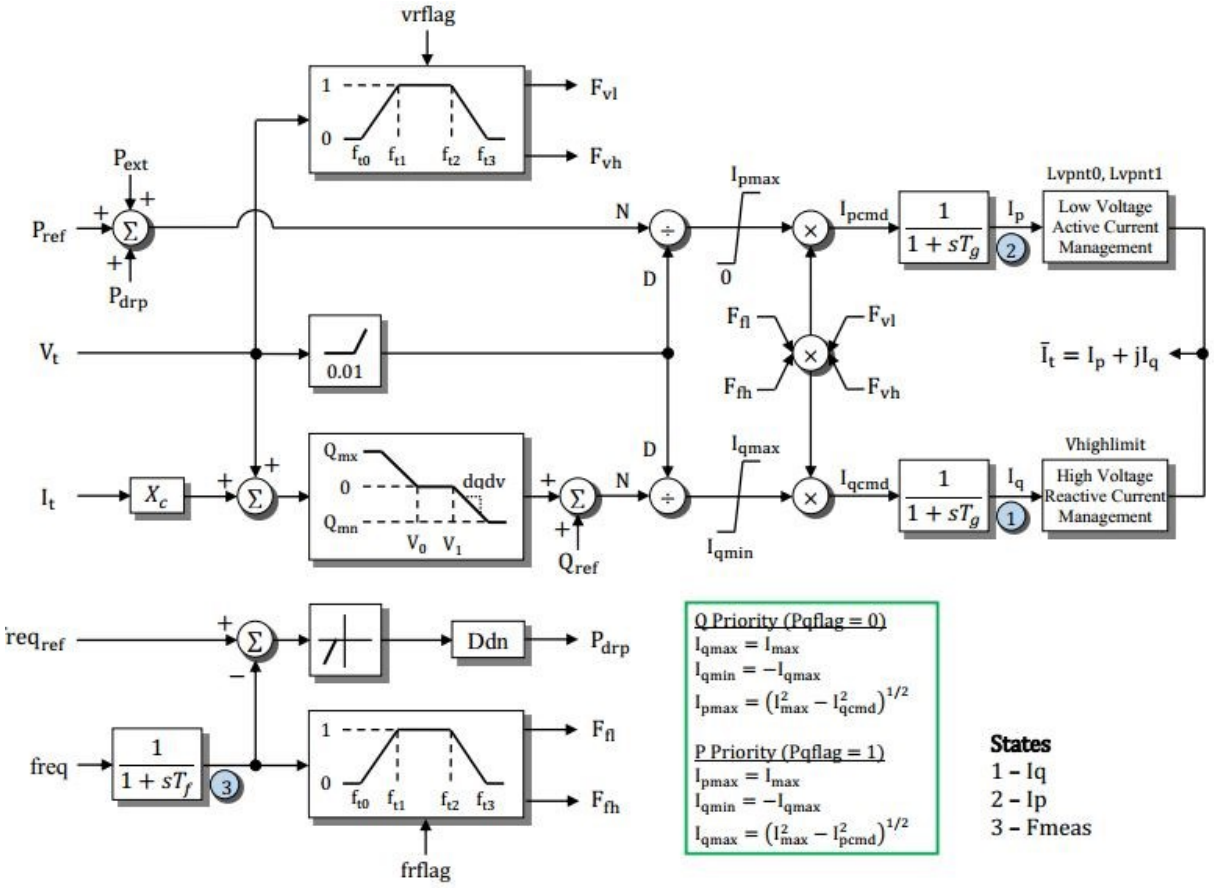

Figure 3-14 Block diagram of PVD1 distributed PV system model [26]

3.4 POWER – FLOW SOLUTION

Power-flow is the computation of voltage magnitude and phase angle at each bus in a power system under balanced three-phase steady-state conditions. Powerworld can solve the network based on several methods such as the Gauss-Seidel method, the Newton-Raphson

method and the Fast decoupled method. In standard mode, simulator solves the power flow equations using the Newton-Raphson power flow solution, which is the most accurate among the methods. Data entry for the power flow problem can begin from a single line diagram of the power system from which the input data for computer solutions can be obtained. The input data consists of bus data, transmission line data, transformer data, load data and other power system components data as was discussed in section 3.3. Each bus in the power system is classified into three different categories, which are:

a) Swing bus (or Slack bus) – Voltage (V) and load angle (δ) are known

b) Load (PQ) bus – Real power (P) and reactive power (Q) are known

c) Voltage controlled (PV) bus – Real Power (P) and Voltage (V) are known

The power flow solves the complex matrix equations

$$YV=I= S^*/V^* \qquad (3.1)$$

Where Y is the network nodal admittance matrix, V is the unknown complex node voltage vector, I is the nodal current injection vector, and S=P+jQ is the apparent power nodal injection vector that represents the specified load and the generation at demand or generation nodes respectively. It is a solution to a nonlinear equation using non-linear method.

3.4.1 Newton – Raphson Method

The Newton – Raphson method is a mathematical approach using a Jacobian matrix method of finding better approximations to find solution for sets of coupled nonlinear equations. The method starts with an initial guess, which is close to a true root and obtains a solution after several iterations such that the results are accurate to with defined convergence criteria. This

method uses the power balance equations (3.2) and (3.3) as shown below for convergence criteria.

$$P_k = V_k \sum_{n=1}^{N} Y_{kn} V_n \cos(\delta_k - \delta_n - \theta_{kn}) \quad (3.2)$$

$$Q_k = V_k \sum_{n=1}^{N} Y_{kn} V_n \sin(\delta_k - \delta_n - \theta_{kn}) \quad k=1, 2\ldots N \quad (3.3)$$

Where,
- P, Q : Real and Reactive power
- V : Voltage
- Y : Admittance
- δ : Phase angle of voltage
- θ : Impedance angle
- K : bus number

This chapter discussed about the modeling aspects and challenges in building a Powerworld model. It briefly explains about the simulation software used in this study, how every component of the system is modeled using the Powerworld software.

CHAPTER 4. SIMULATION RESULTS AND ANALYSIS

This study conducted extensive simulations using the model and recorded the results, this chapter discusses about the analysis and results done on the model.

4.1 TRANSITION TO MICROGRID OPERATION

Figure 4-1 shows the flow of events while forming a microgrid. The microgrid is assumed to be formed if the entire grid goes down by some means. The microgrid controller will take care of identifying the situation to form a microgrid by various islanding detection techniques. The details of islanding detection and microgrid transition are not included in this thesis. First, when the grid goes down, the appropriate transmission interties are identified and opened remotely to form an island. Then, the distribution fuses are opened manually and smart switches are opened remotely using existing SCADA systems. The hydro generators can quickly go from zero power to maximum output; this is an advantage in this microgrid.

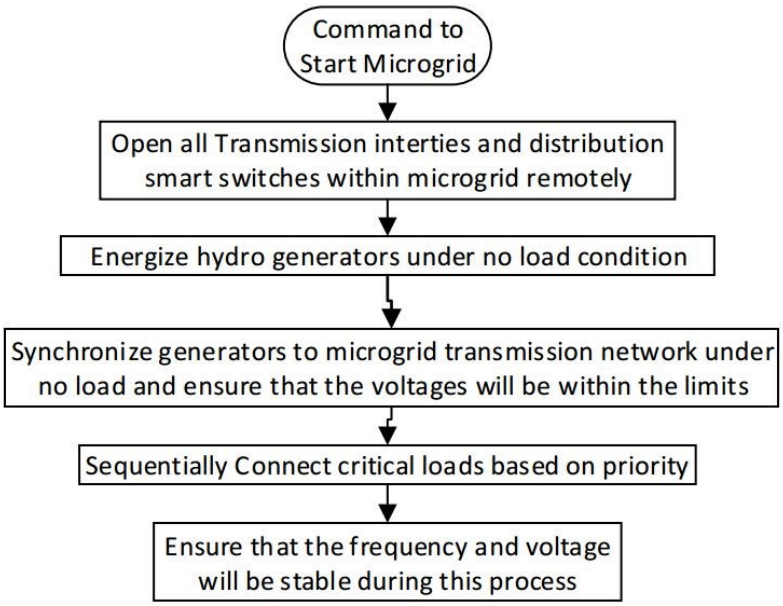

Figure 4-1 Transition to microgrid plan

The two hydro generators can be bought into running mode under no load condition and then connected to the microgrid transmission network. In this case, there is a chance of over voltages at different buses, so the capacitor banks need to be disconnected during this process. Finally, the critical loads are added sequentially based on the priority making sure that the frequency and voltage attains stability. Capacitor banks are switched in according to the requirement to maintain the voltage limits.

4.2 LOAD AND GENERATION FORECAST STUDIES

The load and generation profiles acquired from utility were analyzed over a three year period. They were used in terms of system planning by providing information about reactive compensation requirements and any additional components. This forecast information of microgrid based on historic profiles would also be useful to plan and perform the load-shedding schedule ahead of time so that the information can be shared with the customer affected by the shedding. It can also identify any special requirements that may be needed.

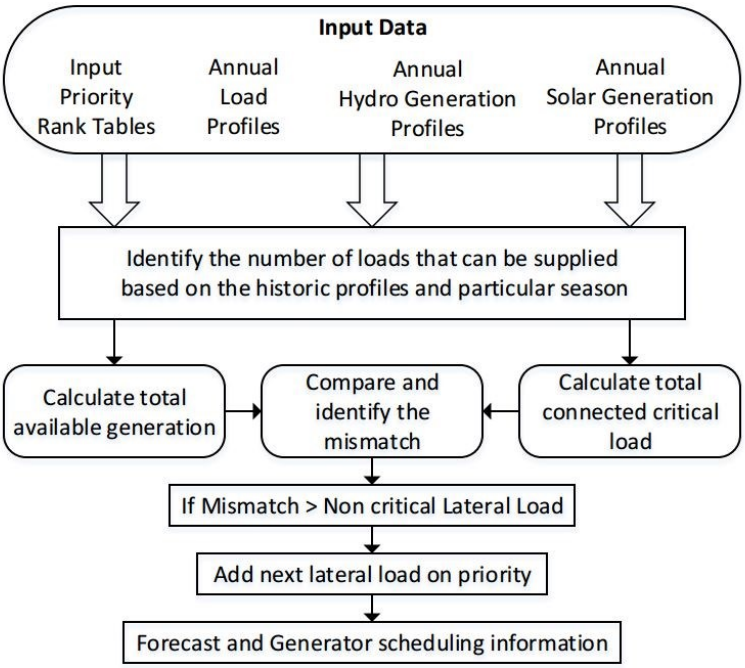

Figure 4-2 Utilizing forecast information for the microgrid short term planning

Figure 4-2 shows the different steps involved in generating this information, which are discussed in detail below.

4.2.1 Step-1

In this step, the historic profiles of different loads in the microgrid, hydro generation and solar generation are used for estimation. The profiles are divided into four seasons (i.e.) spring, summer, fall, and winter by averaging across the seasons. This determines the approximate behavior of load and generation in these seasons. The priority/rank table of the critical loads is developed with different cases changing the priority based on the requirement of utility how they can operate. Figure 4-3 shows three ranking tables of critical loads based on different applications, which are created for demonstration. This table is useful to determine the loads to shed when there is dearth in generation. The table from top to bottom shows the breaker closing sequence and the reverse direction shows the trip order.

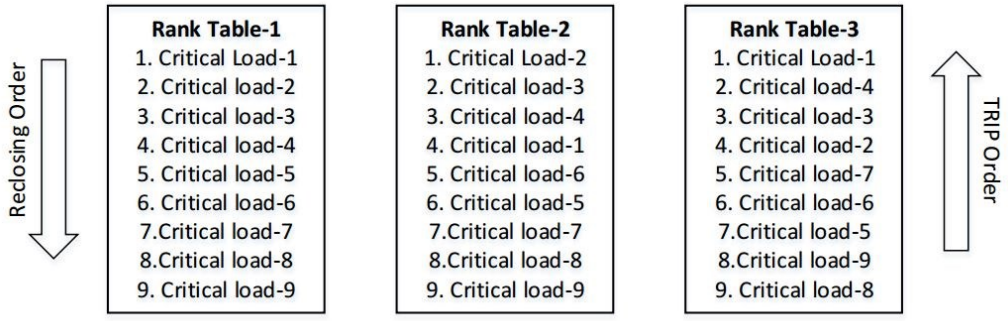

Figure 4-3 Possible rank tables for critical loads in the microgrid

4.2.2 Step-2

This step identifies the loads that can be supplied during an hour of the day in a particular season. The averaged load and generation profile values across a 24-hour period are taken and added to compare the difference between load and generation. Figure 4-4 shows the graph of load versus generation in a day in each season as a reference. These graphs show the total sum

of all nine critical loads included in the microgrid and the total generation including the two hydro generators and solar generation estimation estimated in section-2.2.3.

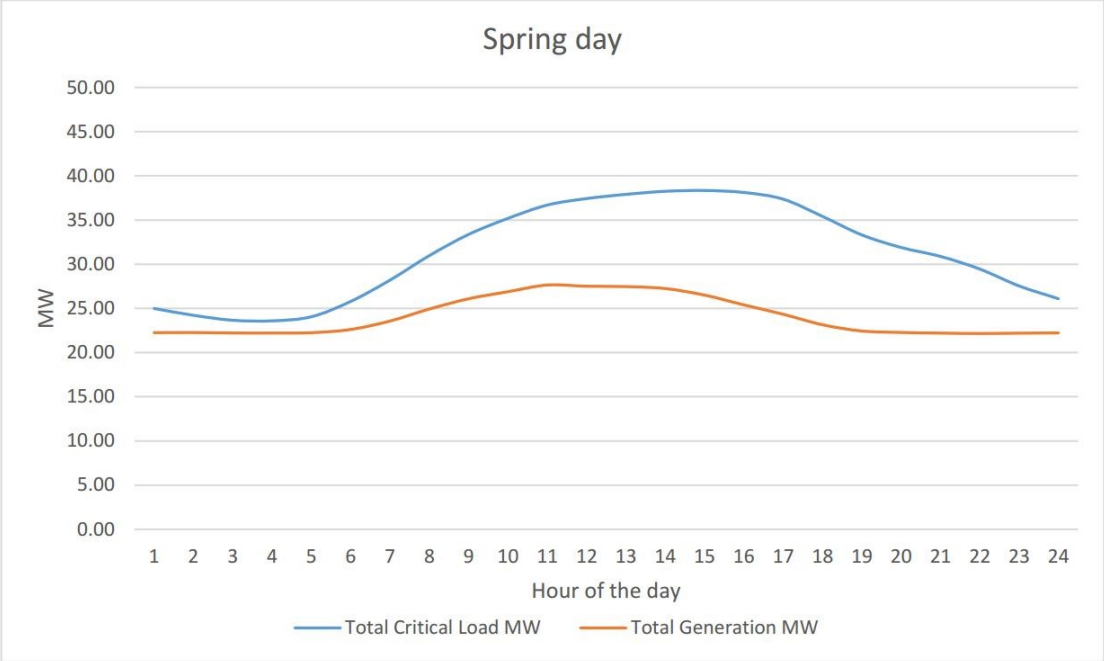

Figure 4-4 Total load vs total generation on a spring day averaged over three years

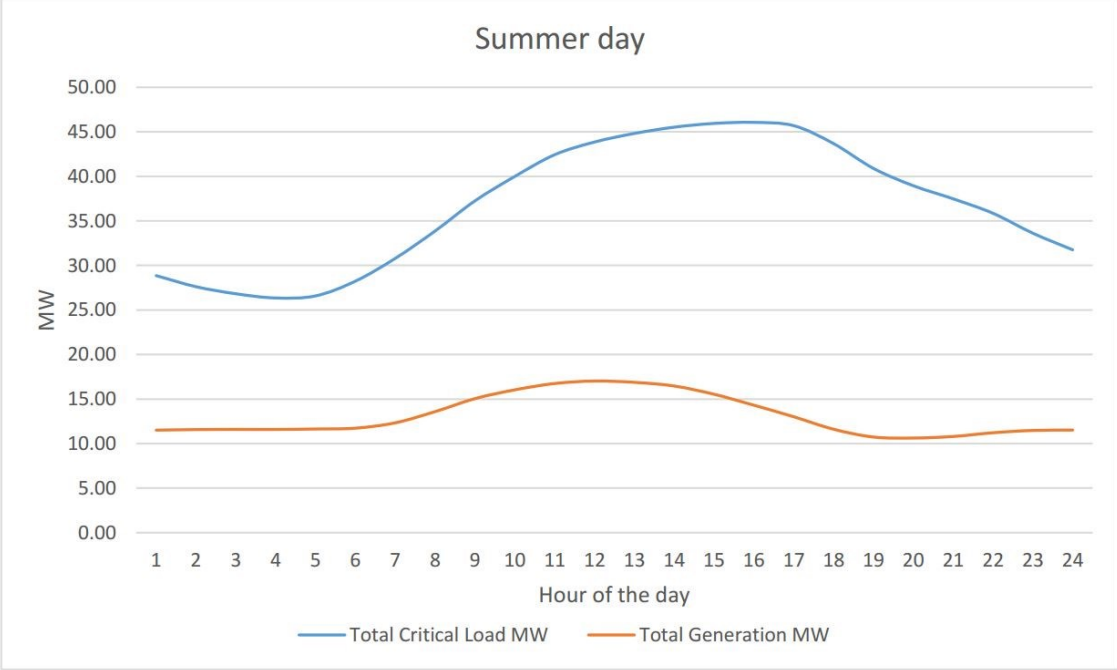

Figure 4-5 Total load vs total generation on a summer day averaged over three years

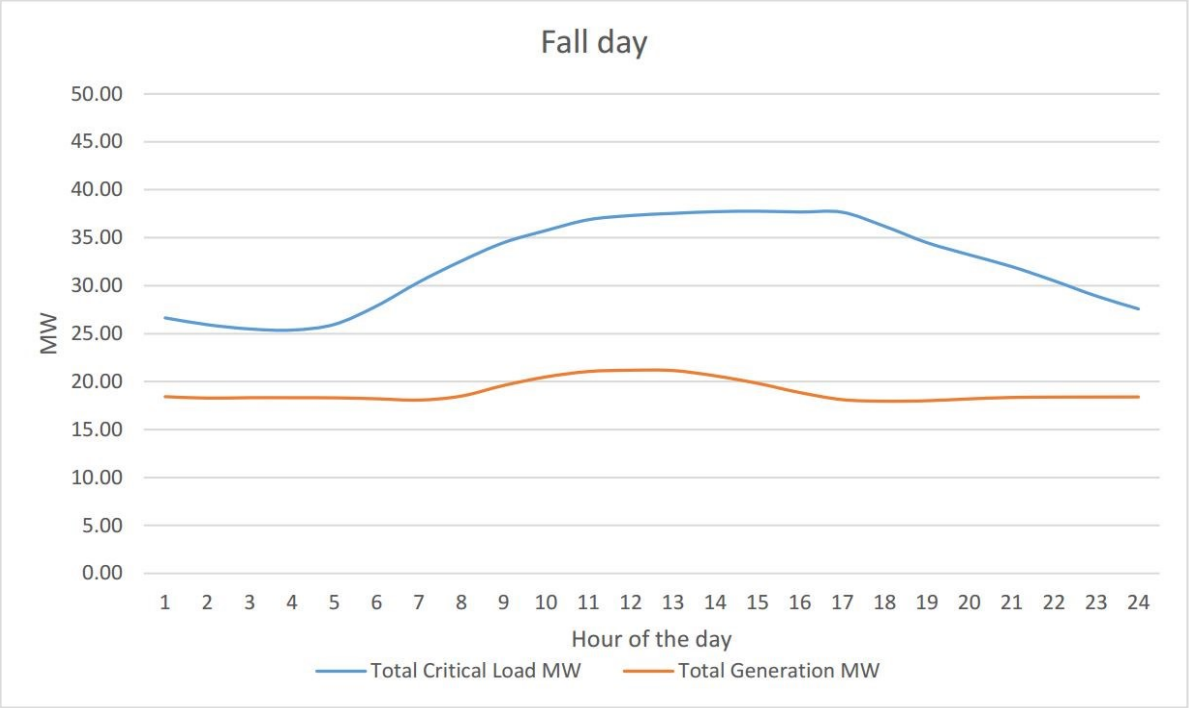

Figure 4-6 Total load vs total generation on a fall day averaged over three years

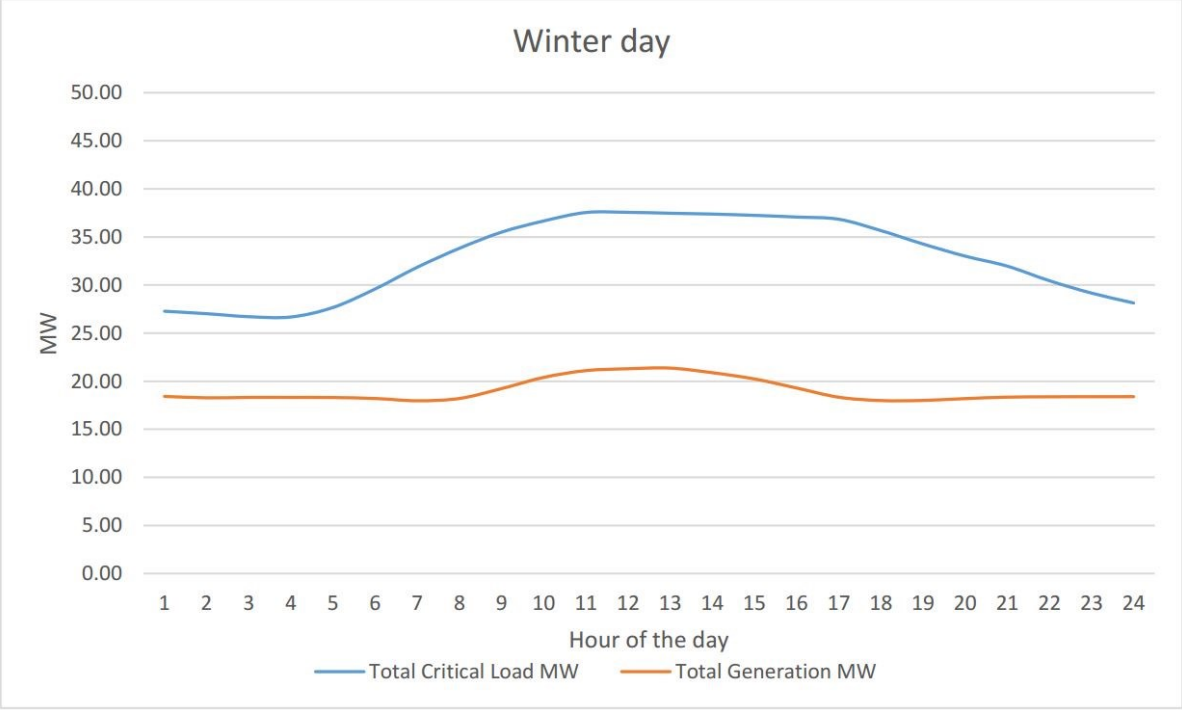

Figure 4-7 Total load vs total generation on a winter day averaged over three years

All the load profiles follow a typical shape with a rise in the power demand around 6 AM and drop in the power demand at about 6 PM each day. The generation from hydro generators, which depends mostly on water flow availability in the river, will be mostly constant throughout the day in each different season but varies significantly by season. The solar energy estimation added to the generation mix changes the profile shape to better follow the load profiles, as the solar energy is mostly available from 6AM to 6PM in a day. The summer season has the highest demand around 45MW of peak demand value all loads aggregated during the afternoon and the other three seasons mostly follow similar profiles of loads peaking around 35MW around noontime.

There is a gap between the available generation and connected critical load in each season, particularly this gap is more during summer. Therefore, loads need to be shed based on the available generation, as not every load can be supplied in every hour in each season. The main cause for the variation in this case is the variation in hydro energy generated due to variation in water flow availability. The results identify the loads that need to be shed in each season. The load exceeds generation for a shorter duration with a difference in total real power of the load and real power of generation less than 2MW. The reliability of supplying the loads during that time can be provided by having a battery with proper controls. This battery can charge when the generation exceeds the total load. Figure 4-8 to Figure 4-11 shows the load versus generation profiles after load shedding and as well as battery addition (which is sized to be 2MW maximum output, more information about battery sizing is discussed in section - 4.3). The number of loads among the critical loads that can be supplied in each hour of a season are identified and the rest other critical loads are shed when the demand exceeds supply.

a) Spring day

Figure 4-8 shows the load versus generation profile on a spring day. Seven critical loads (peak demand of 26.9MW around 2 PM) can be supplied continuously on this day and the eighth critical load can be supplied from 12:00 AM to 6:00 AM. Figure 4-8 shows that the total critical load dropped from 23.4MW to 20.7 MW at around 6:00 AM, which is due to shedding of 2.7 MW at critical load-8. Loads are treated as fixed based on historical data. Demand response or other load shedding by the load owners is not considered in this study. The battery is switched into the microgrid (stays online) around 2:00PM to contribute towards small variation between load and generation. It is switched off from the microgrid at 7 PM, as it is no longer needed after that time. It supplied 7 MW-hr on this day. The mismatch shown in the figure is the difference between the power consumed by all the loads and power generated by generators. It gives the idea of power available for storage. Typically, the area under this mismatch curve is greater than the area under battery curve. More information about the potential storage and battery sizing is discussed in section 4.3.

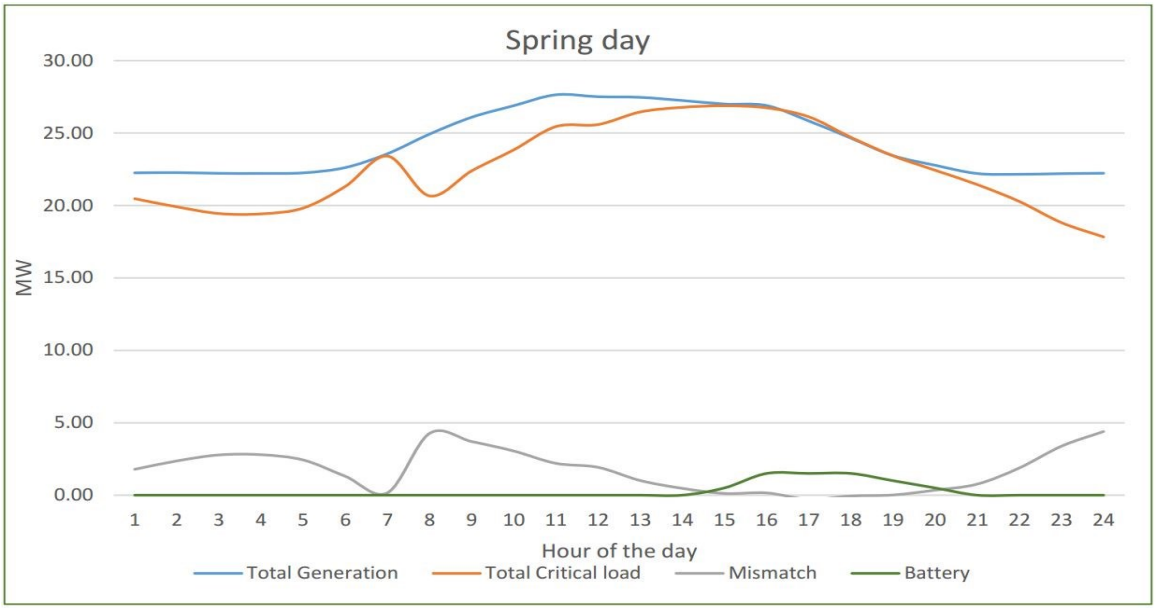

Figure 4-8 Total load vs Total generation on a spring day after load shedding

b) Summer day

Figure 4-9 shows the load versus generation profile on a summer day. On this summer day, four critical loads can be supplied based on their priority (with a peak demand of 16.7MW around 11 AM) as there is a huge gap between the available generation and total critical load. This is due to the unavailability of water to generate power from the hydro generators. Though there is a maximum output from solar energy during this season, it is able to supply only a fraction of the critical load. The critical load-5 can only be supplied from 1:00 AM to 11:00 AM, and it needs to shed at 11:00 AM as the total demand crosses the available generation after that point. The plot shows a drop from 16.7 MW to 12.7 MW total load at 11:00 AM due to the 4 MW reduction of critical load-5. The battery is switched into the microgrid from 4:00 PM to 9:00 PM, supplying 6.0 MW-hr on this day.

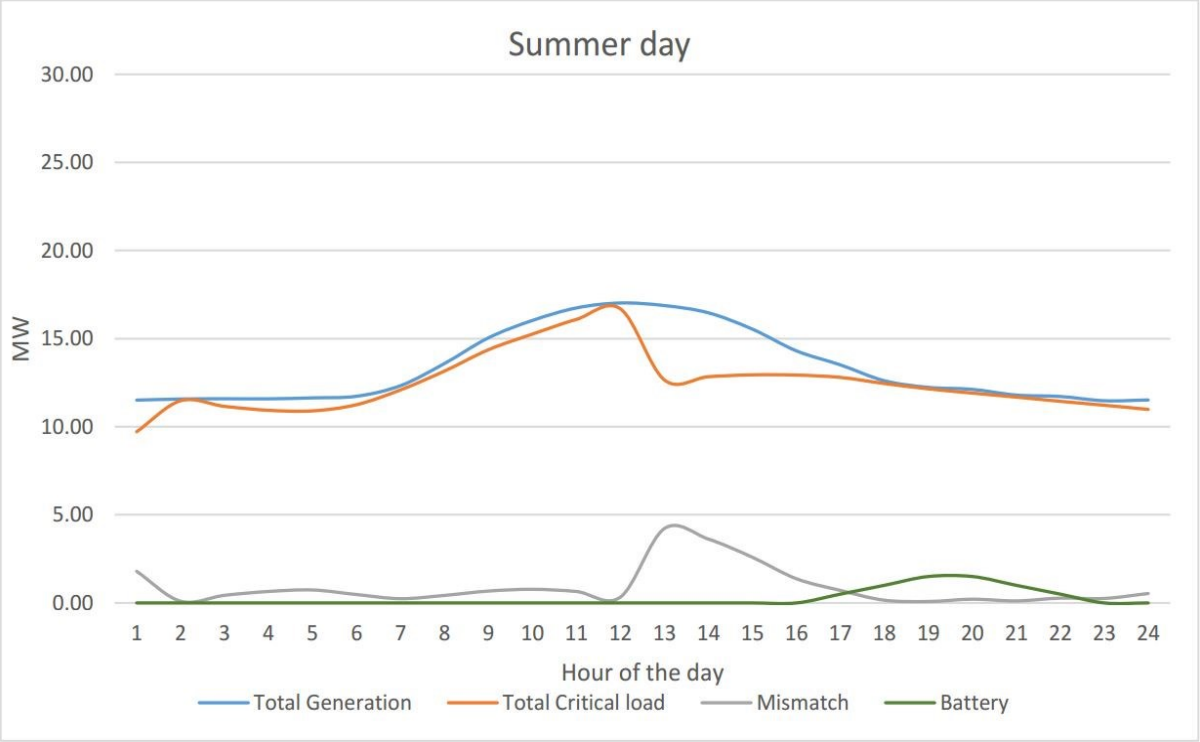

Figure 4-9 Total load vs total generation on a summer day including load shedding

c) Fall day

Figure 4-10 shows the load versus generation profile on a fall day. Six critical loads can be supplied continuously on this day based on priority (with a peak demand of 21.18 MW around 11:00AM). The seventh critical load can be supplied from 12:00 AM to 5:00 AM and needs to be disconnected after 5:00 AM due to increase in demand. The plot shows it as a drop from 18 MW to 14.6 MW total load around 5:00 AM due to 3.4MW reduction by shedding critical load-7. The battery is switched on from 2:00PM to 6:00 PM supplying 3.5 MW-hr on this day.

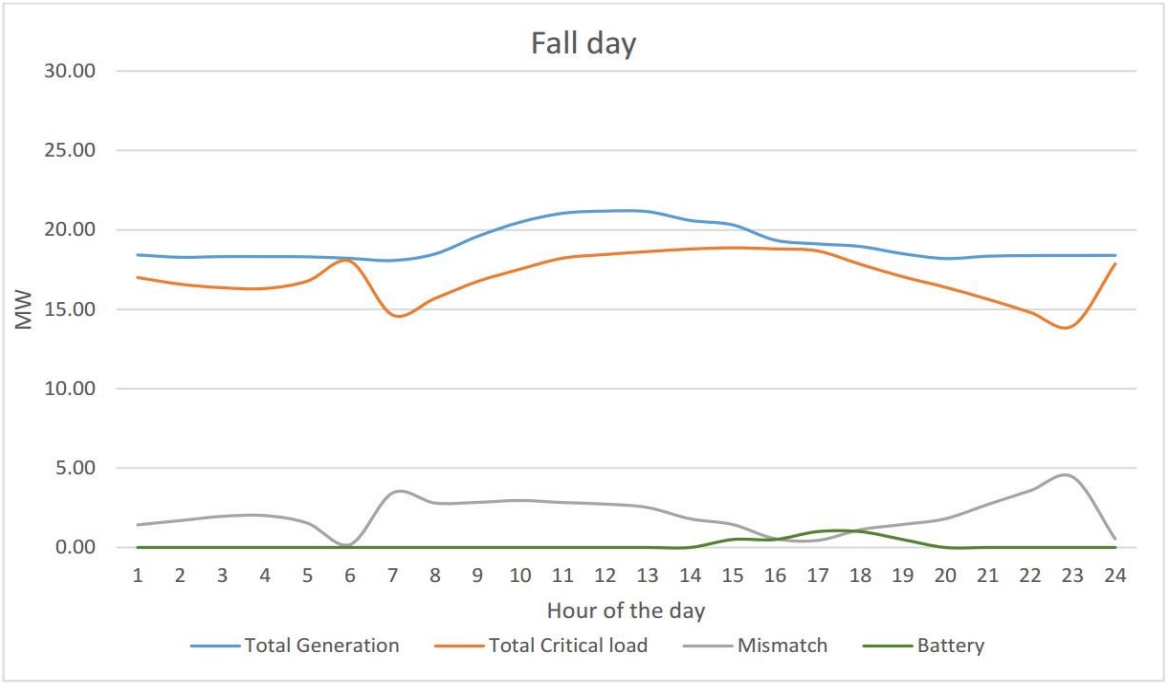

Figure 4-10 Total load vs Total generation on a fall day including load shedding

d) Winter day

Figure 4-11 shows the load versus generation profile on a winter day. Six critical loads can be supplied based on priority on this day (with a peak demand of 17.86 MW around 10:00 AM). The seventh critical load can be supplied from 12:00 AM to 4:00 AM and needs to be

disconnected after that. The plot shows it as a drop from 17.25 MW to 13.5 MW around 4 AM due to reduction of 3.75MW contribution from critical load-7. The battery is switched into the microgrid from 3:00 PM to 7:00 PM supplying only 2.5 MW-hr.

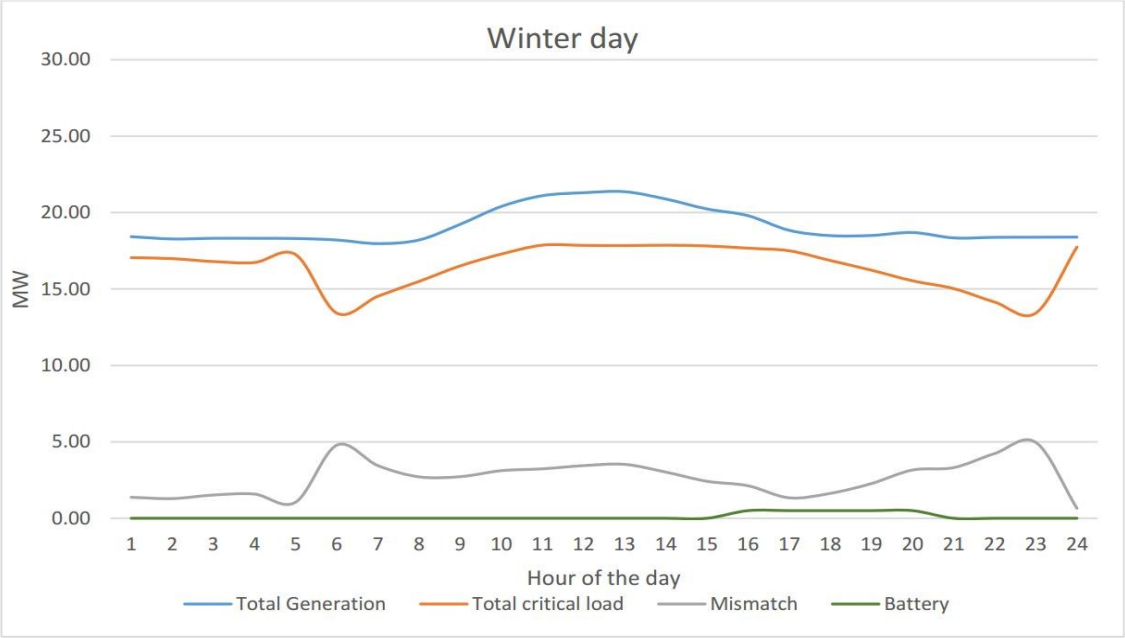

Figure 4-11 Total load vs total generation on a winter day including load shedding

Table 4-1 summarizes the load shedding criteria and the forecast information created based on the analysis on the historic profiles over the year.

Table 4-1 Summary of load shedding and forecast study

Season	**Total critical loads supplied**	**Additional critical load**	**Load shed value**	**Additional critical load duration**		**Battery switching duration**		**Peak demand of the day**		**Lowest demand on the day**	
			MW	Start time	End time	Start time	End time	MW	Occurred Time	MW	Occurred Time
Spring	7	Critical load-8	2.7	12:00 AM	6:00 AM	2:00 PM	7:00 PM	26.90	2:00 PM	17.83	11:00 PM
Summer	4	Critical load-5	4	1:00 AM	11:00 AM	4:00 PM	9:00 PM	16.70	11:00 AM	11.00	11:00 PM
Fall	6	Critical load-7	3.4	12:00 AM	5:00 AM	2:00 PM	6:00 PM	21.18	11:00 AM	13.95	11:00 PM
Winter	6	Critical load-7	3.75	12:00 AM	4:00 AM	3:00 PM	7:00 PM	17.86	10:00 AM	13.42	11:00 PM

4.2.3 Step-3

In this step, the mismatch value between total generation and total critical load in each hour of the day is calculated. This value is shown in the Figure 4-8 to Figure 4-11. The non-critical loads are modeled as laterals in the Powerworld microgrid model. These non- critical loads can be supplied if the mismatch value crosses the non-critical load value at any point of the day. This means the available generation at that point of time is able to supply all the critical loads possible and additional non-critical loads, which are less than the next critical load in priority. This particular feature is optional and depends on the requirement of the non-critical load to be supplied at that point of time. There is also an assumption that they can be picked up through SCADA controlled switch. The microgrid controller uses the forecast information based on this analysis to make appropriate decisions according to the situation of the microgrid.

4.3 BATTERY SIZING STUDY

The peak power rating and storage capacity of the batteries in the microgrid needs to be properly determined based on several factors. It is important to size the battery appropriately, as it can improve the balance between generation and demand trends, and thus, the battery size will have significant impact on the grid's economic operation. The microgrid dynamics and stability rely on the amount of stored energy in the microgrid. In case of the conventional power system, the large generators in the network act as the main source of energy, and the combined inertia of the machines acts as a stored energy and feeds the grid disturbances to stabilize. The microgrid has low inertia due to small hydro machines; therefore, storage will have significant stabilizing effects.

The battery size is estimated based on two different criteria, one is the availability of power that can be stored in different seasons and the other one is deficit in power availability

in supplying critical loads in any hour of the day. This study does not include the economic aspects in optimizing the size of the battery.

4.3.1 Potential for Storage

Figure 4-12 and Figure 4-13 are the examples used to demonstrate the basic idea of estimating the energy storage rating. In Figure 4-12, case-1 depicts the situation when the total generation exceeds the total critical load in the microgrid. In this case, the additional energy available after supplying all the critical loads is the potential energy storage available for battery. In case-2, the total energy available is less than the total critical load consumption in the microgrid, in this case there is no potential energy storage available, rather load shedding is required to bring the generation and load in balance as shown in case-3. Case-3 is the desired operation state. These figures show the comparison of the generation and load power consumption.

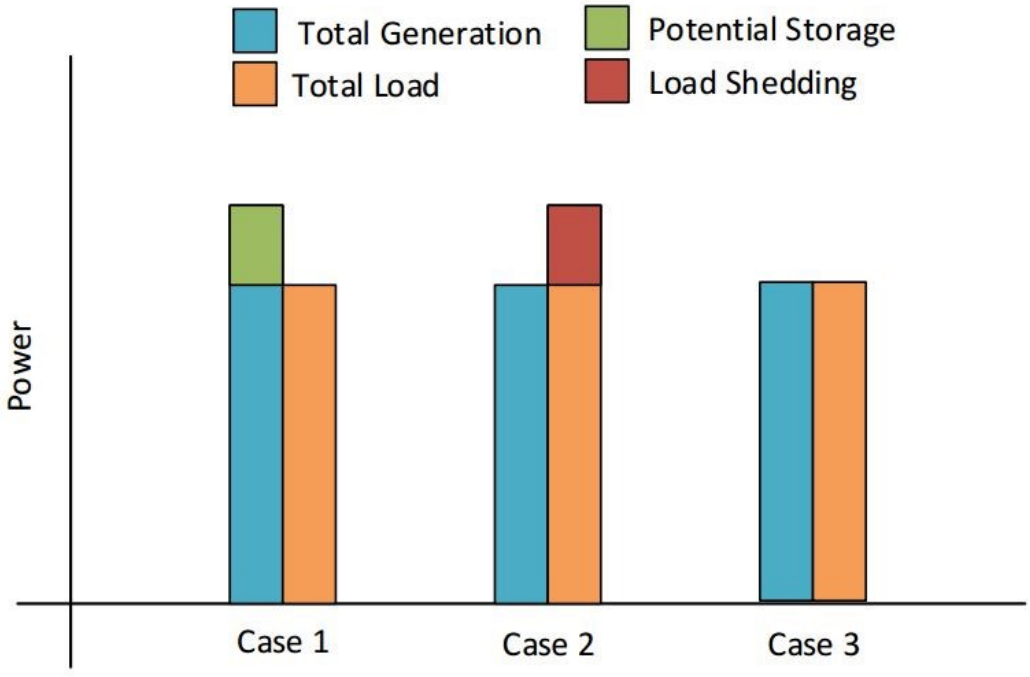

Figure 4-12 Example of the storage estimation for battery

Figure 4-13 demonstrates the process in detail. In case-1, if the total critical load is the summation of individual critical loads L1 to L6. In this case, the next critical load, L7, can be added if it does not exceed the total generation available, and the remaining energy is the potential energy storage that can be transferred to an energy storage device. In case-2, the critical load-7 exceeds the total available generation at that point of time. Therefore, in this case the critical load-7 cannot be added, instead the available energy above the total critical load consumption is used as potential energy storage. The excessive generation after the battery is completely charged need to be shed by using generator-shedding techniques with the help of governor and AGC.

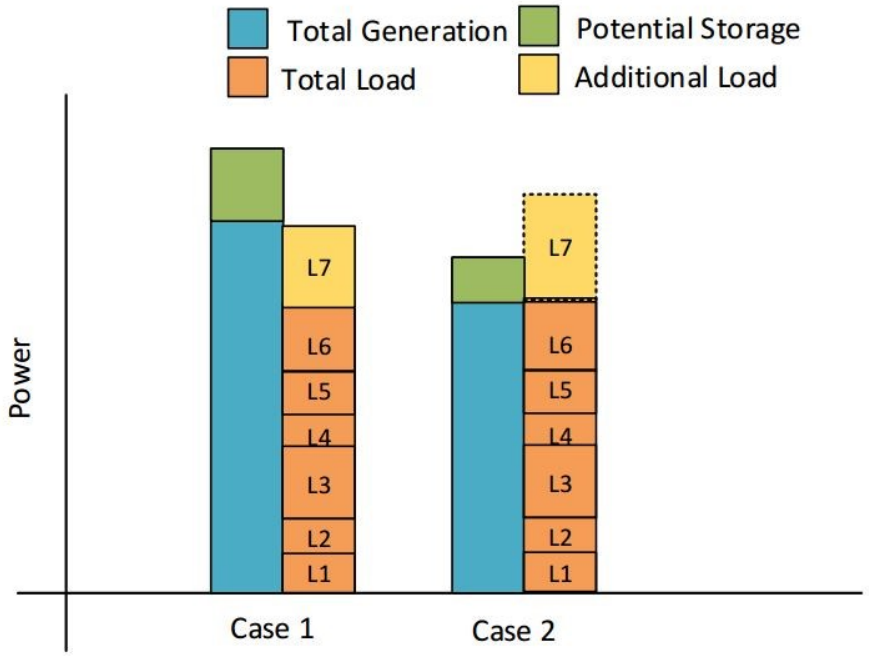

Figure 4-13 Battery addition criteria

The potential energy storage of the battery is estimated based on the same approach. The available energy that can be stored is determined. The discrete values of energy mismatch between the total generation and total connected critical load are recorded and added together.

Figure 4-14 shows the total energy in MW-hr available to store without supplying any additional loads within a day and MW-hr available for storage while also supplying an additional critical load for part of the day.

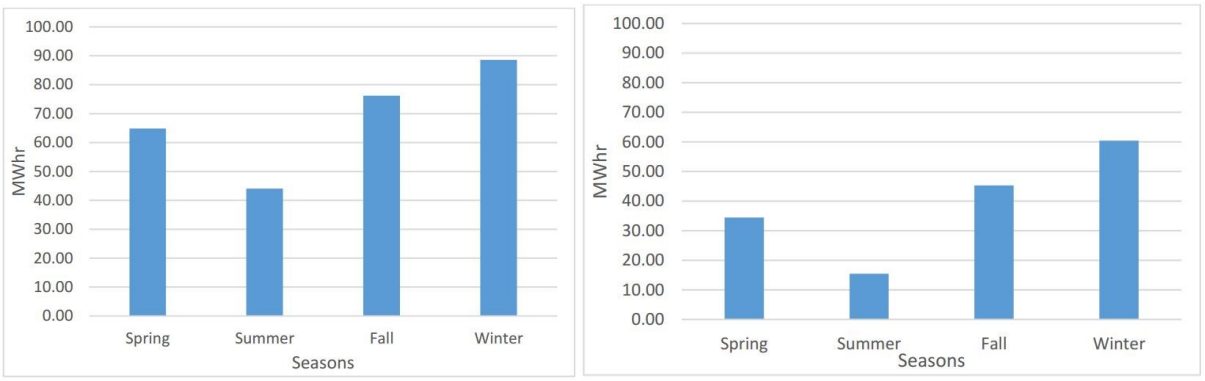

Figure 4-14 Potential energy storage available for battery

4.3.2 Critical Load Supplying Capability

The available generation capability including the predicted power generated by hydro generators and hypothetical photovoltaic cells combined together cannot supply all of the critical loads in the microgrid at the peak time of the day. There is potentially energy available to supply some portion of the next critical load, but the load cannot be supplied in that way. Instead, the additional energy is used to charge the battery as discussed in the previous section. Moreover, the extra power available after the battery is completely charged can instead be reduced by governor action. The Automatic Generation Controller (AGC) sends the command to reduce the power output of the generator.

If there is a minor deficit in power required by the critical loads, the generators are not capable of supplying additional power if they are already operating at their maximum output. In this case, the entire critical load needs to be shed due to a minor difference between available generation and connected critical load. In such a situation, the battery helps a lot in avoiding

that load shedding by supplying the power during those hours that stores the energy in the off peak hours assuming sufficient energy capacity. Identifying the minimum difference between the load and generation in all the seasons is used in sizing the battery.

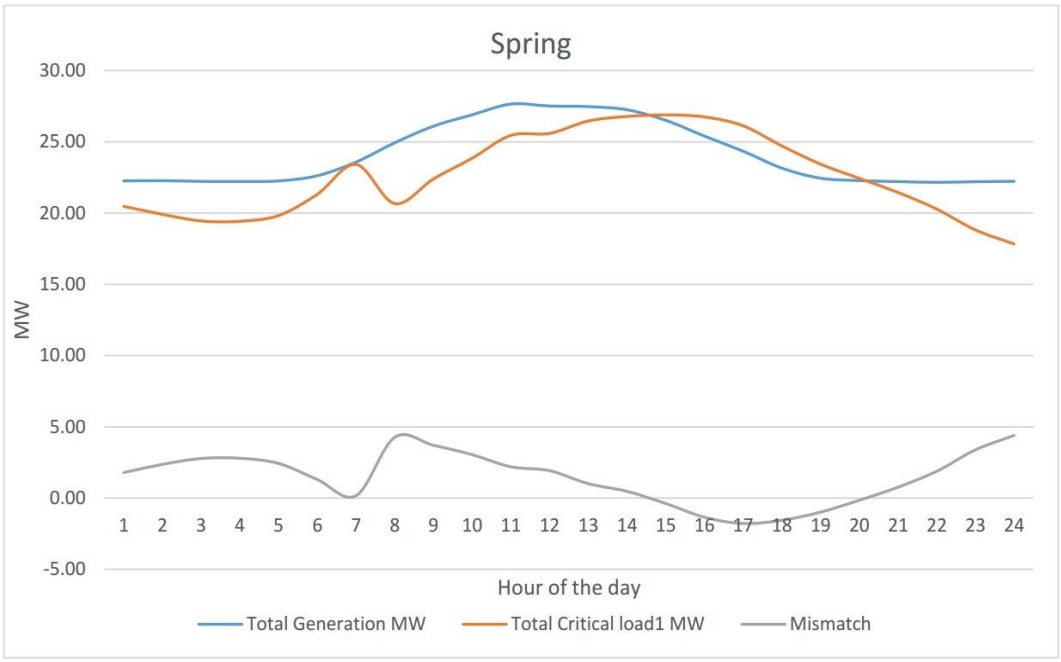

Figure 4-15 Total generation, total critical load and mismatch during spring season

The forecast study performed in Section 4.2 provides the power deficit information. For better understanding of this case, the spring and summer seasonal profiles are shown for a typical day. Figure 4-15 shows a plot of spring season load and generation profiles, the total critical load exceeds the available generation from 2:00 PM to 7:00 PM and the maximum deficit value on this day is 1.78MW in the lower curve in the figure, which occurred around 4:00 PM. Figure 4-16 shows the plot of summer load and generation profiles for a typical day, the critical load exceeds the available generation on this day from 5:00 PM to 9:00 PM with a peak deficit of 1.45MW that occurred around 6:00PM (Note that the total generation and load is substantially lower in the summer case). Table 4-2 summarizes the load profile analyses for

the other seasons. The maximum deficit value is used size of the battery (peak power rating) and it is sized to be 2MW maximum capacity. The need for 6 hours of discharge needs a total of 12MWhr of energy storage.

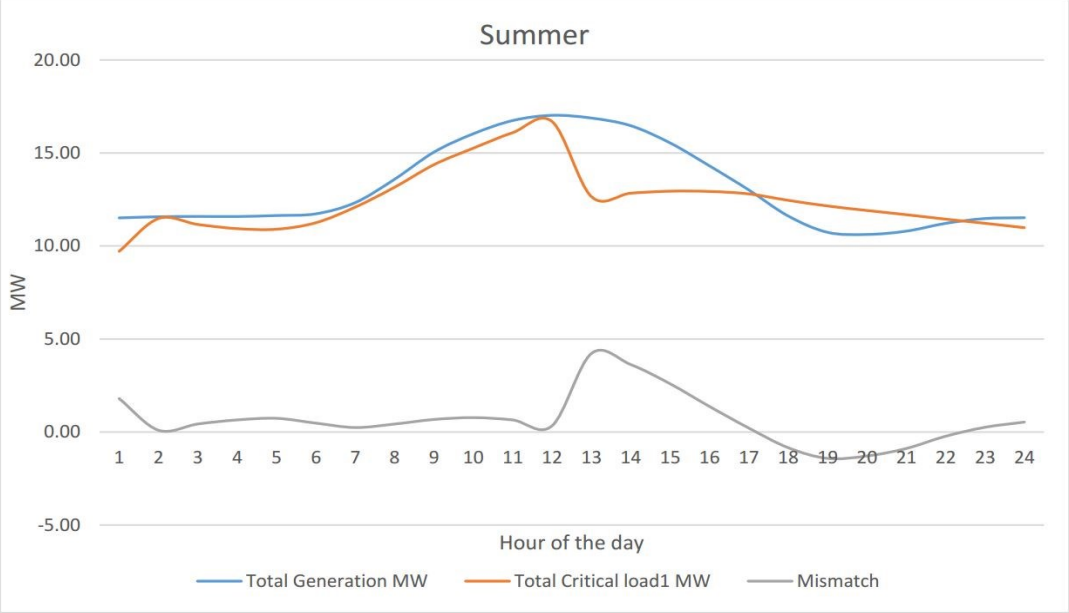

Figure 4-16 Total generation, total critical load and mismatch during summer season

Table 4-2 Summary of battery peak power requirement study

Season	Total critical loads supplied	Peak Deficit value	Deficit duration	
		MW	Start time	End time
Spring	7	1.78	2:00PM	7:00PM
Summer	4	1.45	5:00PM	9:00PM
Fall	6	0.6	4:00PM	4:59PM
Winter	6	0	NA	NA

4.4 BATTERY LOCATION IDENTIFICATION

The physical placement of energy storage elements plays an important role in a microgrid. Good locations improve the voltage and power quality at different buses. It also reduces the requirement of capacitor banks to improve the voltage. Several past studies were

reviewed to learn methods to find the quasi-ideal location for the battery placement in the microgrid. References [61] and [62] seems provide methods specific to microgrids. Reference [61] talks about identifying the location based on study of line loading percentages and line loading in different cases. Reference [62] discusses using voltage sensitivity analysis to identify the ideal locations in a microgrid. These two different techniques are used to identify the location of the battery in this microgrid.

The voltage sensitivity technique is widely used in power system analysis to identify the relationships between voltage magnitude and active or reactive power transfer at a particular bus. These relationships are depicted in terms of P-V and Q-V curves. In a transmission system, the Q-V curve is commonly adopted to evaluate the impact of reactive power on voltage magnitude in terms of dQ/dV, in contrast active power usually has negligible impact on voltage magnitude [61]. In distribution systems, the relation between voltage magnitude and active or reactive power are not linear due to more significant line resistances. Therefore, it is useful to have an active power supplier (battery) along with a reactive power injection. The microgrid in this study is a combination of both transmission and distribution networks, so it is more complex to derive relations of active power and reactive power with bus voltages.

The voltage sensitivity of each of the buses in this microgrid is calculated to determine the most sensitive bus to place the battery in this study. The rate of change of voltage at every bus is calculated with respect to unit change in real power (dV/dP) is calculated at every bus. This simulation is done with the help of the time step simulation in Powerworld, which can simulate different step changes and provide outputs based on different inputs. More information about time step simulation is provided in later sections. The test setup contains the microgrid Powerworld model developed in this study. The generation input of the microgrid model is kept

at a constant value and all the loads are increased in steps of 0.5 MW each to evaluate dV/dP. The bus voltages are measured at each step. The percentage change of voltage for each step change of real power is calculated. Figure 4-17 shows the percentage change of voltage taken on the ordinate and size of the step changes of load taken on abscissa.

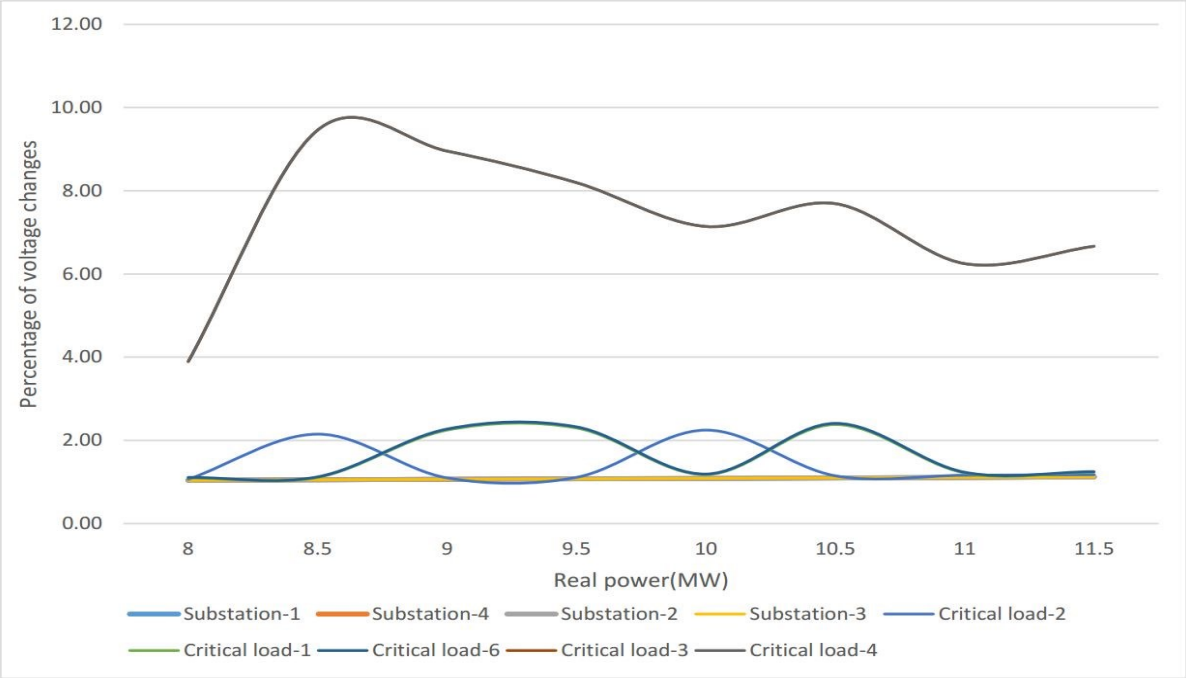

Figure 4-17 Percentage voltage change with respect to power

The critical loads are varied in steps of 0.5 MW each, the percentage changes in the plot show that the bus voltages at the locations of critical load 3 and critical load 4 are affected the most by these changes and they are the most sensitive bus among others. The next most sensitive bus is the bus at critical load 6.

Powerworld does not have a built-in battery model for steady-state studies. Therefore, the battery is modeled in the Powerworld power flow as a generator that switches on or off at certain times. This option is possible with the help of time step simulation in Powerworld. The battery is placed at the two sensitive buses identified above, to evaluate the performance and

identify the improvements. The voltage at all the buses with batteries placed at the critical load-3 and critical load-6 buses is shown in Figure 4-18 and 4-19. The Figure 4-18 shows the bus voltage improvement at critical load-3 bus when the battery is placed at two locations identified. Figure 4-19 shows the bus voltage improvement at critical load-6 bus when a battery is placed at the two different locations.

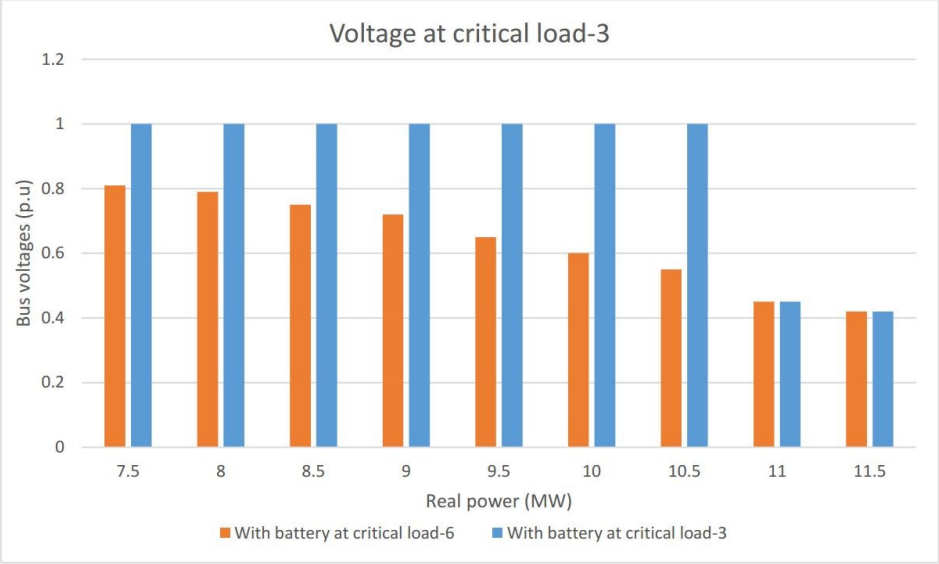

Figure 4-18 Bus voltage at critical load-3 with battery at two locations identified

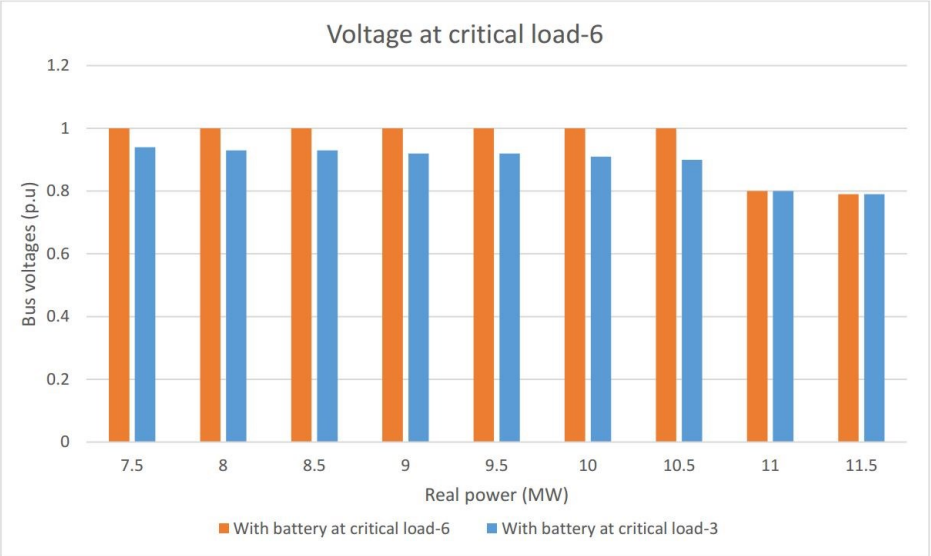

Figure 4-19 Bus voltage at critical load-6 with battery at two locations identified

Analyzing the comparison plots show that there is more improvement in the voltage at the two buses when the battery is placed at critical load-3 bus.

The line loading rating of all the lines is verified to identify the lines that are overloaded or are close to overload. In this study, the battery is placed at the two locations identified above and line-loading percentages are evaluated. The percent line loading did not vary much as the loads were changed in steps of 0.5 MW. Figure 4-20 shows the percentage line loading violations (the lines exceeding 100 % loading) when the all the critical loads are at very high values. This gives a comparison of line loading characteristics. The feeder lines supplying critical load-6 are affected the most by the heavy load conditions. Placing the battery at the bus for critical load-6 will reduce the line loading percentages on the most overloaded lines. However, there is not a significant improvement in this case as the loads were varied in steps of 0.5 MW.

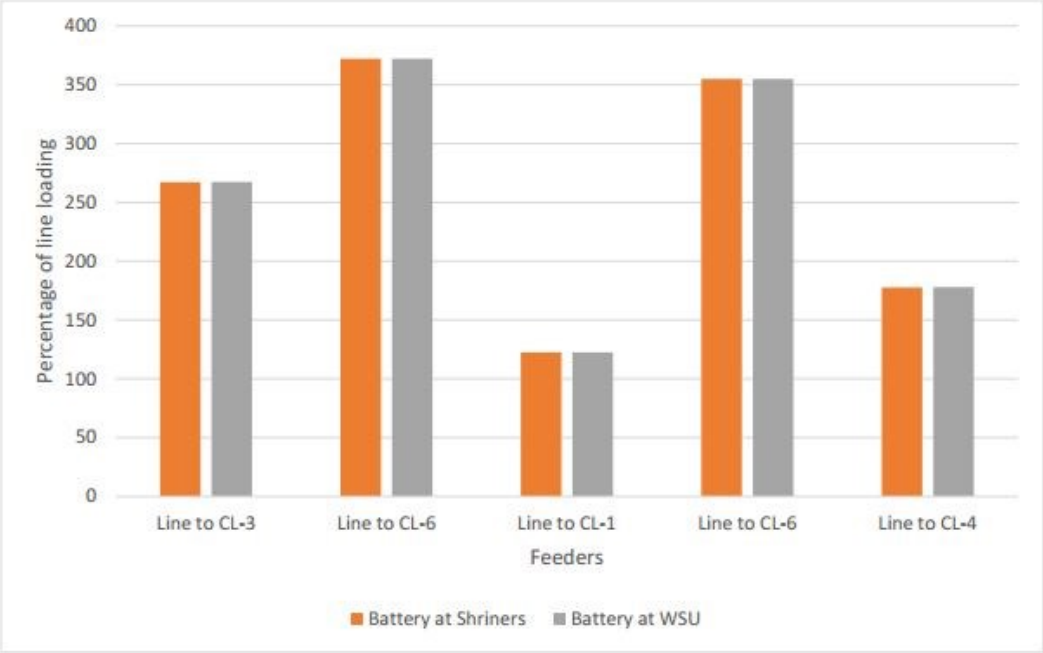

Figure 4-20 Line loading percentage violations with high load

4.5 STEADY-STATE STABILITY ANALYSIS

Power system stability is the ability of an electric power system, for a given initial condition, to regain a state of operating equilibrium after being subjected to a physical disturbance, with most system variables bounded such that practically the entire system remains intact [63]. Though the stability of the system is a single phenomenon, for the ease of analysis it is classified based on types of studies such as steady-state stability analysis and transient stability analysis. However, there are many categories and subcategories of the power system stability as shown in Figure 4-21. Many disturbances can occur in a microgrid such as sudden changes in load, switching operations, reduction in generation, and faults. The microgrid should have the capability to withstand the disturbances and operate in a stable fashion. Therefore, steady-state stability analysis of the system is an important aspect while planning a microgrid.

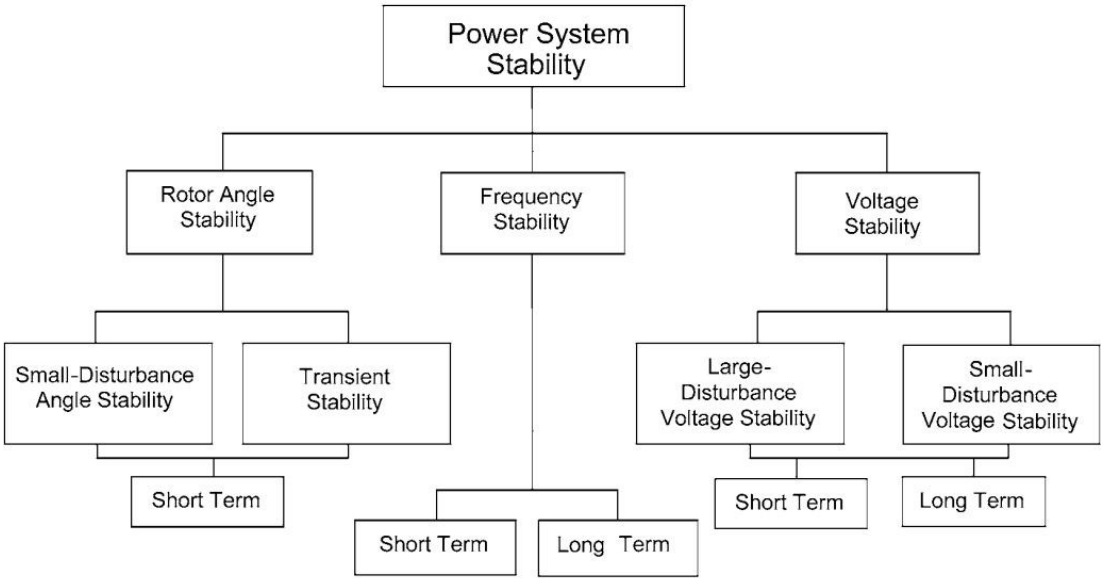

Figure 4-21 Classification of power system stability [63]

The power flow simulation is used as a steady-state analysis tool; it determines the quasi-steady-state operating condition for a power system. The assumption here is the sum of

total load and losses in the system is always equal to the total generation. The generation mismatch is usually made up at the slack bus. According to the microgrid start up plan, the microgrid transmission system is energized under no load conditions. There is a chance of rise in the voltage at substation buses under the no-load condition due to shunt capacitance effect of transmission lines. If there is an overvoltage, shunt reactors are needed to bring the voltage down. In order to determine this condition, simulation is performed under the no-load condition. The bus voltages remain close to one per unit if the capacitor banks are disconnected from the system. Removing the shunt capacitors under the no-load condition will eliminate the need for shunt reactors. Table 4-3 summarizes the simulation results for this case. Simulation is also performed when the high summer loading values entered in the model. The voltages at four different substations are recorded under no load condition and the full load condition. The full load condition here means the generators are supplying their maximum capability while supplying five of the critical loads. Shunt cap-1 is placed at critical load-5; shunt cap-2 is placed at substation-2, shunt cap-3 is placed at critical load-2, and shunt cap-4 is placed at critical load-3.

Table 4-3 Steady-state voltages under no load and full load condition

Bus	Bus Voltages		Capacitor	Shunt Capacitor	
	No Load Condition (Without capacitors)	Full Load condition (With capacitors)		No Load Condition	Full Load condition
Substation-1	1.02 pu	0.99 pu	Shunt Cap-1	0 MVAR	0.3 MVAR
Substation-2	1.02 pu	0.99 pu	Shunt Cap-2	0 MVAR	1.5 MVAR
Substation-3	1.02 pu	0.99 pu	Shunt Cap-3	0 MVAR	0.9 MVAR
Substation-4	1.02 pu	0.99 pu	Shunt Cap-4	0 MVAR	1.2 MVAR

The bus voltages at four substations are close to one per unit when the capacitor banks are switched off and by switching on the appropriate capacitor banks as shown in Table 4-3 at four locations, the voltage is brought back to 0.99 per unit under full load condition.

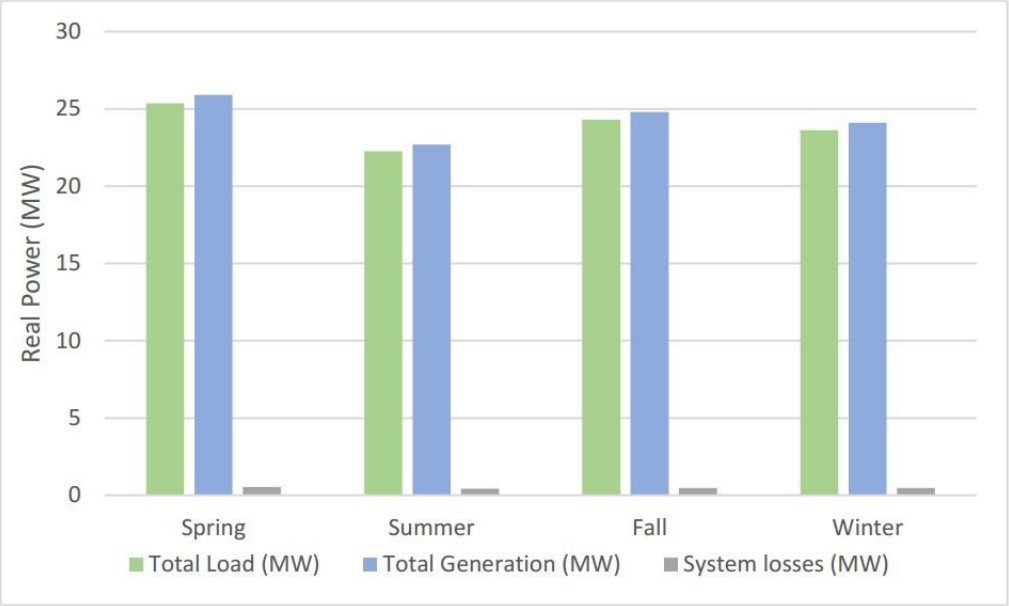

Figure 4-22 Comparison of generation and load at peak days in four seasons

Power flow analysis is performed while considering different seasons high and low demand values. The system is stable under the steady-state condition when the critical loads are supplied up to hydro resource capabilities. The total generation in the model is the sum of the total critical load and system losses in the same four different conditions, observed in the Figure 4-22. Figure 4-23 shows the bus voltages at four substations in four different seasons. The voltage is maintained well within the limits as per the ANSI/NEMA C84.1-2011 standards [39]. Table 4-4 shows the summary of the simulation results for four different seasons each with high and low demand values. There is a variation in the number of critical loads supplied in different seasons based on the available generation resource. The voltages are maintained within the limits by varying the capacitors accordingly. Table 4-5 shows the capacitor ratings under the

different conditions. The capacitor banks are assumed as available in steps of 300kVAr according to the sponsoring utility standard. Section-4.8.1 discusses the capacitor sizing and placing them in more detail.

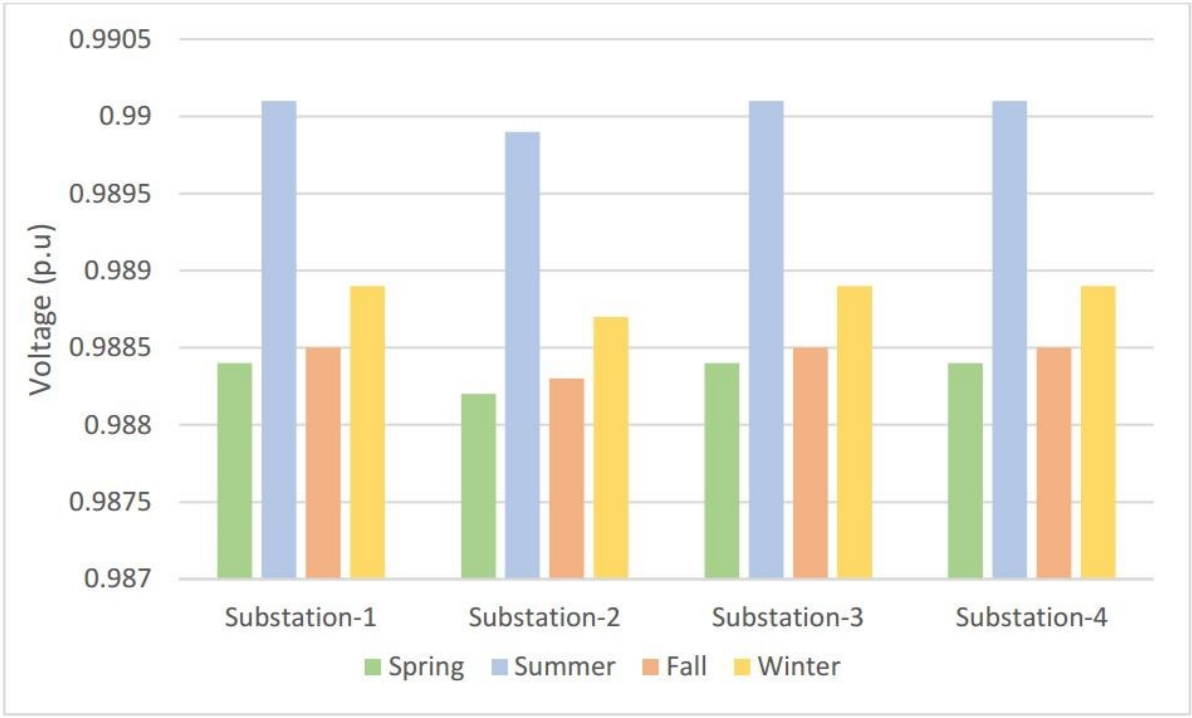

Figure 4-23 Comparison of generation and load in four seasons

Table 4-4 Steady-state power-flow analysis results for four seasons

Season	Demand	No of critical loads served	Total Load (MW)	Total Generation (MW)	System losses (MW)	Voltage (p.u)			
						Substation - 1	Substation - 2	Substation - 3	Substation - 4
Spring	High	6	25.37	25.9	0.53	0.988	0.988	0.988	0.988
	Low	4	5.94	6.09	0.08	1.001	1.001	1.001	1.001
Summer	High	5	22.27	22.7	0.42	0.99	0.99	0.99	0.99
	Low	4	4.06	4.09	0.03	1.002	1.002	1.002	1.002
Fall	High	6	24.31	24.8	0.48	0.989	0.988	0.989	0.989
	Low	4	3.57	3.61	0.04	1.002	1.002	1.002	1.002
Winter	High	6	23.62	24.1	0.48	0.989	0.989	0.989	0.989
	Low	6	11.9	11.928	0.1	0.998	0.998	0.998	0.998

Table 4-5 Steady-state power-flow analysis results including capacitor values for four different seasons

Season	Demand	Cap1 MVAR	Cap2 MVAR	Cap3 MVAR	Cap4 MVAR
Spring	High	0.6	1.5	0.6	0.9
	Low	0	0	0	0
Summer	High	0.3	1.5	0.9	1.2
	Low	0	0	0	0
Fall	High	0.3	1.5	0.3	0.3
	Low	0	0	0	0
Winter	High	0.3	0	0	0
	Low	0	0	0	0

4.6 TRANSIENT STABILITY ANALYSIS

Transient stability is the ability of the power system to maintain synchronism when subjected to a severe transient disturbance, such as a fault on transmission facilities, loss of generation, or loss or insertion of a large load. The system response to such disturbances involve large excursions of generator rotor angles, power flows, bus voltages and other system variables [64]. The factors that influence transient stability are [64]:

a) How heavily the generators are loaded
b) The generator output during the fault or disturbance. This also depends on the fault location and type.
c) The fault clearing time
d) The post fault transmission system reactance
e) Generator reactance. Lower reactance increases peak power and reduces initial rotor angle
f) The generator inertia. The higher the inertia, the slower the rate of change in angle.

g) The generator internal voltage magnitude. This depends on field excitation.

The dynamic behavior in an electrical power system due to disturbances is a contribution of many different components. The electrical power system equipment can be classified into mechanical equipment and electrical equipment as shown in Figure 4-24. There is interdependency between them. The mechanical equipment requires a control system and communication infrastructure, which are electrical components. Moreover, the electro-mechanical components have many mechanical components interacting with electrical [65].

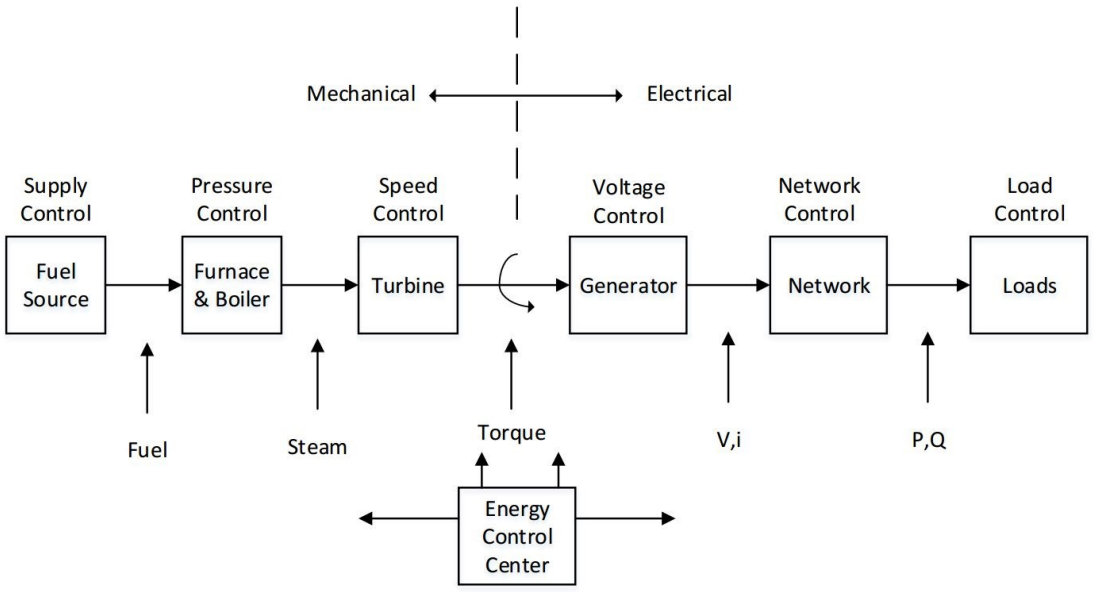

Figure 4-24 Electromechanical system in electrical power system [65]

The time scale response properties of power systems that defines the position of transient stability is in the range of 10 milliseconds to 100 seconds range as shown in the Figure 4-25 [65]. Interconnected power systems have guidelines of maintaining the stability in the system. The specifications that are particular to the western region of the U.S are defined in the WECC criteria TPL-001-WECC-CRT-2 [66]. This criterion is a combination of National Energy Regulator Committee (NERC) and Western Electricity Coordination Council (WECC)

requirements. This criterion discusses the acceptable ranges of voltage and frequency during a transient condition. Table 4-6 summarizes the criteria requirements.

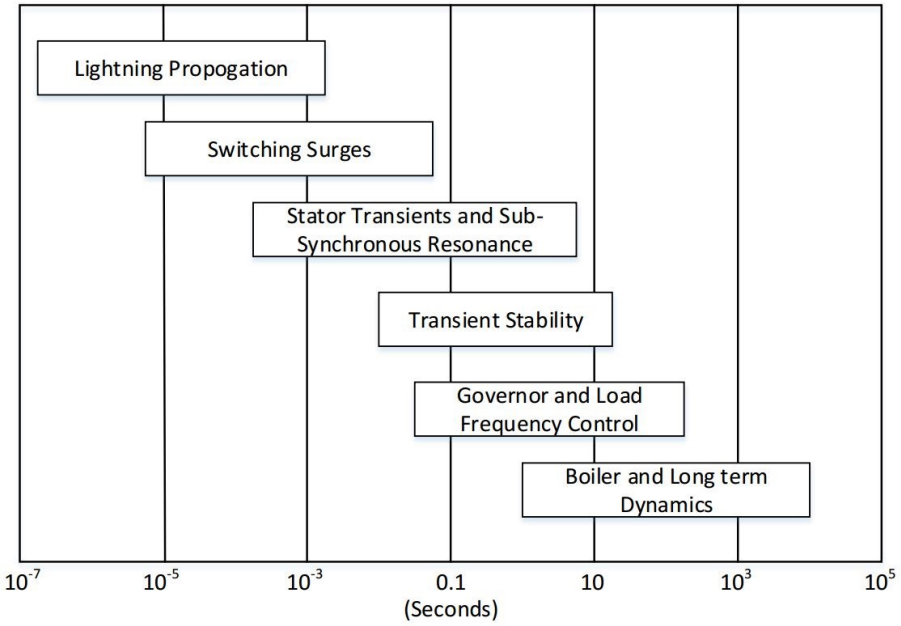

Figure 4-25 Phenomena time scales in electrical power systems [65]

Table 4-6 TPL-001-WECC-CRT-2 criteria guidelines [66]

NERC and WECC Categories	Outage Frequency Associated with the Performance Category (outage/year)	Transient Voltage Dip Standard	Minimum Transient Frequency Standard	Post Transient Voltage Deviation Standard (See Note 3)
A	Not Applicable	Nothing in addition to NERC.		
B	≥ 0.33	Not to exceed **25%** at load buses or **30%** at non-load buses. Not to exceed **20% for more than 20 cycles** at load buses.	Not below **59.6** Hz for 6 cycles or more at a load bus.	Not to exceed **5%** at any bus.
C	0.033 – 0.33	Not to exceed **30%** at any bus. Not to exceed **20% for more than 40 cycles** at load buses.	Not below **59.0** Hz for 6 cycles or more at a load bus.	Not to exceed **10%** at any bus.
D	< 0.033	Nothing in addition to NERC.		

The A, B, C, D categories in the first column represent the types of disturbances. Category A represents a case with all bulk electric system (BES) elements in service, which is the ideal condition. Category B represents a case in which there is loss of single bulk electric system (BES) element, it specifies a requirement for voltage dip to not to exceed 25% at load buses, 30% at no load buses, and no voltage drop of 20% for more than 20 cycles at any load bus. The frequency should not be below 59.6Hz for 6 cycles or more, and the post transient deviation should not be more than 5% at any load bus. Category C and D are for more severe faults, which can be interpreted in the same way. Figure 4-26 shows an example of applying standard for transient stability voltage response at a load bus. A fault occurred at time t=0 seconds then the voltage dropped near to zero, and the voltage recovers after the fault is cleared going through several oscillations due to rotor angles and power angles.

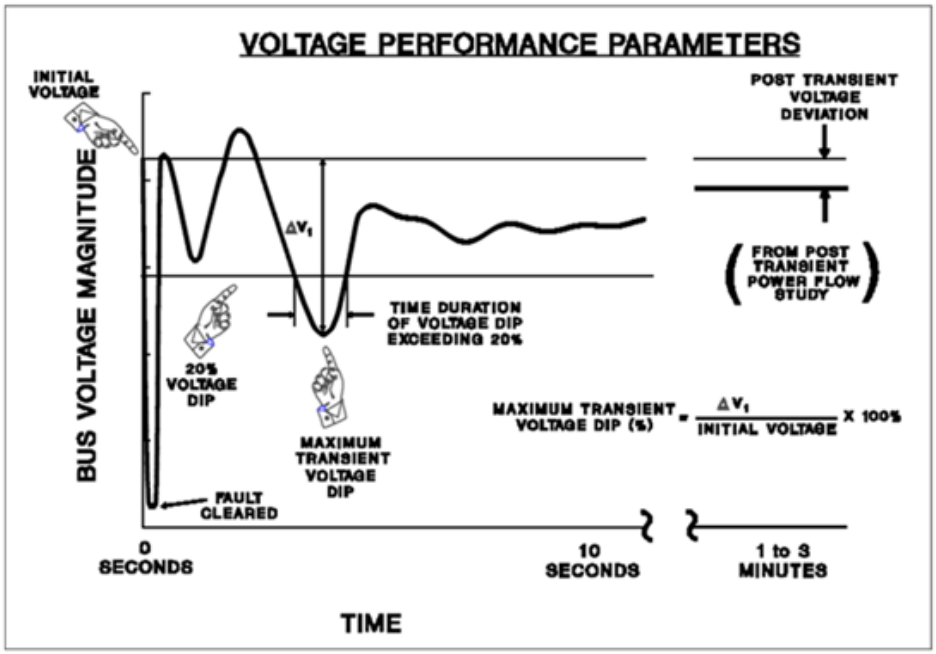

Figure 4-26 Transient voltage performance parameters [66]

These standards are defined for application to large bulk electric systems, which are interconnected systems. There are no similar standards defined specially for microgrids, yet. It

is assumed that the utility operating the microgrid will comply with these standards in the microgrid operation.

Transient stability analysis was performed on the microgrid model using Powerworld. The dynamics that are considered in this thesis are in the order of a few milliseconds to seconds. As discussed in section 3.3, dynamic machine models, exciter models, and governor models are included in the model to perform the transient stability study. The goal of this study is to verify how the generators behave during the startup of the microgrid, switching of loads, and fault conditions when the microgrid isolated from the main power grid. Powerworld offers many options to perform transient stability study by inserting actions like applying a fault, opening or closing an element. These actions can be applied to buses, lines, breakers, loads, generators, and transformers.

Figure 4-27 shows the frequency response of the microgrid model when critical load-6 is added after 2 cycles. The frequency dropped to 59.54 Hz at the instant the breaker closed and it attained a steady-state condition after 25 cycles at 59.94 Hz. In the transient stability study, simulations normally do not bring the frequency to nominal (60Hz). Instead, the AGC control in the generators will bring the system frequency to 60Hz, which is normally in the order of minutes. Figure 4-28 shows the generators response for the same transient condition. Generator-1 and generator-2 responded to the change in the load and increased output to new operating points of 10.2 MW and 10.8 MW respectively. The photovoltaic cells are modeled as supplying constant power in this case; the transient models for photovoltaic cells are not included in this study. Therefore, the output power from photovoltaic cells remains the same even after the load addition. A similar response can be observed in terms of reactive power outputs of the generators. Figure 4-29 shows the voltage profiles at all of the buses in the system, in response

to the transient condition; the voltage dropped a little and attained a steady-state condition with new values within 6 cycles.

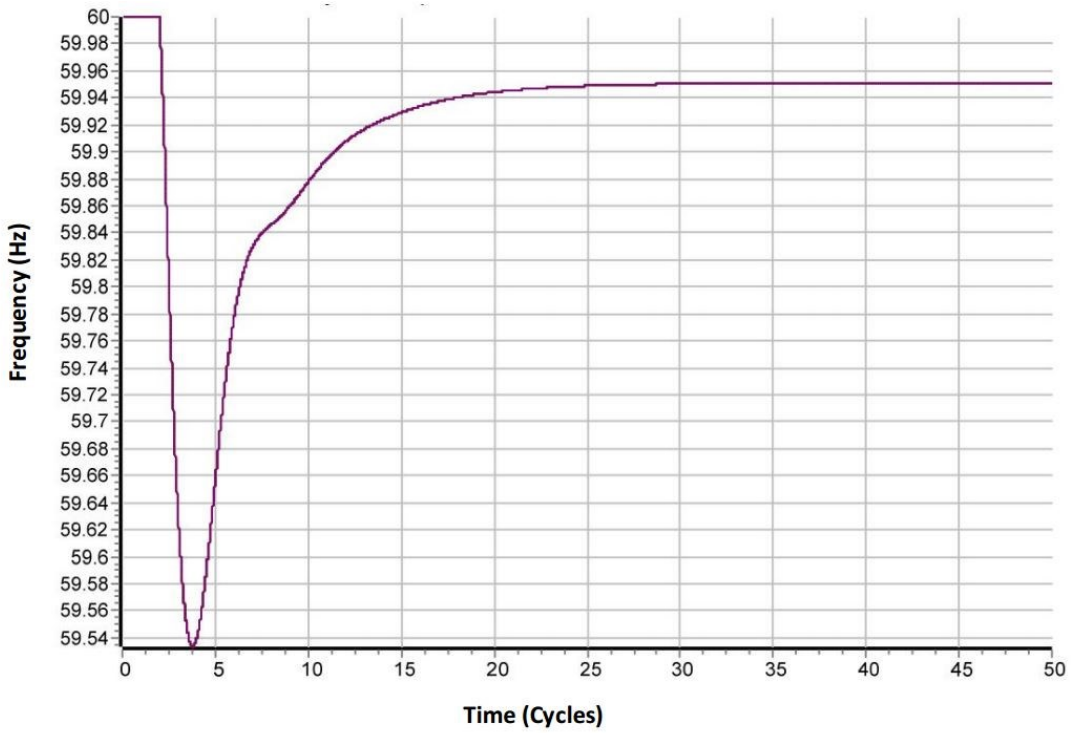

Figure 4-27 Frequency response to transient load pickup condition

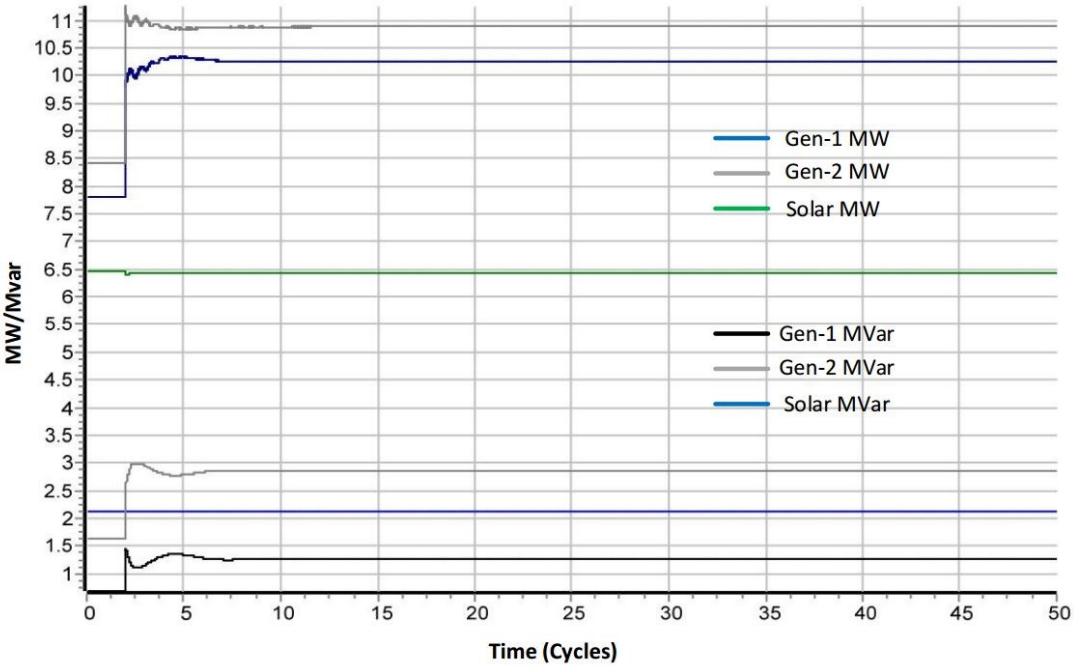

Figure 4-28 Generators power output response for transient condition

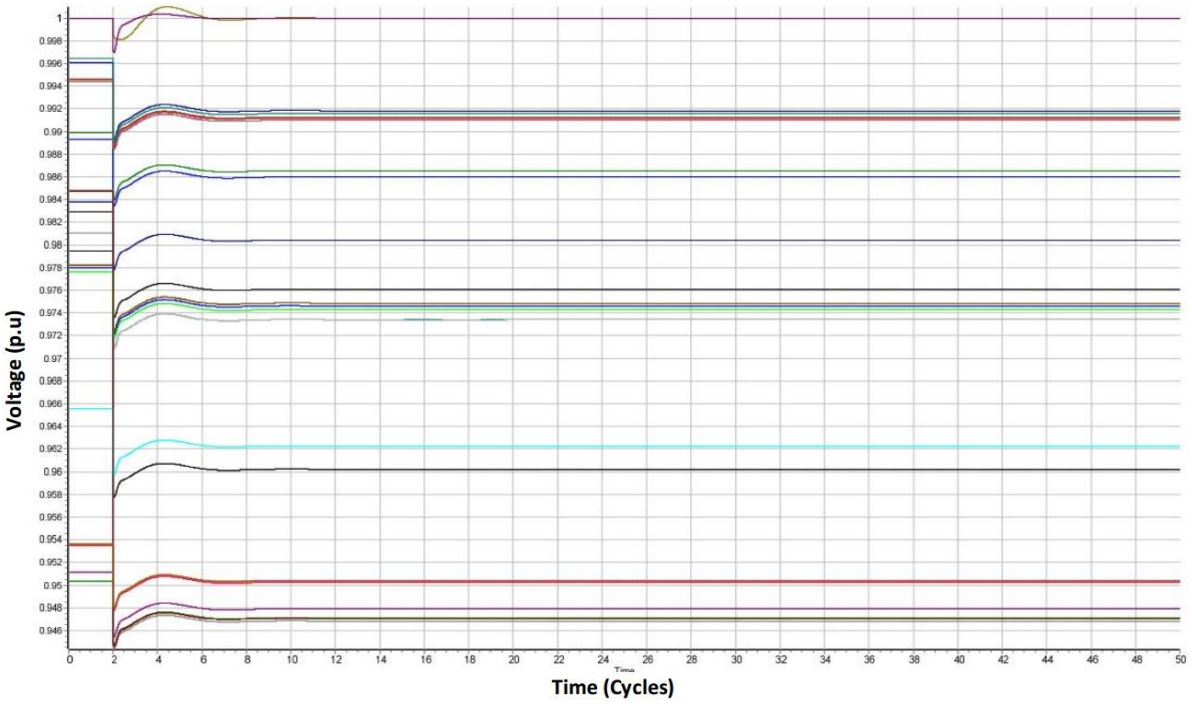

Figure 4-29 Voltage response for transient condition

Table 4-7 shows the summary of the transient stability cases studied on the microgrid model; these cases are classified as microgrid start cases, microgrid stop cases, load changes, generator switching, battery switching, and fault conditions. The microgrid model attained a new stable state after applying the transient condition in all of the cases except for a fault that was not cleared. In the fault study cases, the microgrid model attains a steady state condition if it has the ability to clear the faults on it. The time taken to reach the new steady state condition that is expressed in number of cycles, and generators final steady state values are shown in the Table 4-7. The response of the machines to these transient conditions can be improved by tuning the governor and exciter controls of the generator further. As the Generator-1 actual parameters are not available now, approximations of machine model that are more reasonable can be made to improve the overall response. Additional study is needed to identify the system response, which is beyond the scope of this thesis.

Table 4-7 Summary of Transient stability study results

Category	Case	Condition	Critical Load	Transient case	Stable	No of cycles to stable Frequency	Initial Frequency	Steady state Frequency	No of cycles to stable voltage	Gen-1 (MW)	Gen-2 (MW)	Solar (MW)
Microgrid start up Cases (loads are sequentially added one after the other)	1	Addition of critical load	Critical load-1	Open to close	Yes	28	60	59.96	4	0	1.8	0
	2	Addition of critical load	Critical load-2	Open to close	Yes	28	60	59.85	5	0	9.5	0
	3	Addition of critical load	Critical load-3	Open to close	Yes	26	60	59.96	5	9.6	4.5	0
	4	Addition of critical load	Critical load-4	Open to close	Yes	25	60	59.99	1	7.8	6.6	0
	5	Addition of critical load	Critical load-5	Open to close	Yes	25	60	59.94	6	11.4	4.2	6.45
	6	Addition of critical load	Critical load-6	Open to close	Yes	26	60	59.95	6	10.1	10.8	6.45
Microgrid Stop Cases (loads are sequential-ly removed one after the other)	7	Removal of critical load	Critical load-6	Close to Open	Yes	27	60	60.05	5	5	11.25	6.45
	8	Removal of critical load	Critical load-5	Close to Open	Yes	30	60	60.01	2	7.1	7.6	0
	9	Removal of critical load	Critical load-4	Close to Open	Yes	25	60	60	1	6.8	7.55	0
	10	Removal of critical load	Critical load-3	Close to Open	Yes	26	60	60.04	6	5.7	4.6	0
	11	Removal of critical load	Critical load-2	Close to Open	Yes	30	60	60.015	1	0	1.8	0
	12	Removal of critical load	Critical load-1	Close to Open	Yes	24	60	60.04	4	0	0	0
Load changes	13	Removal of critical load	Critical load-2	Close to Open	Yes	26	60	60.08	5	3.6	4.1	6.45
	14	Addition of critical load	Critical load-2	Open to close	Yes	25	60	59.92	6	11.4	3.8	6.45

Battery	15	Addition of battery	Critical load-6	Open to close	Yes	20	60	60	0	NA	NA	NA
	16	Removal of battery	Critical load-6	Close to Open	Yes	25	60	59.98	4	NA	NA	NA
	17	Addition of battery	Critical load-3	Open to close	Yes	22	60	60	0	NA	NA	NA
	18	Removal of battery	Critical load-3	Close to Open	Yes	25	60	59.98	4	NA	NA	NA
Generator switching	19	Addition of generator	Generator-2	Open to close	Yes	21	60	60	1	NA	NA	NA
	20	Removal of generator	Generator-2	Close to Open	Yes	30	60	59.85	8	NA	NA	NA
	21	Addition of generator	Generator-1	Open to close	Yes	25	60	59.85	6	NA	NA	NA
	22	Removal of generator	Generator-1	Close to Open	Yes	22	60	60	0	NA	NA	NA
	23	Removal of generator	Solar	Close to Open	Yes	11	60	60	0	NA	NA	NA
	24	Addition of generator	Solar	Open to close	Yes	26	60	59.94	4	NA	NA	NA
Fault on Transmission line	25	Fault not cleared	Line-Sub1 to Sub2	Apply	No	NA	60	NA	NA	NA	NA	NA
	26	Fault cleared in 4 cycles	Line-Sub1 to Sub2	Apply and Clear	Yes	20	60	60	6	NA	NA	NA
	27	Fault cleared in 18 cycles	Line-Sub1 to Sub2	Apply and Clear	Yes	18	60	60	6	NA	NA	NA
Fault on Distribution line	28	Fault cleared in 18 cycles	Line to Critical load-2	Apply and Clear	Yes	22	60	60	6	NA	NA	NA

4.7 AUX FILE GENERATION

Powerworld has a feature to import the data to/ from data sources other than power flow models into the Powerworld Simulator. This is implemented using auxiliary (aux) files. The aux files are text files that exchange data and execute batch script commands. These files are called data auxiliary files in the Powerworld simulator and typically have the file extension .AUX. The script language and auxiliary data formats are incorporated together [67]. Auxiliary data formats are used in this model to load the model parameters. The format is shown below

```
SCRIPT ScriptName1
{
script_statement_1;

script_statement_n;
}
DATA DataName1 (object_type, [list_of_fields], file_type_specifier, create_if_not_found)
{
data_list_1

data_list_n
}
```

The microgrid model has many different load and generation profiles available across different seasons in a year. The load and generation profiles are averaged over three years (2013-2015) and the high and low values in all the four seasons are identified. In the same way, averaged 24-hour profiles have 96 values of load generation, which are comprised of 24 values over 24hours in each season. It will be a tedious task to enter all these values individually to analyze different cases. Instead, these values are entered in data auxiliary files and loaded into Powerworld model. Generating 96 + 8 = 104 auxiliary files is also a difficult task. This process is automated with the help of a JAVA program (Appendix-C) that generates the auxiliary files by fetching the data loaded into CSV files. The CSV files are used to organize the forecast

information data; the JAVA program loads this data and inserts it into auxiliary files. This makes it easier to study different cases. A sample auxiliary file is shown in the appendix-A.

4.8 TIME STEP SIMULATION

The load and generation outputs of the microgrid are not constant; they vary every second of the year. It is difficult to manually enter all the different values and run power flow solutions. To address this issue, Powerworld has a time step simulation. The time step simulation in Powerworld allows the user to specify operating conditions and obtain power flow solutions for a set of points in time. It is very useful to assess how power system quantities vary hour by hour or by intervals down to one second due to changes in load or generation, and transmission line status. The time step simulation is further useful for optimizing capacitor sizes, modeling the battery, and developing contour diagrams based on voltage magnitude or angle.

The averaged profiles of load and generation are divided into four representative days, one for each of four seasons in a year. This data is modified according to the forecast study performed in Section 4.2 that determined how many loads could be supplied in each season along with capacitor bank values, and transformer tap positions. The data is then loaded into auxiliary files according to the process described in Section- 4.7. These auxiliary files are loaded into the time step simulation.

4.8.1 Capacitor Sizing and Placement

The time step simulation is helpful to determine which bus voltages are very low in different seasons. This helps in placing the capacitors at those buses to improve the system voltage profile. The simulation is performed based on the forecast study as discussed earlier.

Figure 4-30 shows the time-step simulation results, which provide the voltage profile at all buses in the microgrid. The abscissa contains dates that are only for the purpose of time step simulation and are not real; the seasons are shown separately. The ordinates show the bus voltage in per unit.

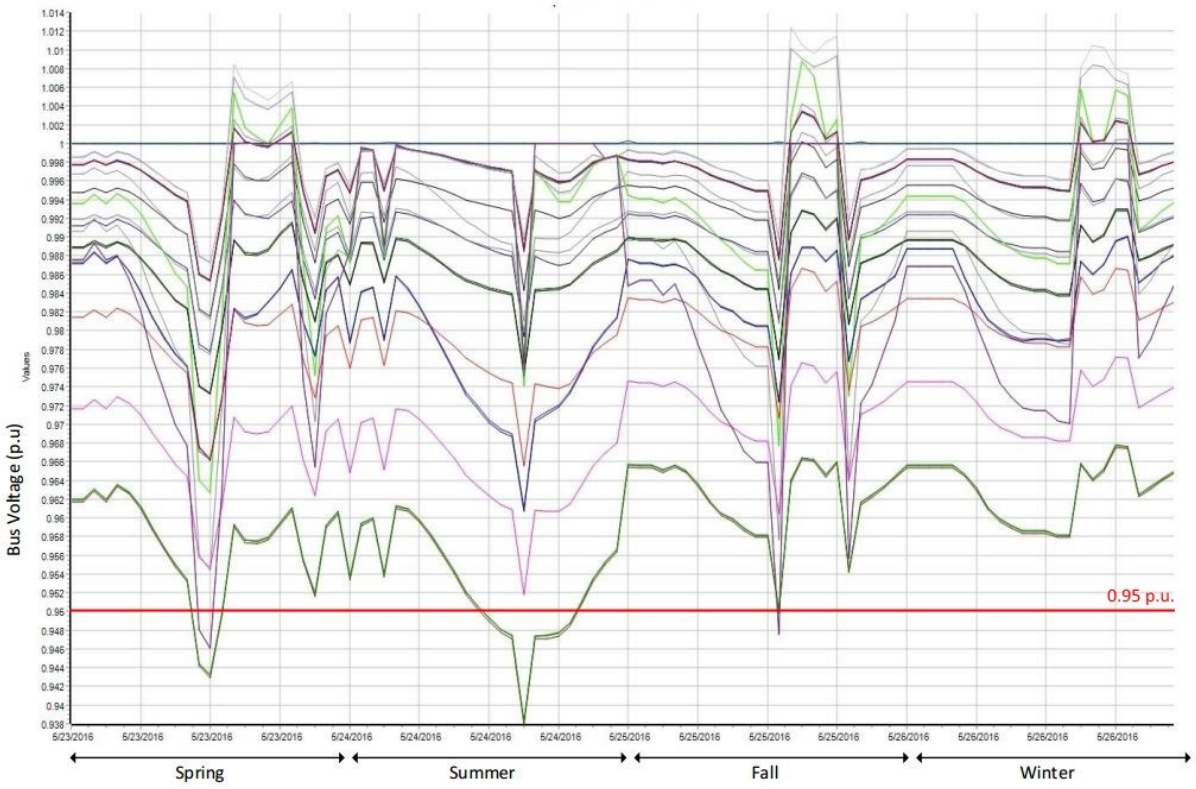

Figure 4-30 Bus voltages at all the buses without capacitors

The bus voltage magnitudes at some buses are low without the capacitor banks in all the seasons, particularly in spring and summer, the voltage at critical load-3 falls below the lower threshold of 0.95 per unit. In order to avoid these poor voltage profiles, the capacitors are sized performing several simulations. The capacitors are placed at the buses which are mostly affected by the under voltages. The capacitors are available in steps of 300kVar according to the utility sponsor's standard. Table 4-8 shows the four capacitors identified and the locations where they are placed. Figure 4-31 shows the results of the time step simulation performed after

placing these capacitors. The voltage profile at all the buses improved in four different seasons after placing the capacitors.

Table 4-8 Capacitor sizes and their locations in different seasons

Season	**MVAR**			
	Shunt cap-1	**Shunt cap-2**	**Shunt cap-3**	**Shunt cap-4**
Spring	1.5	0.6	0.6	0.9
Summer	1.5	0.3	0.9	1.2
Fall	1.5	0.3	0.3	0.3
Winter	0	0.3	0	0
Location	Critical load-6	Substation-2	Critical load-2	Critical load-3

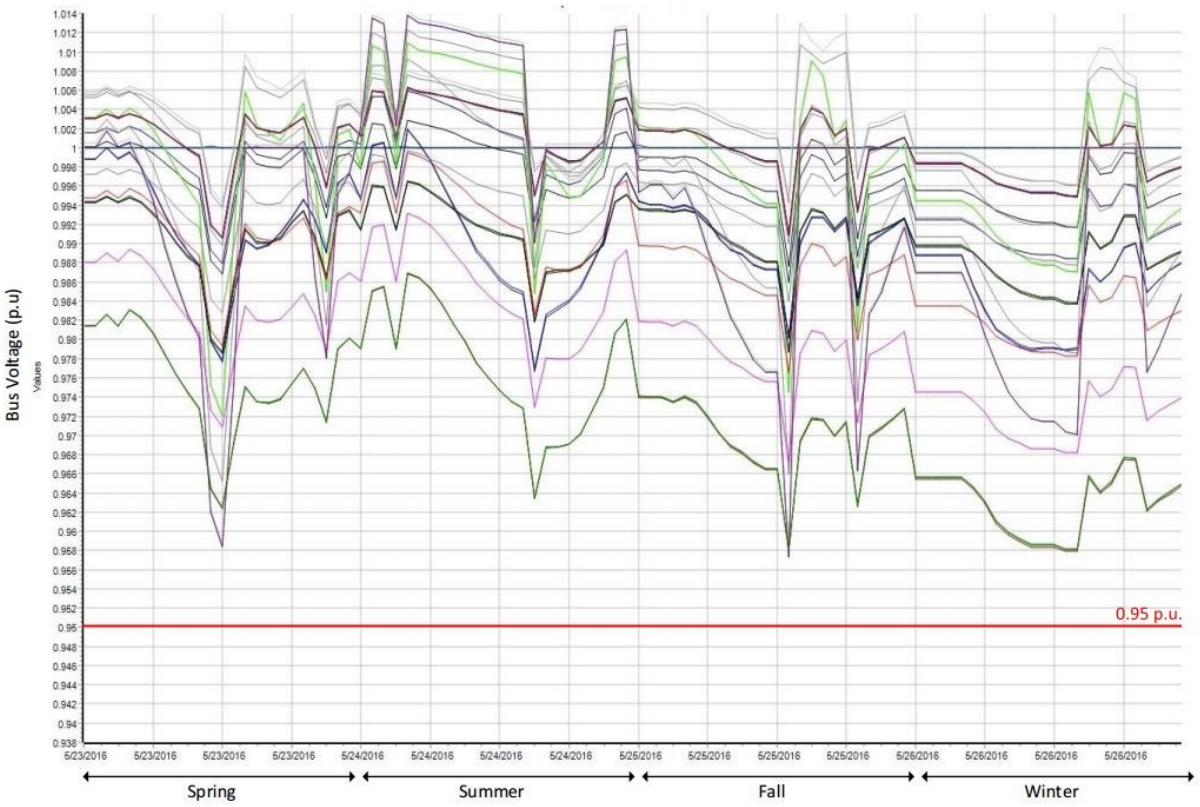

Figure 4-31 Bus voltage magnitudes at all the buses with capacitors added

The capacitors are sized according to worst-case need; they can be switched as needed each hour as well. By switching in that fashion, the spikes in the plot can be avoided.

4.8.2 Transformer Taps

Several of the transformers in the system contain tap changers with the tap positions set as discussed in Section 3.3.3. A separate study is performed to identify how the capacitor sizes can be reduced while using the Load Tap Changer (LTC) of the transformers. Table 4-9 shows the new capacitor bank sizes and the transformer tap ratios of the transformers 1T2, 1T2 at sub-1 and 3T1, 3T2 at sub-3.

Table 4-9 Capacitor sizes, tap ratios and their locations in different seasons

Season	**MVAR**				Tap ratios		
	Shunt cap-1	**Shunt cap-2**	**Shunt cap-3**	**Shunt cap-4**	**1T1 & 1T2**	**3T1**	**3T2**
Spring	0	0	0	1.2	0.97489	0.97676	0.97482
Summer	0	0	0	1.2	0.97489	0.97676	0.97482
Fall	0	0	0	1.2	0.97489	0.97676	0.97482
Winter	0	0	0	1.2	0.97489	0.97676	0.97482
Location	Critical load-6	Substation-2	Critical load-2	Critical load-3	Substation -1	Substation -3	Substation -3

Figure 4-32 shows the voltage profile at all buses in four different seasons. By varying the tap positions of the transformers, the capacitor banks can be sized down which leads to potential savings in terms of cost of installation. However, there are pros and cons by using capacitors and LTC transformers. The LTC's provide better voltage control, flexibility, and cost saving in terms of total lifecycle cost. However, they need proper maintenance, probability of failure is higher, and now many utilities prefer not to switch LTCs very often these days. The capacitors have lower life expectancy, which adds to the total life costs, but they are flexible and easily placed at the load centers when compared with LTCs. It is the utility's decision to choose where to use LTCs for active voltage regulation or install cap banks. Figure 4-33 shows the time-step simulation results of bus voltages at all the buses when the tap changers are used

alone to improve the voltage profile. The bus voltages are within tolerances except for the buses at critical load-3 where the capacitor was placed in other case to improve voltage profile.

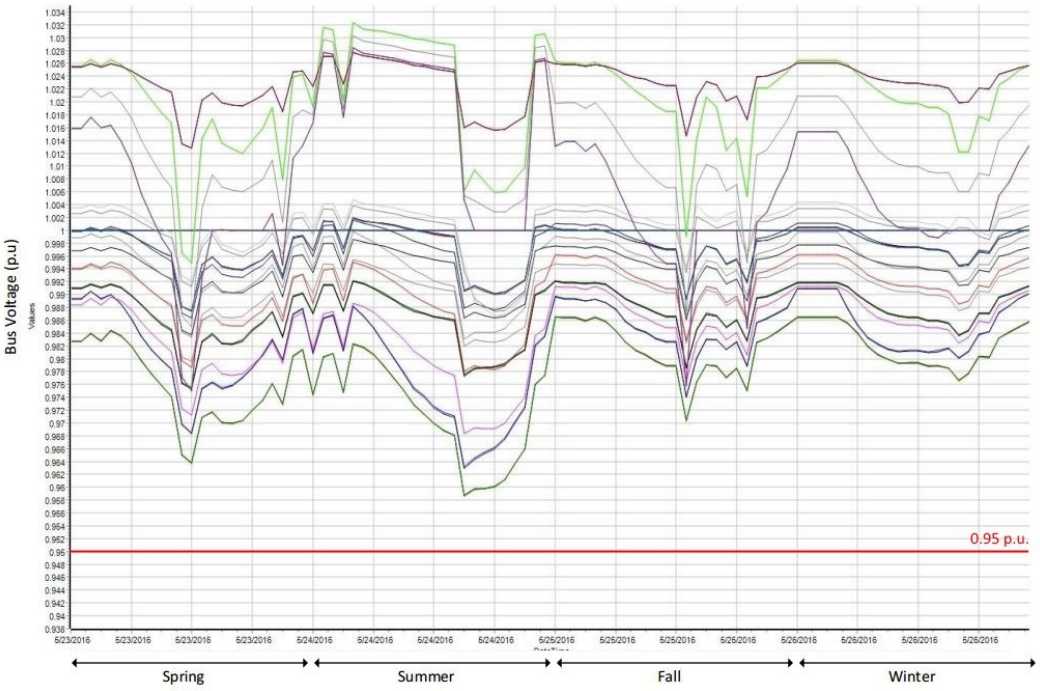

Figure 4-32 Bus voltage magnitudes at all the buses with capacitors and LTCs

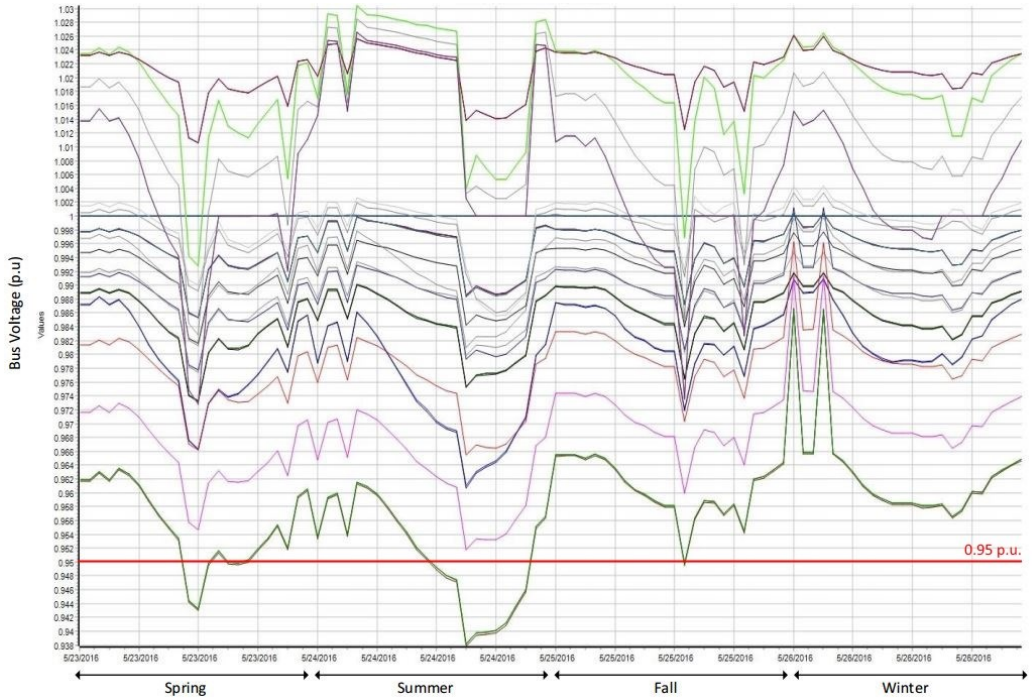

Figure 4-33 Bus voltage magnitudes at all the buses with LTCs and no caps

4.8.3 Line Limit Monitoring

The transmission and distribution lines have limits based on the physical features of the conductors; these limits vary according to weather conditions as well. Therefore, there are different line limits in different seasons. The line limits are configured in the model according to the limits mentioned in Section 3.3.1. The time step simulation is performed to identify the lines that are overloaded at times over a year. Figure 4-34 shows the plot in which the ordinate represents the percentage of line loading for all the different conductors in the model and abscissa represents the different seasons. This plot is simulated when there are no capacitors or LTC used in the model. A few lines are overloaded in all the seasons. The lines that are overloaded are the distribution lines supplying the critical load-6 from both substation-1 and 3.

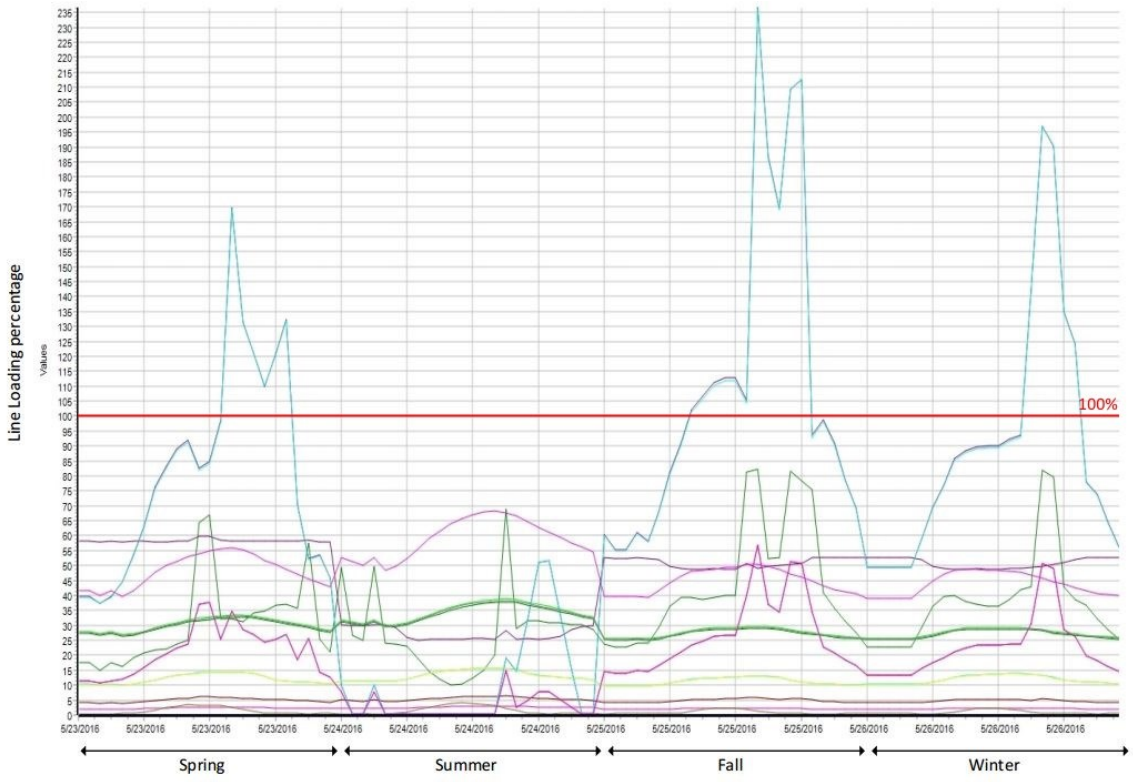

Figure 4-34 Line loading percentages at all the buses without capacitors and LTCs

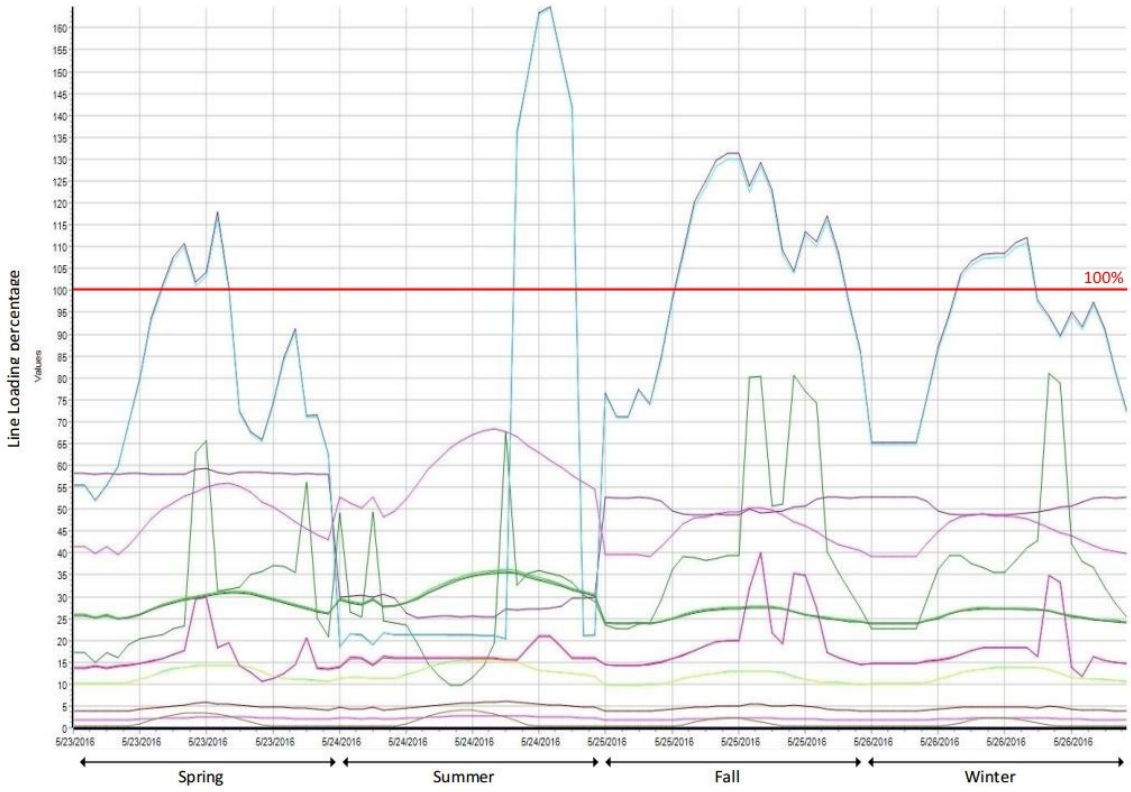

Figure 4-35 Line loading percentages at all the buses with capacitors and LTCs

The line loading percentages are next simulated when the capacitors and LTC's are properly sized. It is observed in Figure 4-35 that the percentage of loading is reduced when the capacitors and LTCs are used. The two distribution lines mentioned earlier are overloaded even after the caps and LTCs were included. The lines need to be reconductored in order to have them within the limits. The reason for the violation is that these conductors are normally open under ideal grid connected operating conditions. They are not designed to handle higher currents that would flow in microgrid operation.

4.8.4 Battery Impact Study

The location for battery in the microgrid was identified in section 4.4. Time step simulation is used to compare the voltage magnitude improvements by placing the battery at the two locations identified. Figure 4-36 and Figure 4-37 show the voltages profiles at all the

buses when the battery is placed at critical load-3 and critical load-6 respectively. There is a reasonable improvement in voltage profile in all the seasons, when the battery is placed at critical load-3. The battery supplies both real and reactive power while improving the voltage.

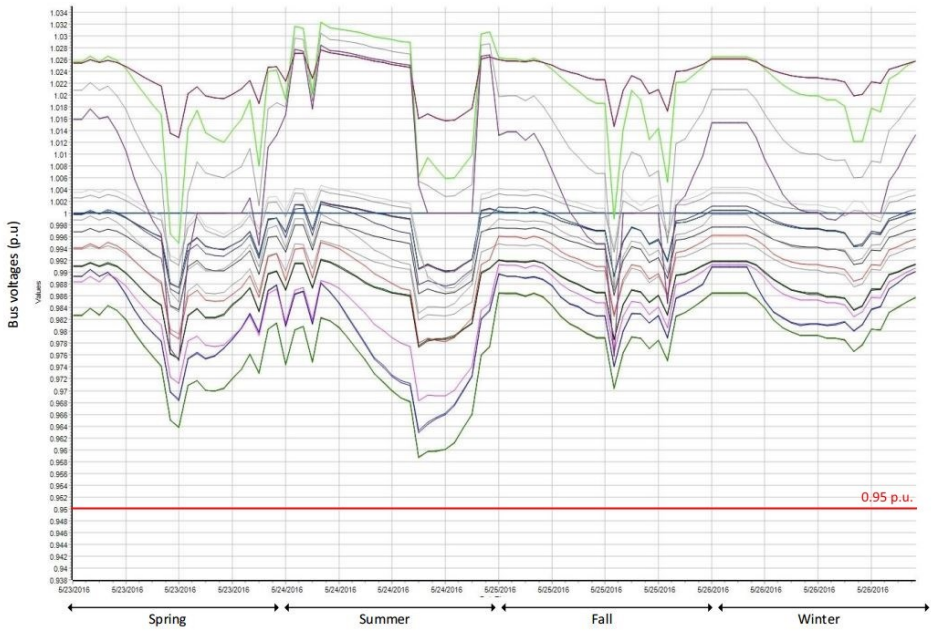

Figure 4-36 Bus voltages at all the buses when battery placed at critical load-6

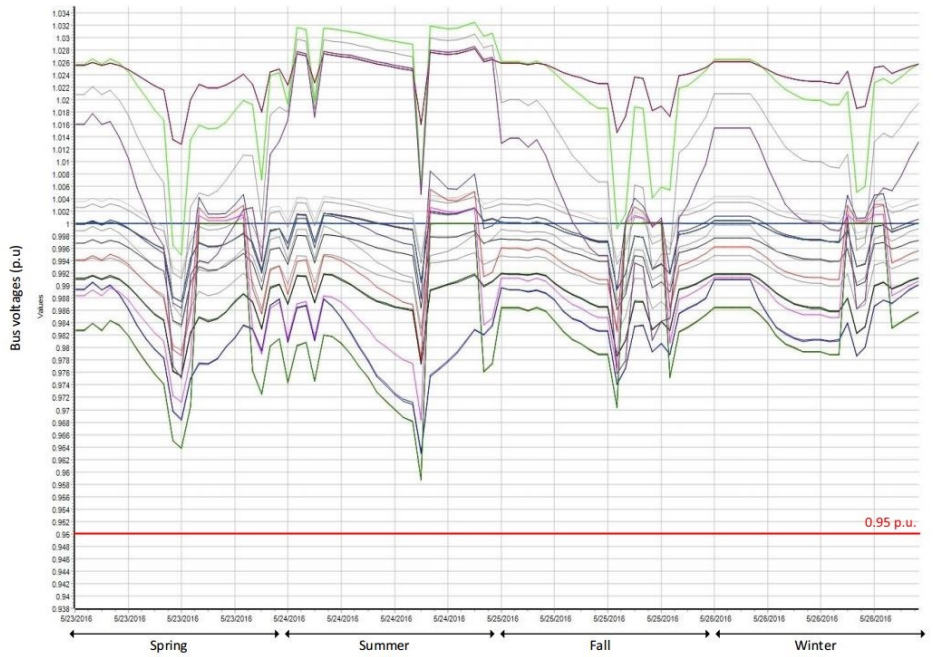

Figure 4-37 Bus voltages at all the buses when battery placed at critical load-3

4.8.5 Generation and Load Profile with Time Step Simulation

Figure 4-38 and Figure 4-39 show the real and reactive power output profile of the hydro generators, the PV generation, and the battery on representative days over four different seasons in the time step simulation. Generator-2 acts as slack bus and operates in the isochronous mode responding to the load fluctuations. The plot shows several sharp peaks supplying the fluctuations. Generator-1 is operated in droop mode, supplying fixed amount of power by varying its speed according to a droop characteristics. The solar energy is only available during the day and peaks in early afternoon. The battery switches in and out to balance load, and it is operated and controlled according to the forecast study.

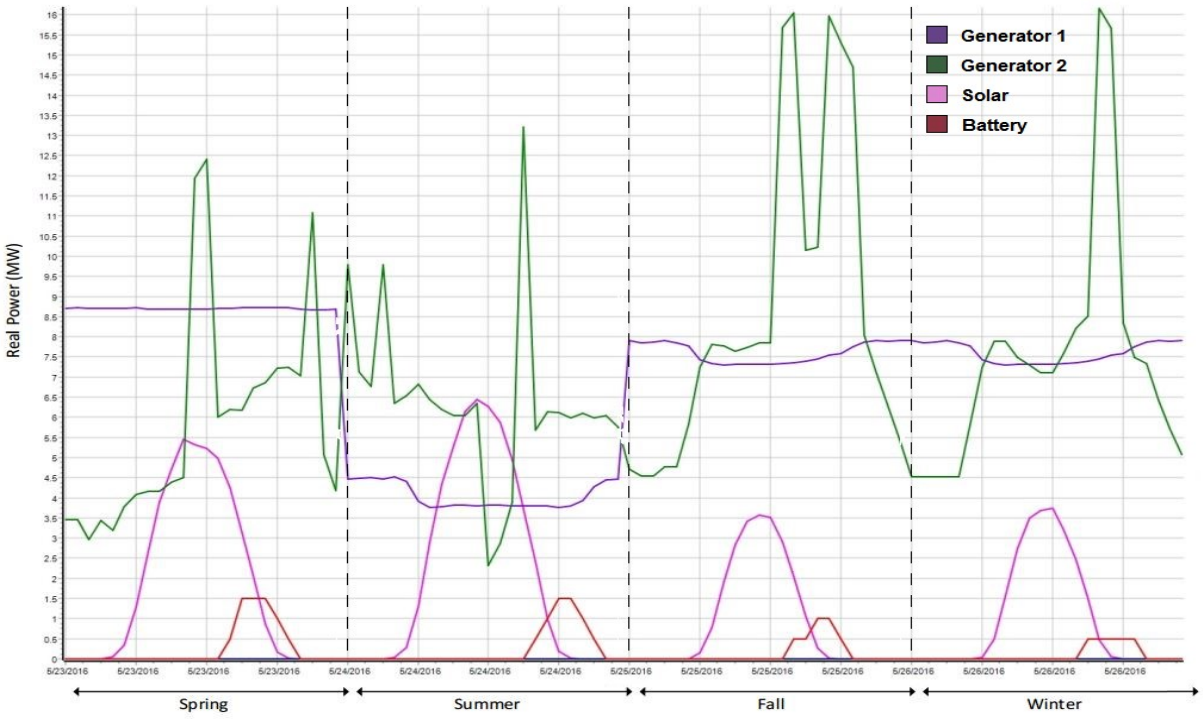

Figure 4-38 Real power output profile of all the generators along with the battery over single day in each of four seasons

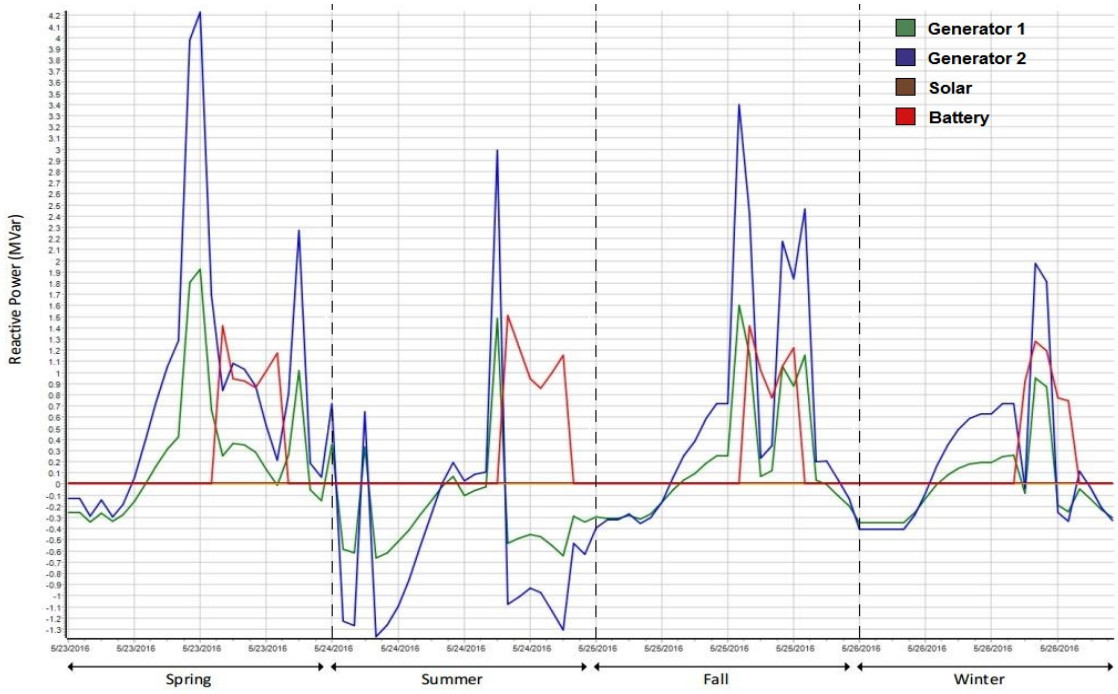

Figure 4-39 Reactive power output profile of all the generators along with the battery over single day in each of four seasons

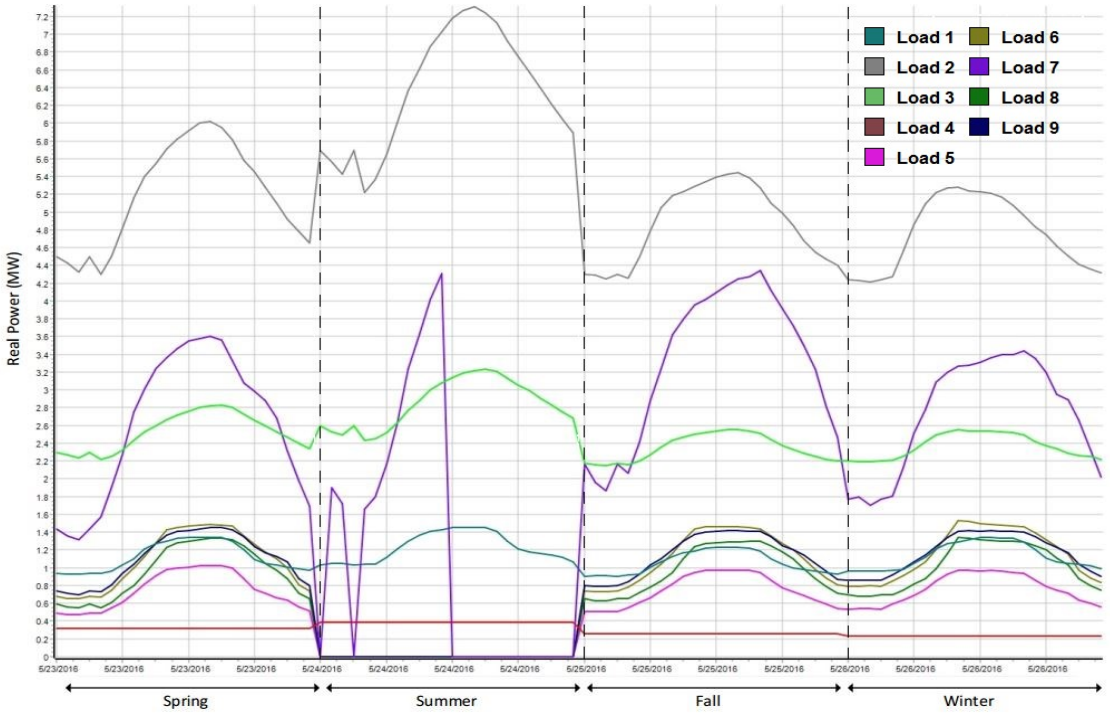

Figure 4-40 Real power consumption of all the critical loads over single day in each of four seasons

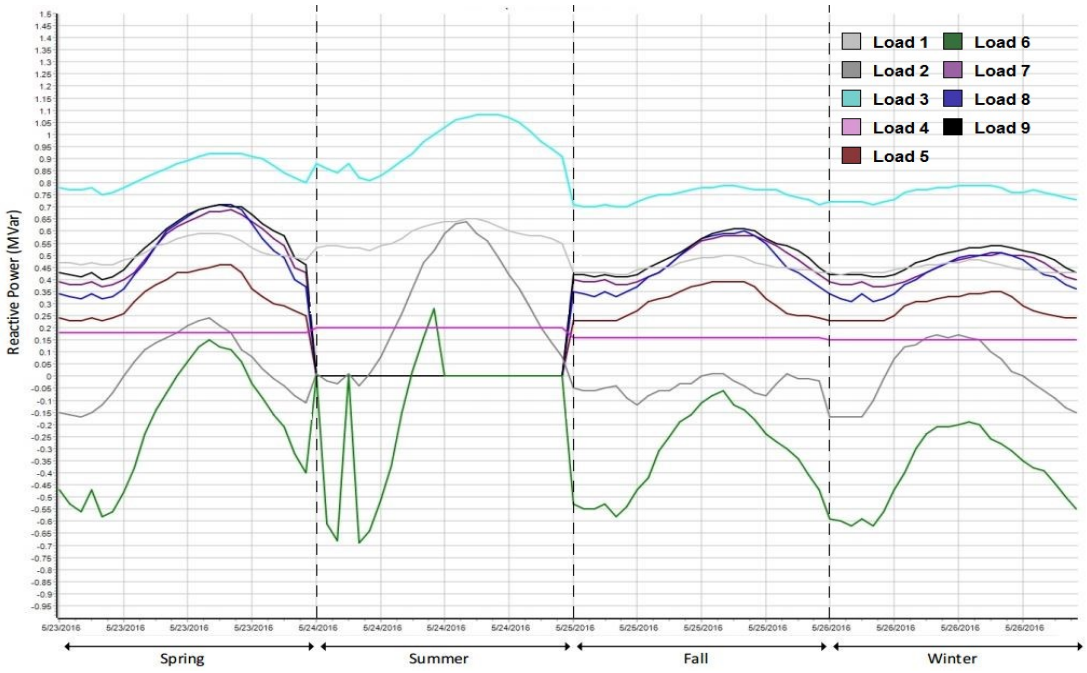

Figure 4-41 Reactive power consumption of all the critical loads in four seasons

Figure 4-40 and Figure 4-41 shows the real and reactive power consumption of all the critical loads supplied in four different seasons. Most of the critical loads are supplied in all the seasons except in summer in which only four of the critical loads are supplied. Critical load-2 consumes the maximum power when compared to other loads. The loads are managed to switch on and off according to the forecast study. It can be seen in the figures as sudden fall in real and reactive power to zero. The critical load-4 actual profile was not available, hence it is assumed as constant load across a day in each season. Apart from this, most of the other loads follow a typical profile of increase in the demand around 7 AM and reduce in the demand around 6 PM. Critical load-6 and critical load-2 are supplying capacitive reactive power during certain times of the day.

4.9 CONTINGENCY BASED ANALYSIS

The microgrid should be scheduled and operated in such a way that overloads do not occur even under load variation or under any statistically likely contingency. This is also called

maintaining the system operational security. The contingency can be anything ranging from loss of a shunt capacitor to loss of the entire generating unit. Load or generation shedding may be required in response to some contingencies, but equipment should not be overloaded. Contingency-based analysis is performed on the microgrid model to identify the worst-case contingencies that can bring down the system. Table 4-10 shows the list of a few violations recorded by simulating all the contingencies related to equipment outages on the system

Table 4-10 Summary of the contingency analysis done on the microgrid model

Contingency	No of violations caused	Violations	Contingency Value	Actual Limit	Percentage of loading
Loss of Transformer GSU1	3	GSU-2 to Substation-1 line overload	22.54	20	112.71
		Substation-1 to critical load-6 line overload	4.369	2.812	155.38
		Substation-1 to critical load-6 line section overload	4.301	2.81	153.07
Loss of Transformer GSU2	3	GSU-1 to Substation-1 line overload	23.24	15	154.91
		Substation-1 to critical load-6 line overload	4.383	2.812	155.88
		Substation-1 to critical load-6 line section overload	4.311	2.81	153.42
Loss of transmission line from Substation-1 to substation-2	15	Substation-1 to critical load-6 line overload	19	2.812	675.68
		Substation-1 to critical load-6 line section overload	17.56	2.81	624.81
		substation-2 to critical load-6 line overload	11.21	3.68	304.65
		substation-2 to critical load-6 line section overload	3.823	3.68	103.9
		critical load-6 bus section-1 under voltage	0.845	0.9	
		critical load-6 line section-2 under voltage	0.7757	0.9	
		critical load-6 bus under voltage	0.7753	0.9	

The limits for voltage that are considered while performing the contingency analysis are 0.9 to 1.1 per unit; this means the voltages that fall below 0.9 p.u and above 1.1 p.u are considered as violations. In the same way, the line loading percentages crossing 100% are considered as violations. More violations are caused in the microgrid model during the loss of transmission line from substation-1 to substation-2. The worst-case violations can be identified and proper planning need to be done in order to avoid system collapse during such violations by appropriate load shedding or generator shedding. This task can be accomplished by microgrid controller by including such algorithms to avoid abnormal situations.

4.10 GENERATOR CAPABILITY CURVES

The generator capability curves are calculated using the machine data as discussed in Section 3.3.2 and Appendix-B. This information is loaded into the Powerworld microgrid model. Figure 4-42 and Figure 4-43 shows the generator capability curves with operating points for generator-1 and generator-2 respectively that are captured when the high summer load and generation profiles are loaded into the microgrid model.

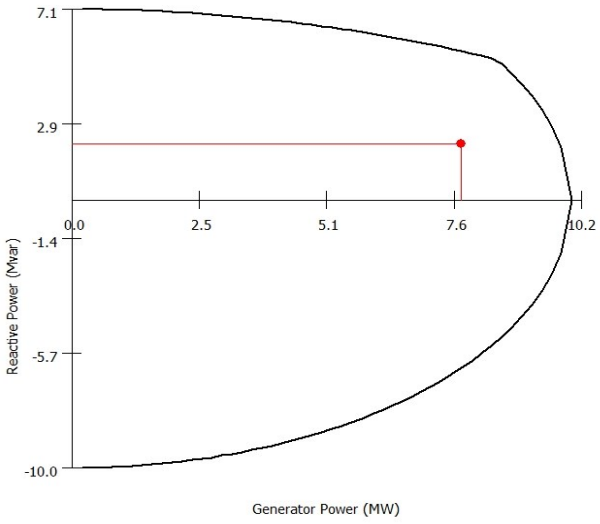

Figure 4-42 Generator capability curve of the generator-1

The instance at which these operating points are captured are when the generator-1 is supplying 7.8 MW real power and 2.1 MVAR reactive power. Generator-2 is supplying 14.17 MW and 4.52 MVAR. The reactive power supplied by each machine is within the limits of the respective generators. The figure shows that the reactive power value is within the limits and within the capability curve as are the real power outputs.

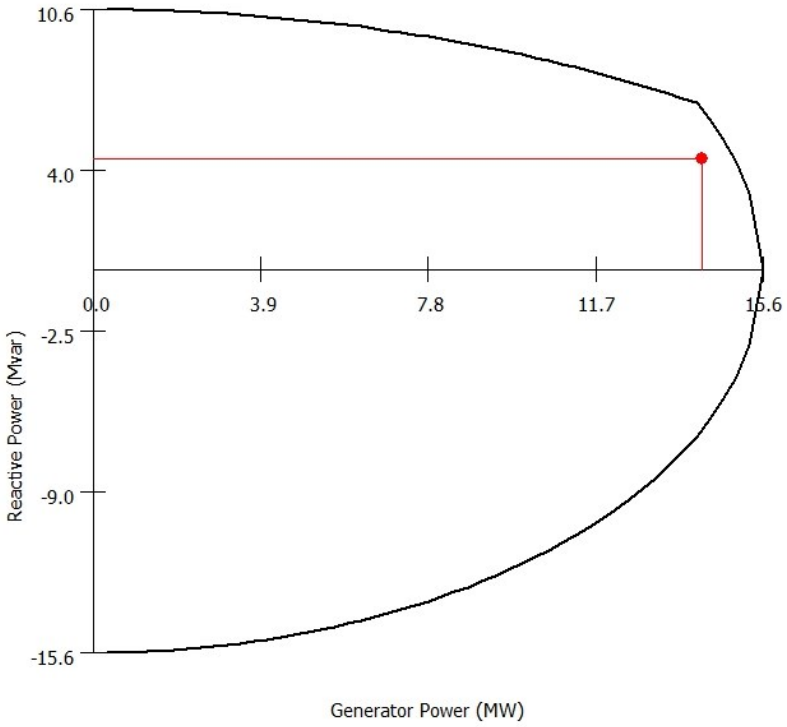

Figure 4-43 Generator capability curve of the generator-2

4.11 MICROGRID ENERGY MANAGEMENT SYSTEM (MicroEMS)

The Microgrid Energy Management System (MicroEMS) is an essential component of the microgrid. Figure 4-44 shows a potential architecture for a MicroEMS [41]. A Microgrid Supervisory Control and Data Acquisition (MicroSCADA) system acquires the data from measurement devices such as protection relays, smart energy meters that are located at loads and generators. A MicroEMS will have the control logic in it to maintain operation of the

microgrid under stable operating conditions. This microgrid controller is not implemented as a part of this thesis, and will need to be developed and implemented if the microgrid is implemented.

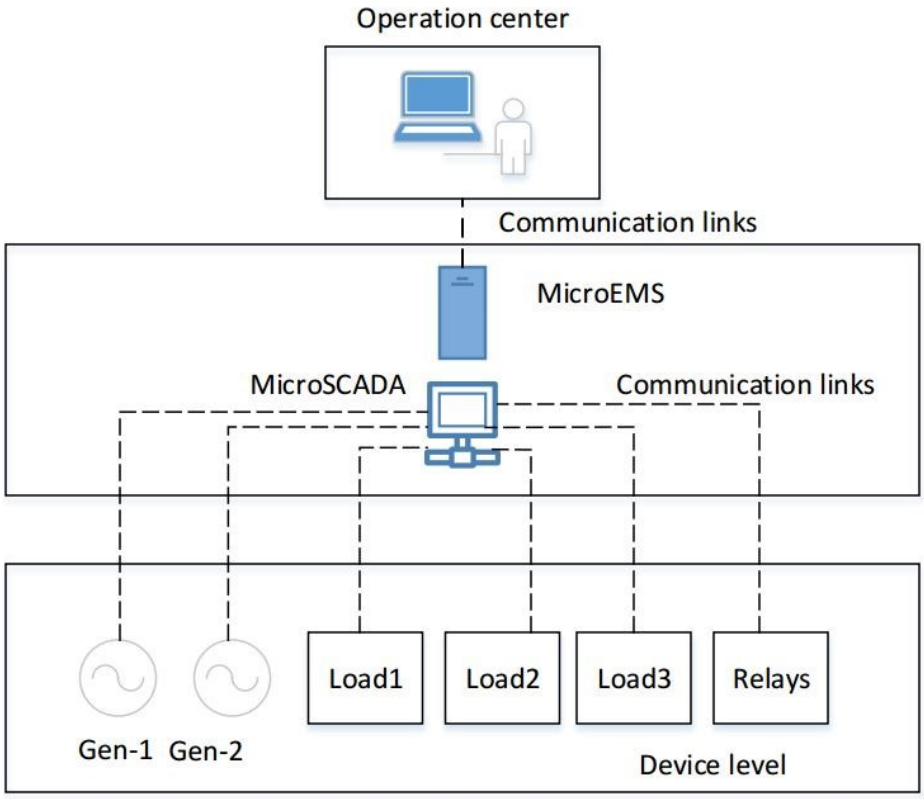

Figure 4-44 Overview of a microgrid energy-management system

Many different control strategies for microgrids have been proposed and some have been implemented in the field in the recent years. Usually, the real time generation control of microgrids is performed using droop controllers that react to frequency and voltage, while non-real-time decisions are taken by well-defined Energy Management System (EMS) [68]. References [69] [70] [71] [72] discusses different strategies that can be used to control the microgrids. One option is developing agent-based control associated with all of the devices in a microgrid. The grid agent sends explicit set points to device agents to control. The MicroEMS

system can be centralized or decentralized. A few of the relevant challenges in microgrid control and protection include handling the following: bidirectional power flows, stability issues, modeling, low inertia, and uncertainty. The desirable features of control system include output control, power balance, demand side management, economic dispatch, and transition between modes of operation [73].

Figure 4-45 shows the high-level flow chart of a control strategy proposed for the microgrid in this study. In this process, the load and forecast information along with ranking tables are loaded into the controller. The rank tables are the look up tables that contain the priority of the loads as discussed in Section 4.2.1. The controller acquires the real time metering data from smart devices like smart energy meters, protection relays with communication capability for example, devices using IEC 61850 for communication.

The controller then processes the metering data including, voltage at all the buses, system frequency, real and reactive power consumption and generation, and the battery state of charge. The sum of measured real power (P_{total}) and reactive power (Q_{total}) of all the loads and all the generators is used to estimate losses and calculate a mismatch. If there is an excessive generation available from Solar more than the peak demand, that can be stored in the battery. The frequency and voltage of the microgrid is constantly monitored, if the frequency drops below the limit, load shedding is performed to maintain the frequency. AGC will take corrective actions to stabilize the frequency after the load shedding is performed. If the frequency crosses the limit, the AGC will send a command to reduce the power output of the machines. The voltage at all the buses can be maintained by switching the capacitors at all the buses and varying LTCs of transformers. This is the proposed model and it is not implemented as a part of this thesis.

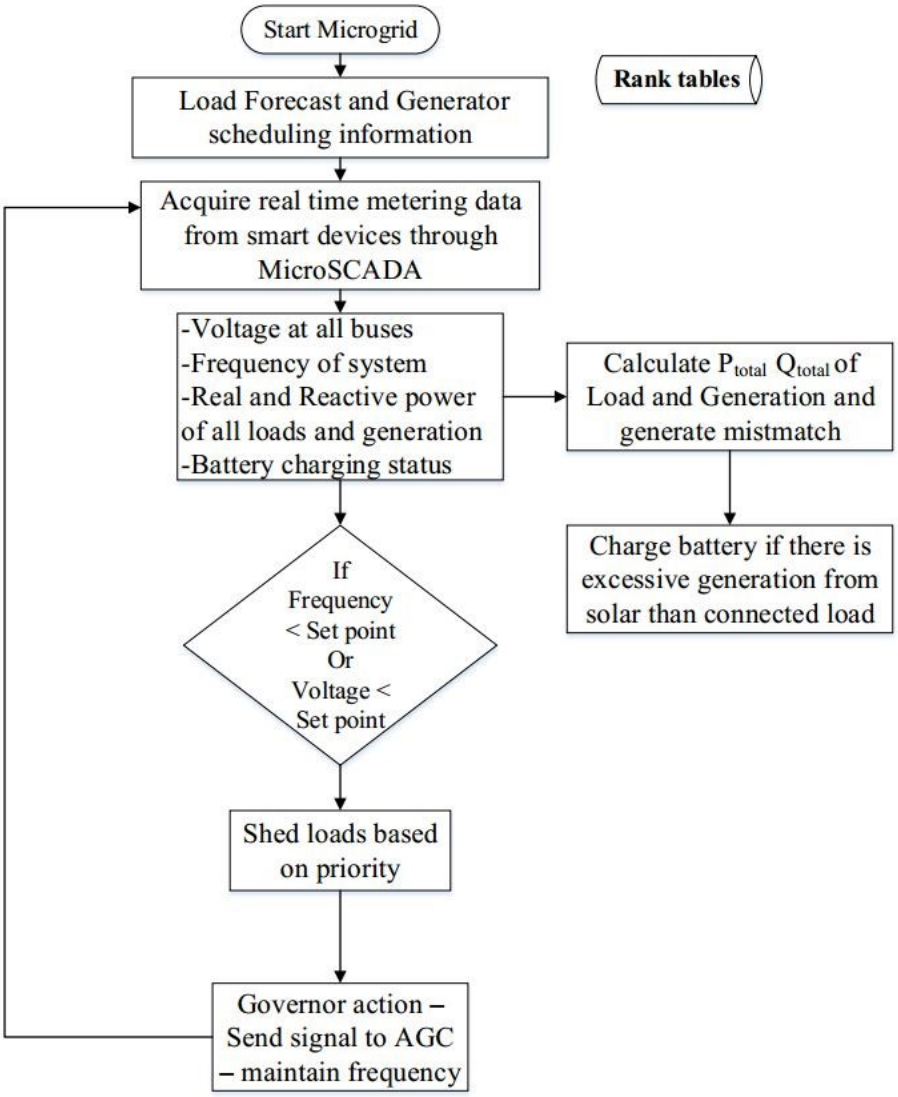

Figure 4-45 Higher-level flow diagram of energy management system

4.12 RTDS MODEL DEMONSTRATING LOAD SHEDDING

A simplified model of the microgrid is implemented in Real Time Digital Simulator (RTDS). RTDS provides opportunity to perform hardware in loop simulations. It provides low-level output signals, which resembles the real system data such as current transformer outputs or voltage transformer outputs. These outputs can be directed to intelligent electronic devices to perform protection or automation operations. RTDS has set of processor cards, analog and digital input/output cards, network and synchronization cards. All of these components

constitute a rack in RTDS. RSCAD is the user interface that provides a platform to draft the models and visualize the outputs in a runtime.

Figure 4-46 shows the simplified model developed in RTDS. The RTDS racks have limit on number of nodes that it can model. The available test bed contains two racks. Owing to these limitations, the components are aggregated to form a simplified model. There are two synchronous machines modeled with exciter and governor, a power system stabilizer is used to stabilize the output from these machines. EXST4B exciter and HYGOV governor dynamic models are included. The transmission lines are modeled using the data from Powerworld model as coupled RL branches by ignoring the capacitance affect. The transformers are modeled with 0.1 per unit leakage inductance. The critical loads are modeled same way they were modeled in Powerworld except critical loads 3 and 4, critical loads 5 and 7, critical loads 8 and 9 are aggregated together as single load.

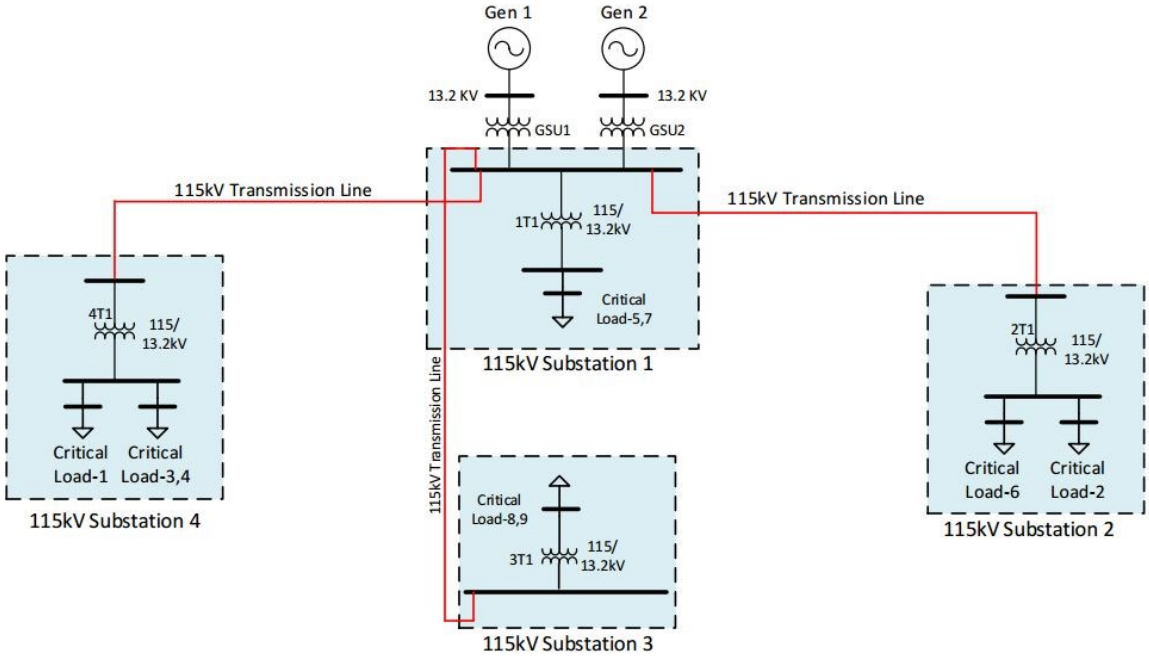

Figure 4-46 Simplified microgrid model developed in RTDS

The system is stable with initial load flow simulations. A runtime file is created to record the frequency response of the system and the voltages at different buses. The system is stable with the simplified model of the microgrid. The complete model of the microgrid including the distribution system is not modeled at the time of writing the thesis. The plan is to perform hardware in loop simulation by including a real time automation controller which receives the microgrid model data such as breaker statuses, real and reactive power values at loads and generators through standard communication protocols (ex: IEC 61850 or Modbus).

Load shedding and generator shedding logic can be included in the controller to maintain the stability in the microgrid in terms of voltage and frequency. The contingencies or the disturbances that might arise in the microgrid are load switching and generation variation and faults. There would also be conditions such as battery switching, capacitor bank switching, and reactor switching if any. These all cases can be simulated to identify the system response and behavior. There can be cases such as communication failures or disturbances that can be caused by cyber-attacks. These cases can be simulated to perform the system behavior. The microgrid controller can be designed to handle such situations.

CHAPTER 5. CONCLUSIONS AND FUTURE WORK

5.1 CONCLUSION

The microgrids are proliferating across the world. This thesis modeled a proposed real world microgrid as part of scoping study for a system that may be established soon. The study identified the available generation resources and critical loads based on their priority and the system topology. The potential amount solar energy that can be generated within the footprint of the microgrid based available locations is estimated. The PCC breakers that need to be opened to form a microgrid were identified and electrical boundaries for the microgrid were defined. The transmission and distribution line parameters were acquired from different simulation packages and a unified model representing the microgrid was implemented in Powerworld. Historical measured load profiles and estimated generation resource profiles for the past three years were used to analyze the daily and seasonal behavior of different loads. Owing to seasonal variation of various parameters, different scenarios were created using aux files in Powerworld to run the simulations over representative days in different seasons.

Power flow simulation was performed to identify the steady-state behavior of the system. The steady-state voltages were within limits in both no load and full load conditions when the capacitor banks were switched appropriately. Transient stability cases were simulated by including the machine dynamic models and for the set of case studies, the system attained stability after a certain amount of time. A load and generation forecast study was performed to identify the forecast information for the microgrid. In addition, a study was performed to determine feasibility of adding battery storage, followed by determination of optimal locations, and rating of the potential battery storage systems. Several auxiliary files were created to study

the system behavior in different seasons using time step simulation. The voltage magnitudes and line loading are mostly within the limits in four different seasons by optimally sizing and placing the capacitors and using the load tap changers. However, segments of two distribution lines were still overloaded. Contingency-based analysis was performed to identify the worst-case contingencies.

A few microgrid controller ideas were proposed to develop schemes that maintain voltage and frequency stability. The guidelines from IEEE 1547 standards were followed to design this microgrid. It was confirmed based on the results that it is feasible to form a microgrid in that region with the available resources. Performance can be improved by adding PV generation on roofs of larger buildings and parking areas and with addition of a battery. However, the microgrid is feasible without the additional resources, although additional load shedding will be required. Further analysis of the system including microgrid energy - management system and better generator governors would improve the system behavior. The microgrid has a very good potential to improve the resilience of the system as it is predominantly supplied by hydro generation that is very close to the critical loads.

5.2 FUTURE WORK

5.2.1 Nanogrid

The microgrid could become more resilient if nanogrids were formed within it. A nanogrid is defined as a small microgrid, typically serving single building or a group of buildings. Substation-3 contains two of the critical loads (critical load-8 and critical load-9) which are of the lowest priority for supplying from the microgrid. There is no potential for the microgrid to supply these critical loads in any of the seasons with existing generation capability or the proposed added PV. If an additional solar is installed on local buildings and combined

with demand-response capabilities, then the area around critical load-8 and 9 supplied from substation-3 can be operated as a nanogrid. It can potentially disconnect itself from the microgrid and later resynchronize during times of the day when there is excess generation available.

5.2.2 Further Analysis of the Microgrid Model

Studies including economic aspects while optimizing the solar generation and storage sizing in the microgrid can be performed. A study examining the economic benefit of solar generation and energy storage when not operated, as a microgrid would be a priority. Additional transient stability studies can be performed including dynamic models of smart photovoltaic converters. Many other cases in transient stability study can be performed using any Electromagnetic Transients Program (EMTP) that can simulate the response in smaller time steps or by using the Powerworld dynamic studio. Also the governors presently installed at the hydro generators are not sufficient for microgrid operation, so better governors at generators are needed. These governors can be designed based on simulation studies. In addition, more realistic modeling of the operation of the batteries and their controls are needed, including use of models that maintain energy balance. Studies include cold load pick up, magnetizing inrush, and motor starting should be performed. The generator-1 parameters were assumed due to lack of test data, and the model can be more accurate if parameters are determined. Analysis based on other smart grid software tools such as DER-CAM, Homer Energy, GridLab-D, and Open DSS can help to improve the performance of the microgrid.

5.2.3 Microgrid Energy Management System

The existing transmission and distribution systems in the microgrid region are managed using SCADA and distribution automation systems. A microgrid master controller or microgrid

energy-management system (MicroEMS) can be developed, which communicates with both transmission and distribution networks within the microgrid. The controller sends control commands to the microgrid automatic generation controller to better optimize the microgrid operation. Inclusion of a demand response system would improve the system behavior, as the available generation is not able to supply all of the critical loads within the microgrid at present. This MicroEMS can act as a central controlling entity that can communicate with the decentralized control equipment. The concept of transactive energy can be introduced where the customers will have the capability to buy and sell power dynamically. References [74] [75] [76] [77] [78] and [79] discuss the management system that can be developed building from considerations for a microgrid. Similar concepts can be implemented while designing the MicroEMS. The development of an adequate situational awareness tool that enables the effective and timely decision-making could thus play a key role in preserving resilience during emergencies [10]. Hardware in loop simulations can be performed using RTDS along with MicroEMS.

5.2.4 Improved Load Shedding Techniques

Load shedding is a process to identify and curtail non-critical loads based on preset preference. It includes different schemes for determining the amount of load to be shed. The loads to be shed are usually determined by operator selectable priorities. The advanced load shedding techniques can be included in MicroEMS. Conceptually, the load shedding system is divided into two functional categories - pre-event calculations and event actions. The system performs pre-event calculations to determine which loads to shed and to build a load shed table dynamically. The system monitors contingency trigger signals and generates load shed signals when a trigger is detected based on the load-shed table. Secondary backup under-frequency

load shedding schemes can be implemented such that if the system falls below a certain threshold, load shedding can be initiated. In addition, the system would benefit from having the ability to do more precise load shedding within critical loads. References [80] and [81] considers the different load shedding schemes implemented practically.

5.2.5 Distributed Control of Microgrids

Decentralized control of the microgrid will have many opportunities in enhancing the cost effectiveness and security performance [8]. The need for resiliency also drives the real time control development for microgrids. Applying the concept of multi-agent systems can improve the autonomous control of microgrids in which each local intelligent controller is operated as an agent. Coordinated algorithms and communication between the agents through system wide organization can improve the overall efficiency. The local agents can have certain autonomy allowing them to make decisions without a central controller. The multi-agent system algorithms can be implemented to optimize the economic operation of the microgrid as well.

Internet technologies such as the Internet of things (IoT) will play a dominant role in the deployment of microgrids. For example, smart homes (Wi-Fi enabled homes) with more precise demand response that can actively control devices in the household and LV networks can contribute for better optimization strategies [8].

5.2.6 Adaptive Protection and Control Schemes

The basic protection functions that can be employed in a microgrid are line current differential protection, transformer protection, and directional overcurrent elements. However, the bi-directional power flow in the case of a microgrid and the complexity of the system makes the protective relaying for a microgrid a complicated task. In order to overcome this, improved protection and control equipment can to be employed. Protective relays equipped with micro

phasor measurement units (PMUs) with small angle resolution capabilities and IEC 61850-communication capability can make better state estimation decisions within the microgrid. The existing protection equipment can have different settings groups that can be changed by a trigger from the microgrid controller. The settings need to be changed between grid connected operation and islanded or microgrid operation. Additional circuit breakers may be needed as well due to the changes in current flow direction.

The increasing complexity of power systems and uncertainty in the events that might occur call for the development of smarter, more adaptive protection schemes capable of adapting to the evolving system conditions and dynamically determining the best actions to take based on unfolding events, and not on predetermined criteria. However, these schemes have not been widely implemented yet due to concerns about reliability [10].

REFERENCES

[1] S. S. M. Venkata and N. Hatziargyriou, 'Grid resilience: Elasticity is needed when facing catastrophes,' *IEEE Power Energy Mag*., vol. 13, no. 3, pp. 16–23, 2015.

[2] World Economic Forum, *The Global risks report 2016*, 11th Edition Available: http://www3.weforum.org/docs/Media/TheGlobalRisksReport2016.pdf, accessed on: 06/17/2016.

[3] S. Parhizi, H. Lotfi, A. Khodaei and S. Bahramirad, 'State of the Art in Research on Microgrids: A Review,' in IEEE Access, vol. 3, no. , pp. 890-925, 2015. doi: 10.1109/ACCESS.2015.2443119.

[4] National centers for environmental information, *National Oceanic and Atmospheric Administration (NOAA)*, Billion-Dollar Weather and Climate Disasters: Table of Events Available: http://www.ncdc.noaa.gov/billions/events, accessed on: 06/17/2016.

[5] Y. Wang, C. Chen, J. Wang and R. Baldick, 'Research on Resilience of Power Systems Under Natural Disasters—A Review,' *IEEE Transactions on Power Systems*, vol. 31, no. 2, pp. 1604-1613, March 2016.

[6] Ward Bower, Dan Ton, Ross Guttromson, Steve Glover, Jason Stamp, Dhruv Bhatnagar, and Jim Reilly, *The Advanced Microgrid Integration and Interoperability*, Sandia Rep., no. March, pp. 1–56, 2014.

[7] Amory Lovins, *Resilience in Energy Strategy*, Rocky mountain Institute, Available http://www.rmi.org/Knowledge-Center/Library/1977-02_ResilienceInEnergyStrategy accessed on 05/07/2016.

[8] G. Strbac, N. Hatziargyriou, J. P. Lopes, C. Moreira, A. Dimeas, and D. Papadaskalopoulos, 'Microgrids: Enhancing the resilience of the European megagrid,' *IEEE Power Energy Mag*., vol. 13, no. 3, pp. 35–43, 2015.

[9] K. P. Schneider, F. K. Tuffner, M. A. Elizondo, C. C. Liu, and Y. Xu, *Microgrid as a resiliency resource*, PNNL-23674, Pacific Northwest Nat. Lab., Richland, Washington, Sept. 2014.

[10] M. Panteli and P. Mancarella, 'The grid: stronger, bigger, smarter? Presenting a conceptual framework of power system resilience,' *IEEE Power Energy Mag*., vol. 13, no. 3, pp. 58–66, 2015.

[11] Galvin Project Inc., *What are the Benefits of the Smart Microgrid Approach?* Galvin Electricity Initiative. [Online]. Available: http://www.galvinpower.org/resources/microgridhub/smart-microgrids-faq/benfits, accessed on: 05/09/2016.

[12] G. Venkataramanan and C. Marnay, 'A larger role for microgrids,' *IEEE Power and Energy Magazine*, vol. 6, no. 3, pp. 78-82, May-June 2008.

[13] D. T. Ton and W. T. P. Wang, 'A more resilient grid: The U.S. Department of Energy joins with stakeholders in an R&D plan,' *IEEE Power Energy Mag*., vol. 13, no. 3, pp. 26–34, 2015.

[14] U.S. Department of Energy, *DOE Microgrid Workshop Report*, Off. Electr. Deliv. Energy Reliab. Smart Grid R&D Program, San Diego, California, pp. 1–32, 2011.

[15] N. Hatziargyriou, H. Asano, R. Iravani, and C. Marnay, 'Microgrids,' *IEEE Power Energy Mag.*, vol. 5, no. 4, pp. 78–94, 2007.

[16] *IEEE Guide for Design, Operation, and Integration of Distributed Resource Island Systems with Electric Power Systems*, IEEE Std 1547.4-2011, vol., no., pp.1-54, July 20 2011.

[17] Nikos Hatziargyriou, 'The Microgrids Concept,' in *Microgrids:Architectures and Control* , 1, Wiley-IEEE Press, 2014, doi: 10.1002/9781118720677.ch01.

[18] *Microgrid activities*, Office of electrical delivery & energy reliability, energy.gov. Available: http://www.energy.gov/oe/services/technology-development/smart-grid/role-microgrids-helping-advance-nation-s-energy-syst-0, accessed on: 06/17/2016.

[19] D. E. Mcnair, D. J. Phelan, and L. Coleman, 'Voices of Experience,' *Insights into Advanced Distribution Management Systems*, U.S. Department of Energy, Feb 2015, no. 159, 2012.

[20] *Distributed Energy Resources Customer Adoption Model* (DER-CAM), Available : https://building-microgrid.lbl.gov/projects/der-cam.

[21] Grid Lab-D Simulation Software, Available : http://www.gridlabd.org/, accessed on 07/25/2016.

[22] Open DSS, Distribution System Simulator, Available: https://sourceforge.net/p/electricdss/wiki/Home/, accessed on 07/25/2016.

[23] Homer Energy, Microgrid Modeling Software Available : http://www.homerenergy.com/, accessed on 07/25/2016.

[24] Smartgrid.gov, *Renewable and Distribution Systems Integration Program*, Project locations and Information, [online] Available: https://www.smartgrid.gov/recovery_act/project_information.html?pff=r, accessed on: 07/07/2016.

[25] Peter Asmus and Mackinnon Lawrence, *Market Data: Microgrids*, Executive summary, 1Q 2016, Navigant research. Available: http://www.navigantresearch.com/research/energy-technologies/microgrids-energy-technologies, accessed on: 06/17/2016.

[26] PowerWorld, PowerWorld Simulator Overview, [Online]. Available: http://www.powerworld.com/products/simulator/overview, accessed on 05/09/2016.

[27] SynerGEE Electric, Power distribution analysis and optimization - Synergi Electric, Available: https://www.dnvgl.com/services/power-distribution-analysis-and-optimization-synergi-electric-5005, accessed on 05/09/2016.

[28] N. Hatziargyriou, H. Asano, R. Iravani, and C. Marnay, 'Microgrids,' *IEEE Power Energy Mag.*, vol. 5, no. 4, pp. 78–94, 2007.

[29] Janez Potocnik, *European technology platform smart grids: vision and strategy for Europe's electricity networks of the future*, European commission, vol. 19, no. 3. 2006.

[30] R. H. Lasseter, 'MicroGrids,' *IEEE Power Eng. Soc. Winter Meeting*., pp. 305–308, 2002.

[31] B. Kroposki, R. Lasseter, T. Ise, S. Morozumi, S. Papathanassiou, and N. Hatziargyriou, 'Making microgrids work,' *IEEE Power Energy Mag*., vol. 6, no. 3, pp. 40–53, 2008.

[32] J. Varela, N. Hatziargyriou, L. J. Puglisi, G. Bissel, A. Abart, M. Rossi, and R. Priewasser, 'The best of IGREENGrid practices: A distribution network's contribution to resiliency,' *IEEE Power Energy Mag*., vol. 13, no. 3, pp. 81–89, 2015.

[33] M. Shahidehpour, C. Bartucci, N. Patel, T. Hulsebosch, P. Burgess, and N. Buch, 'Streetlights are getting smarter: Integrating an intelligent communications and control system to the current infrastructure,' *IEEE Power Energy Mag*., vol. 13, no. 3, pp.

[34] Woodward, *Governor Fundamentals and Power Management*, Technical Manual 26260, 2004. [online]. Available: www.woodward.com/WorkArea/DownloadAsset.aspx?id=2147483987, accessed on: 07/02/2016.

[35] T. Basso, *IEEE 1547 and 2030 Standards for Distributed Energy Resources Interconnection and Interoperability with the Electricity Grid IEEE 1547 and 2030 Standards for Distributed Energy Resources Interconnection and Interoperability with the Electricity Grid*., vol 5, no. 4, pp. 78-94, 2007.

[36] IEEE Standards Association, '*IEEE SCC21 Standards Coordinating Committee on Fuel Cells, Photovoltaics, Dispersed Generation, and Energy Storage*,' [online] Available: http://grouper.ieee.org/groups/scc21/index.html, accessed on: 07/07/2016.

[37] *IEEE Guide for Design, Operation, and Integration of Distributed Resource Island Systems with Electric Power Systems*, IEEE Std 1547.4-2011, vol., no., pp.1-54, July 20 2011.

[38] *IEEE Standard for Interconnecting Distributed Resources with Electric Power Systems*, IEEE Std 1547-2003, vol., no., pp.1-28, July 28 2003.

[39] National Electrical Manufacturers Association, *ANSI C84.1 Electric Power Systems and Equipment – Voltage Ratings (60 Hertz)*, [online] Available:

www.nema.org/stds/c84-1.cfm, accessed on: 06/27/2016.

[40] *IEEE Standard for Interconnecting Distributed Resources with Electric Power Systems - Amendment 1*, in IEEE Std 1547a-2014 (Amendment to IEEE Std 1547-2003) , vol., no., pp.1-16, May 21 2014.

[41] Yan Xu, 'Complete System-Level Efficient and Interoperable Solution for Microgrid Interoperable Solution for Microgrid Integrated Controls (CSEISMIC),' *2014 IEEE Power Engineering Society General Meeting*, National Harbor, MD, July 2014.

[42] *IEEE Guide for Smart Grid Interoperability of Energy Technology and Information Technology Operation with the Electric Power System (EPS)*, End-Use Applications, and Loads, in IEEE Std 2030-2011, vol., no., pp.1-126, Sept. 10 2011.

[43] F. Leccese, 'An overview on IEEE Std 2030,' *Environment and Electrical Engineering (EEEIC)*, *2012 11th International Conference*, Venice, 2012, pp. 340-345.

[44] United States Geological Survey, USGS 12419000 Spokane river nr post falls id, Available: http://waterdata.usgs.gov/nwis/uv?site_no=12419000, accessed on: 05/08/2016.

[45] National Renewable Energy Laboratory, Weather Bureau Army Navy (WBAN) Identification Numbers, Available: http://rredc.nrel.gov/solar/old_data/nsrdb/19611990/redbook/sum2/state.html, accessed on: 05/08/2016.

[46] National Renewable Energy Laboratory, PVWatts Calculator, Available: http://pvwatts.nrel.gov/, accessed on: 05/09/2016.

[47] National Renewable Energy Laboratory, '*Solar Energy and Capacity Value*,' [online] Available: http://www.nrel.gov/docs/fy13osti/57582.pdf, accessed on: 06/21/2016.

[48] Vladimir Koritarov and Leah Guzowski, *Review of Existing Hydroelectric Turbine-Governor Simulation models*, Decision and Information services, Argonne National Laboratory.

[49] Pouyan Pourbeik, *Power System Dynamic Performance Committee, Dynamic Models for Turbine-Governors in Power System Studies*, IEEE Power & Energy Society, Technical report, Jan 2013.

[50] California Commissioning Collaborative, *Energy Charting and Metrics (ECAM)* tool Available: http://cacx.org/PIER/ecam/, accessed on: 05/09/2016.

[51] D. Rastler, *Electricity Energy Storage Technology Options*, White Paper, 2010. Available: http://large.stanford.edu/courses/2012/ph240/doshay1/docs/EPRI.pdf, accessed on: 06/17/2016.

[52] V Viswanathan, M Kintner-Meyer, P Balducci, C Jin, *National Assessment of Energy Storage for Grid Balancing and Arbitrage*, Phase II, Volume 2: Cost and Performance Characterization, September 2013. Available: http://energyenvironment.pnnl.gov/pdf/Nat.

[53] Susan M. Schoenung, William V. Hassenzahl, *Long vs. Short-Term Energy Storage: Sensitivity Analysis --- A Study for the DOE Energy Storage System Program*, Technical Report SAND2007-4243, Sandia National Laboratories, 2007.

[54] A. K. Barnes, J. C. Balda, A. Escobar-Mejia, and S. O. Geurin, 'Placement of energy storage coordinated with smart PV inverters,' *Innovative Smart Grid Technologies (ISGT)*, *2012* IEEE PES, 2012, pp.1–7.

[55] Farid Katiraei, Reza Iravani, Nikos Hatziargyriou, and Aris Dimeas, 'Microgrid Management,' *IEEE Power & Energy Magazine*, May/June 2008.

[56] Real Time Digital Simulator (RTDS), 'RTDS Technologies,' Available: https://www.rtds.com/, accessed on 05/09/2016.

[57] James Weber, *Description of Machine Models GENROU, GENSAL, GENTPF, GENTPJ*, Powerworld Corporation, October 2015, [online] Available: http://www.powerworld.com/files/GENROU-GENSAL-GENTPF-GENTPJ.pdf, accessed on: 07/02/2016.

[58] Western Electricity Coordinating Council, *The Recommended Synchronous Generator Model: GENTPJ*, A WECC White paper, June 14, 2016, WECC, Utah.

[59] J. Y. Jackson, 'Interpretation and Use of Generator Reactive Capability Diagrams,' *IEEE Transactions on Industry and General Applications*, vol. IGA-7, no. 6, pp. 729-732, Nov. 1971.

[60] University of Wisconsin-Madison, *Estimating Generator Capability Curves*, April 22, 2015. [Online]. Available: http://www.neos-guide.org/sites/default/files/capability_curves.pdf, accessed on: 6/23/2016.

[61] Jiajia Song, T. K. A. Brekken, E. Cotilla-Sanchez, A. von Jouanne and J. D. Davidson, 'Optimal placement of energy storage and demand response in the Pacific Northwest,' *2013 IEEE Power & Energy Society General Meeting*, Vancouver, BC, 2013, pp. 1-5.

[62] L.F. Montoya, Q.Fu, V. Bhavaraju, D.Yu, *Novel methodology to determine the optimal energy storage location in a microgrid and address power quality and stability*, White paper WP083008EN, Eaton, May 2014.

[63] P. Kundur et al., 'Definition and classification of power system stability IEEE/CIGRE joint task force on stability terms and definitions,' in *IEEE Transactions on Power Systems*, vol. 19, no. 3, pp. 1387-1401, Aug. 2004.

[64] Prabha Kundur, Neal J. Balu, Mark G. Lauby, 'Introduction to power system stability problem,' '*Power system stability and control*,' New York, NY, McGraw-Hill, 1994, ch. 2, pp.34.

[65] P. W. Sauer, 'Time-scale features and their applications in electric power system dynamic modeling and analysis,' *Proceedings of the 2011 American Control Conference*, San Francisco, CA, 2011, pp. 4155-4159.

[66] Western Electricity Coordinating Council, *System Performance Regional Criteria - TPL-001-WECC-CRT-2*, 2011, [online] Available: https://www.wecc.biz/Reliability/TPL-001-WECC-CRT-2.1.pdf, accessed on: 07/01/2016.

[67] Powerworld Corporation, *Auxiliary File Format for simulator 19*, June 3, 2016, [online] Available: http://www.powerworld.com/files/Auxiliary-File-Format.pdf, accessed on 07/01/2016.

[68] R. Palma-Behnke, C. Benavides, F. Lanas, B. Severino, L. Reyes, J. Llanos, and D. Saez, ‘A microgrid energy management system based on the rolling horizon strategy,’ *IEEE Trans. Smart Grid*, vol. 4, no. 2, pp. 996–1006, 2013.

[69] A. Bernstein, J. Y. Le Boudec, L. Reyes-Chamorro, and M. Paolone, ‘Real-time control of microgrids with explicit power setpoints: Unintentional islanding,’ *2015 IEEE Eindhoven PowerTech*, PowerTech 2015, 2015.

[70] A. Bernstein, L. Reyes-Chamorro, J.-Y. Le Boudec, and M. Paolone, ‘A Composable Method for Real-Time Control of Active Distribution Networks with Explicit Power Setpoints,’ *Ecole Polytechnique F´ed´erale de Lausanne*, Switzerland, p. 72, 2014.

[71] C.-X. Dou and B. Liu, ‘Multi-Agent Based Hierarchical Hybrid Control for Smart Microgrid,’ *IEEE Trans. Smart Grid*, vol. 4, no. 2, pp. 771–778, 2013.

[72] M. Mao, P. Jin, N. D. Hatziargyriou, and L. Chang, ‘Multiagent-based hybrid energy management system for microgrids,’ *IEEE Trans. Sustain. Energy*, vol. 5, no. 3, pp. 938–946, 2014.

[73] D. E. Olivares *et al*., "Trends in Microgrid Control," in *IEEE Transactions on Smart Grid*, vol. 5, no. 4, pp. 1905-1919, July 2014.

[74] Scott Manson and Saurabh Shah, ‘Automated Power Management Systems for Power Consumers With on-Site Generation,’ *Schweitzer Engineering Laboratories*, Inc., pp. 1–10.

[75] E. R. Hamilton, J. Undrill, P. S. Hamer, and S. Manson, ‘Considerations for generation in an islanded operation,’ *IEEE Trans. Ind. Appl.*, vol. 46, no. 6, pp. 2289–2298, 2010.”

[76] K. G. Ravikumar, T. Alghamdi, J. Bugshan, S. Manson, and S. Krishna Raghupathula, ‘Complete Power Management System for an Industrial Refinery,’ *IEEE Trans. Ind. Appl.*, vol. 9994, no. c, pp. 1–1, 2016.

[77] K. G. Ravikumar, A. Upreti, A. Nagarajan, A. May, ‘State-of-the-Art Islanding Detection and Decoupling Systems for Utility and Industrial Power Systems,’ *69th Annual Georgia Tech Protective Relaying Conference*, Atlanta, GA, 2015.

[78] Guerrero, J. M., Chandorkar, M., Lee, T-L., & Loh, P. C. (2013). Advanced Control Architectures for Intelligent MicroGrids, Part I: Decentralized and Hierarchical Control. *IEEE Transactions on Industrial Electronics*, 60(4), 1254-1262.

[79] J. M. Guerrero, J. C. Vasquez, J. Matas, L. G. de Vicuna and M. Castilla, 'Hierarchical Control of Droop-Controlled AC and DC Microgrids—A General Approach Toward Standardization,' *IEEE Transactions on Industrial Electronics,* vol. 58, no. 1, pp. 158.

[80] W. Allen and T. Lee, 'Flexible High-Speed Load Shedding Using a Crosspoint Switch,' *2006 Power Systems Conference: Advanced Metering, Protection, Control, Communication, and Distributed Resources*, Clemson, SC, 2006, pp. 501-509.

[81] B. Cho, H. Kim, H. E. Co, N. C. Seeley, 'The Application of a Redundant Load-Shedding System for Islanded Power Plants,' *35th Annual Western Protective Relay Conference*, no. 3, pp. 1–9, Spokane, Washington, 2008.

APPENDIX A – SAMPLE AUXILIARY FILE

Auxiliary files are used to model the variations in load and generation in Powerworld. It is a text file as shown below. The data below is a sample auxiliary file that corresponds to the data of a particular season. It contains the data of loads, shunt capacitors, transformer tap positions, generator information.

Auxiliary file

```
DATA                                                                    (Load,
[BusNum,BusName,AreaName,ZoneName,LoadID,LoadStatus,LoadMW,LoadMVR,LoadMVA,
   LoadSMW,LoadSMVR,DistStatus,DistMWInput,DistMvarInput])
{
   12 "Critical load-1" "1" "1" "1 " "Closed"      1.82      1.00      2.08      1.82
1.00 "Closed"     0.00     0.00
   <SUBDATA BidCurve>
     //MW   Price[$/MWhr]
         0.00 10000.00
   </SUBDATA>
   12 "Critical load-2" "1" "1" "2 " "Closed"      2.30      0.93      0.00      2.30
0.93 "Closed"     0.00     0.00
   <SUBDATA BidCurve>
     //MW   Price[$/MWhr]
         0.00 10000.00
   </SUBDATA>
   13 "Critical load-3" "1" "1" "1 " "Closed"      1.47      0.70      1.63      1.47
0.70 "Closed"     0.00     0.00
   <SUBDATA BidCurve>
     //MW   Price[$/MWhr]
         0.00 10000.00
   </SUBDATA>
   13 "Critical load-4" "1" "1" "2 " "Closed"      2.40      0.89      0.00      2.40
0.89 "Closed"     0.00     0.00
   <SUBDATA BidCurve>
     //MW   Price[$/MWhr]
         0.00 10000.00
   </SUBDATA>
   14 "Critical load-5" "1" "1" "1 " "Closed"      2.73      1.00      0.00      2.73
1.00 "Closed"     0.00     0.00
   <SUBDATA BidCurve>
     //MW   Price[$/MWhr]
         0.00 10000.00
   </SUBDATA>
   14 "Critical load-6" "1" "1" "2 " "Closed"      2.17      0.98      2.38      2.17
0.98 "Closed"     0.00     0.00
   <SUBDATA BidCurve>
     //MW   Price[$/MWhr]
         0.00 10000.00
   </SUBDATA>
   15 "Critical load-7" "1" "1" "1 " "Open"      1.93      0.90      2.13      1.93
0.90 "Closed"     0.00     0.00
   <SUBDATA BidCurve>
```

```
     //MW   Price[$/MWhr]
          0.00 10000.00
   </SUBDATA>
   15 "Critical load-8" "1" "1" "2 " "Open"      0.00      0.00      0.00      2.37
0.96 "Closed"     0.00     0.00
   <SUBDATA BidCurve>
     //MW   Price[$/MWhr]
          0.00 10000.00
   </SUBDATA>
   15 "Critical load-9" "1" "1" "2 " "Open"      0.00      0.00      0.00      2.37
0.96 "Closed"     0.00     0.00
   <SUBDATA BidCurve>
     //MW   Price[$/MWhr]
          0.00 10000.00
}
DATA                                                                          (Shunt,
[BusNum,BusName,ShuntID,SSRegNum,SSStatus,SSCMode,SSRegulates,SSAMVR,SSVHigh,
   SSVLow,SSRegVolt,SSDEV,SSNMVR,SSMaxMVR,SSMinMVR])
{
          3 "Cap-1" "1"        3 "Closed" "Fixed" "Volt"    15.00   1.0000   0.9900
1.0000   0.0000    1.50    50.00     0.00
         23 "Cap-2" "1"       23 "Closed" "Fixed" "Volt"     1.50   1.0000   0.9900
1.0000   0.0000     0.30     3.00     0.00
          34 "Cap-3" "1"       34 "Closed" "Fixed" "Volt"     0.00   1.0000   0.9900
1.0000   0.0000     0.30     3.00     0.00
          46 "Cap-4" "1"       46 "Closed" "Fixed" "Volt"    15.00   1.0000   0.9900
1.0000   0.0000    0.30    50.00     0.00
}
    DATA                                                                      (Branch,
[BusNum,BusName,BusNum:1,BusName:1,LineCircuit,LineXFType,LineStatus,LineTap,
       LinePhase,XFAuto,XFRegBus,XFRegValue,XFRegError,XFRegMin,XFRegMax,XFTapMin,
       XFTapMax,XFStep])
     {
         1 "1T1."     5 "Substation-1" "2" "Fixed" "Closed"   1.0   0.00000 "No"     0
0.00000  -0.51000   0.51000   1.50000   0.51000   1.50000   0.00625
     }

DATA                                                                           (Gen,
[BusNum,BusName,GenID,GenStatus,GenMW,GenMVR,GenVoltSet,GenAGCAble,GenAVRAble,
   GenMWMin,GenMWMax,GenMVRMin,GenMVRMax,GenCostModel,GenParFac])
{
    4 "Solar" "1" "Closed"      3.5      0.01  1.00000 "NO " "YES"      0.00  1000.00
0.01     0.01 "None"    10.00
    5 "Gen-1" " 2" "Closed"    9.8    2  1.00000 "NO " "YES"     1.00    10.20     0.05
6.00 "None"     0.16
              <SUBDATA ReactiveCapability>
          //MW   MinMVAR   MaxMVAR
          0.2   -9.99   7.14
          0.4   -9.99   7.13
          0.6   -9.98   7.13
          0.8   -9.96   7.12
          1   -9.94   7.11
          1.2   -9.92   7.1
          1.4   -9.9   7.09
          1.6   -9.87   7.07
          1.8   -9.83   7.06
          2   -9.79   7.04
          8.2   -5.72   5.4
          8.4   -5.42   5.31
          8.6   -5.1   5.1
          8.8   -4.74   4.74
          9   -4.35   4.35
          9.2   -3.91   3.91
```

```
          9.4   -3.41   3.41
          9.6   -2.8   2.8
          9.8   -1.98   1.98
          10   0   0
        </SUBDATA>
    6 "Gen-2" "1" "Closed"    12.83     4.80  1.00000 "NO " "YES"     0.00    15.60
0.00     4.80 "None"    10.00
             <SUBDATA ReactiveCapability>
          //MW   MinMVAR   MaxMVAR
              0.31   -15.59   10.58
              0.62   -15.58   10.57
              0.93   -15.57   10.57
              1.24   -15.54   10.55
              1.56   -15.52   10.54
              1.87   -15.48   10.52
              11.85   -10.13   7.94
              12.16   -9.76   7.79
              12.48   -9.36   7.64
              12.79   -8.92   7.48
              13.1   -8.46   7.32
              13.41   -7.96   7.15
              13.72   -7.4   6.97
              14.04   -6.79   6.79
              14.35   -6.11   6.11
              14.66   -5.32   5.32
              14.97   -4.36   4.36
              15.28   -3.1   3.1
              15.6   0   0
        </SUBDATA>
}
```

APPENDIX B – GENERATOR CAPABILITY CURVES

Generator 1 Capability Curve Calculations

$\text{MVA} = \text{MW}$ $j = \sqrt{-1}$ $lagging = 1$

$S_{base} = 10\ \text{MVA}$ $S_{rated} = 10\ \text{MVA}$ $PF_{rated} = 0.85\ lagging$

$V_{base} = 4.2\ \text{kV}$ $V_{rated} = 4.2\ \text{kV}$

$Z_{base} = \frac{{V_{base}}^2}{S_{base}} = 1.764\Omega$ *Base impedance*

$X_{S_{pu}} = 0.9(1 - 0.15)$ *Per unit synchronous reactance*

$X_S = X_{S_{pu}} \cdot Z_{base} = 1.349\Omega$ *Synchronous reactance*

$V_\phi = \frac{V_{rated}}{\sqrt{3}} = 2.425 \times 10^3\text{V}$ *Per phase voltage*

$Q_0 = \frac{-3 \cdot {V_\phi}^2}{X_S} = -13.072\ \text{MW}$ *Center of rotor current limit cycle*

$I_A = \frac{S_{rated}}{3 \cdot V_\phi} \cdot e^{-j \cdot \cos^{-1}(PF_{rated})}$ *Maximum armature current*

$|I_A| = 1.375 \times 10^3\ \text{A}$

$\arg(I_A) = -31.788°$

$E_A = V_\phi + j \cdot X_S \cdot I_A$ *Maximum generated* E_A

$|E_A| = 3.75\ \text{kV}$

$\arg(E_A) = 24.867°$

$D_E = \frac{3 \cdot E_A \cdot V_\phi}{X_S}$ *Radius of rotor current limit circle*

$|D_E| = 20.214 \text{ MW}$

$S_{rated} = 10 \text{ MW}$ *Radius of stator current limit*

$Q_A = -S_{rated,} - S_{rated} + 10 \text{ kW} \ldots S_{rated}$

$Q_A(P_A) = \pm\sqrt{{S_{rated}}^2 - {P_A}^2}$ *Stator current limits*

$Q_R = Q_A$

$Q_A(P_R) = \sqrt{(|D_E|)^2 - (P_R)^2} + Q_0$ *Rotor current limit*

$P = 1.510^7 \text{ W}$ $Q = 0.510^7 \text{ W}$

$P = \pm\sqrt{{S_{rated}}^2 - Q^2}$ *Stator current limits*

$P = \sqrt{(|D_E|)^2 - (Q - Q_0)^2}$ *Rotor current limit*

$Q > 0 \text{ W}$ $P > 0 \text{ W}$ *Keep result in first quadrant*

$\begin{pmatrix} P_{int} \\ Q_{int} \end{pmatrix} = Find(P, Q)$

$P_{int} = 8.5 \text{ MW}$ $Q_{int} = 5.268 \text{ MW}$ *Intersection point in first quadrant*

$\frac{P_{int}}{{P_{int}}^2 + {Q_{int}}^2} = 0.85 \; lagging$ *Check power factor*

$Q_{cap} = Q_A$

$$Q_{cap}(P_{cap}) = \begin{cases} \sqrt{(|D_E|)^2 - (P_R)^2} + Q_0 \; if \; P_{cap} \le P_{int} \\ \pm\sqrt{{S_{rated}}^2 - {P_{cap}}^2} \; if \; P_{cap} > P_{int} \end{cases}$$

Combined capability curves

$$S_{step} = \frac{S_{rated}}{50} = 2 \times 10^5 \text{ W}$$

$$pnts = 20 \qquad i = 1,2 \ldots pnts$$

$$P_{points_i} = \frac{S_{rated}}{pnts} \cdot i$$

$$Points_i = (P_{points_i} \; Q_{cap}\left(P_{points_i}\right) Q_{cap}(P_{points_i}))$$

$$Points_{20} = (15.6\ 0\ 0) \cdot \text{MW}$$

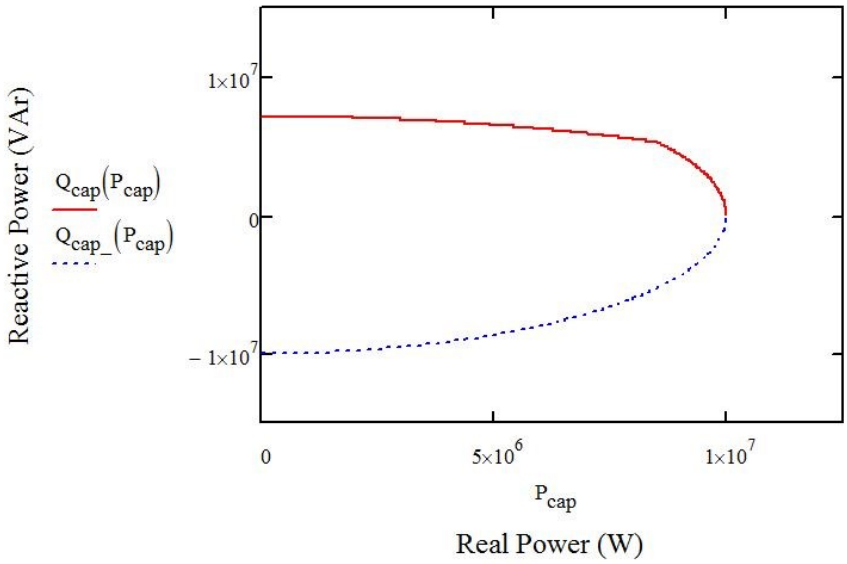

Figure 6-0-1 Generator 1 capability curve from calculations

Generator 2 Capability Curve Calculations

$\text{MVA} = \text{MW}$ $j = \sqrt{-1}$ $lagging = 1$

$S_{base} = 15.6\ \text{MVA}$ $S_{rated} = 15.6\ \text{MVA}$ $PF_{rated} = 0.9\ lagging$

$V_{base} = 13.8\ \text{kV}$ $V_{rated} = 13.8\ \text{kV}$

$Z_{base} = \frac{{V_{base}}^2}{S_{base}} = 12.208\ \Omega$ *Base impedance*

$X_{S_{pu}} = 0.9$ *Per unit synchronous reactance*

$X_S = X_{S_{pu}} \cdot Z_{base} = 10.98\Omega$ *Synchronous reactance*

$V_\phi = \frac{V_{rated}}{\sqrt{3}} = 7.967 \times 10^3\text{V}$ *Per phase voltage*

$Q_0 = \frac{-3 \cdot {V_\phi}^2}{X_S} = -17.333\ \text{MW}$ *Center of rotor current limit cycle*

$I_A = \frac{S_{rated}}{3 \cdot V_\phi} \cdot e^{-j \cdot \cos^{-1}(PF_{rated})}$ *Maximum armature current*

$|I_A| = 652.657\ \text{A}$

$\arg(I_A) = -25.842°$

$E_A = V_\phi + j \cdot X_S \cdot I_A$ *Maximum generated* E_A

$|E_A| = 12.83\ \text{kV}$

$\arg(E_A) = 30.19°$

$D_E = \frac{3 \cdot E_A \cdot V_\phi}{X_S}$ *Radius of rotor current limit circle*

$|D_E| = 27.92\ \text{MW}$

$S_{rated} = 15.6\ \text{MW}$ *Radius of stator current limit*

$Q_A = -S_{rated,} - S_{rated} + 10\ \text{kW} \ldots S_{rated}$

$Q_A(P_A) = \pm\sqrt{{S_{rated}}^2 - {P_A}^2}$ *Stator current limits*

$Q_R = Q_A$

$Q_A(P_R) = \sqrt{(|D_E|)^2 - (P_R)^2} + Q_0$ *Rotor current limit*

$P = 1.510^7\ \text{W}$ $Q = 0.510^7\ \text{W}$

$P = \pm\sqrt{{S_{rated}}^2 - Q^2}$ *Stator current limits*

$P = \sqrt{(|D_E|)^2 - (Q - Q_0)^2}$ *Rotor current limit*

$Q > 0\ \text{W}$ $P > 0\ \text{W}$ *Keep result in first quadrant*

$\begin{pmatrix} P_{int} \\ Q_{int} \end{pmatrix} = Find(P, Q)$

$P_{int} = 14.04\ \text{MW}$ $Q_{int} = 6.8\ \text{MW}$ *Intersection point in first quadrant*

$\frac{P_{int}}{{P_{int}}^2 + {Q_{int}}^2} = 0.9\ lagging$ *Check power factor*

$Q_{cap} = Q_A$

$Q_{cap}(P_{cap}) = \begin{cases} \sqrt{(|D_E|)^2 - (P_R)^2} + Q_0\ if\ P_{cap} \le P_{int} \\ \pm\sqrt{{S_{rated}}^2 - {P_{cap}}^2}\ if\ P_{cap} > P_{int} \end{cases}$ *Combined capability curves*

$S_{step} = \frac{S_{rated}}{50} = 3.12 \times 10^5\ \text{W}$

$pnts = 20 \qquad i = 1,2 \ldots pnts$

$$P_{points_i} = \frac{S_{rated}}{pnts} \cdot i$$

$$Points_i = (P_{points_i}\ Q_{cap}\ (P_{points_i})Q_{cap}(P_{points_i}))$$

$$Points_{20} = (15.6\ 0\ 0) \cdot \text{MW}$$

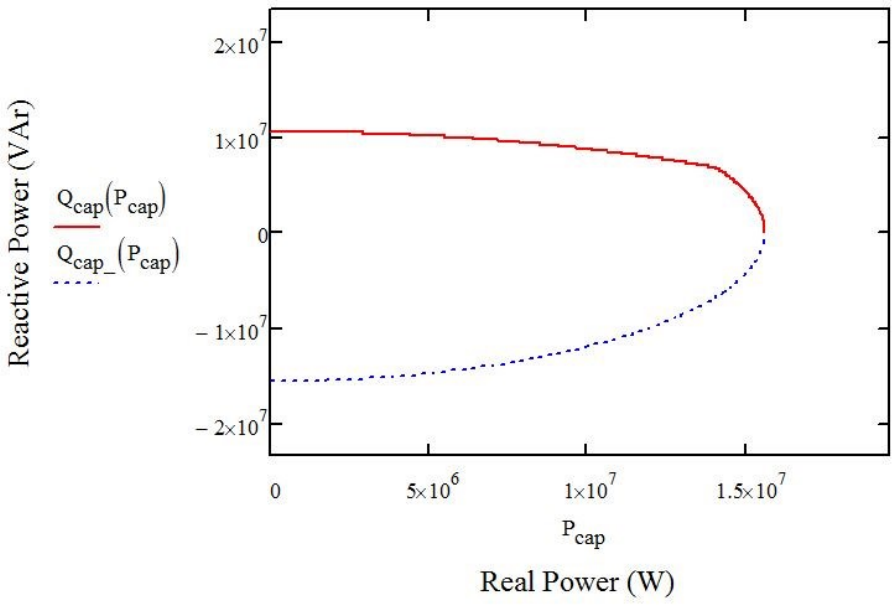

Figure 6-0-2 Generator 2 capability curve from calculations

APPENDIX C – JAVA PROGRAM FOR AUXILIARY FILES

The JAVA program used to create the Auxiliary files is shown below; this is used as a template to generate several files.

```
'use strict'

const xlsx  = require('xlsx')

const fs    = require('fs')

const jx    = require('jquery-extend')

// read excel file

let workbook  = xlsx.readFile('Excel file with forecast information.xlsx')

let ranks     = xlsx.readFile('Rank Tables.xlsx')

// set true if battery is at critical load-6, false if at hospitals

let Batt1 = true;

var seasons = workbook.SheetNames;

seasons.pop();

let rowMW = range(3,26)

let rowMVar = range(28,51)

let checkRowMW = range(58,81)

let cols =
['B','C','D','E','F','G','H','I','J','K','L','M','N','O','P','R','S','T','U
','AA','AB','AC','AD','AE','AF','AG']

let times = ['12:00 AM','1:00 AM','2:00 AM','3:00 AM','4:00 AM','5:00
AM','6:00 AM','7:00 AM','8:00 AM','9:00 AM','10:00 AM','11:00 AM','12:00
PM','1:00 PM','2:00 PM','3:00 PM','4:00 PM','5:00 PM','6:00 PM','7:00
PM','8:00 PM','9:00 PM','10:00 PM','11:00 PM']

let steps = {}

let n = 0

seasons.forEach(function(season) {// get load and gen values

  for(let m = 0; m < cols.length; m++) {// iterate through each load and
gen

    let load = null

    if (cols[m] === 'R' || cols[m] === 'S' || cols[m] === 'T' || cols[m]
=== 'U' || cols[m] === 'AA' || cols[m] === 'AB' || cols[m] === 'AC' ||
cols[m] === 'AD' || cols[m] === 'AE' || cols[m] === 'AF' || cols[m] ===
'AG') {

      load = workbook.Sheets[season][cols[m]+'56'].w

    } else {
```

```
      load = workbook.Sheets[season][cols[m]+'1'].w
    }
    for(let i = 0; i < times.length; i++){// iterate through each hour
      let time = workbook.Sheets[season]['A'+rowMW[i]].w // get times
      let mWCell = null
      if (cols[m] === 'R' || cols[m] === 'S' || cols[m] === 'T' || cols[m]
=== 'U' || cols[m] === 'AA' || cols[m] === 'AB' || cols[m] === 'AC' ||
cols[m] === 'AD' || cols[m] === 'AE' || cols[m] === 'AF' || cols[m] ===
'AG') {
        mWCell = workbook.Sheets[season][cols[m]+checkRowMW[i]]
      } else {
        mWCell = workbook.Sheets[season][cols[m]+rowMW[i]]
      }
      let mVarCell = workbook.Sheets[season][cols[m]+rowMVar[i]]
      let mW = null
      let mVar = null
      let step = {}
      if(mWCell) {mW = mWCell.v.toFixed(2)}
      if(mVarCell) {mVar = mVarCell.v.toFixed(2)}
      step[season] = {
         [load] : {
           [time] : {
             'MW' : [mW],
             'MVar' : [mVar]
           }
         }
       }
       jx(true,steps,step)
    }
  }
})
seasons.forEach(function(season) {// get breaker status
  for (let m = 0; m < cols.length-4; m++) {// iterate through each load
    let load = workbook.Sheets[season][cols[m]+'56'].w
    for (let i = 0; i < times.length; i++) {// iterate through each hour
```

```
      let time = workbook.Sheets[season]['A'+rowMW[i]].w // get times
      let mWCellCheck = workbook.Sheets[season][cols[m]+checkRowMW[i]]
      let status = null
      let step = {}
      if (load.indexOf('Load9') !== -1) {
        status = workbook.Sheets[season]['W'+checkRowMW[i]].w
      } else if (mWCellCheck) {
        status = 'CLOSED'
      } else status = 'OPEN'
      step[season] = {
         [load] : {
           [time] : {
             'status' : [status]
           }
         }
       }
       jx(true,steps,step)
    }
  }
})

let fileCount = 96
let files = {}

for (let i=0; i < 4; i++) {
  let season = seasons[i]
  for (let n=0; n < 24; n++) {
    let time = times[n]
    let content = `DATA (Load,
[BusNum,BusName,AreaName,ZoneName,LoadID,LoadStatus,LoadMW,LoadMVR,LoadMVA,
       LoadSMW,LoadSMVR,DistStatus,DistMWInput,DistMvarInput])
    {
       12 "Critical load-5,7 A" "1" "1" "1 "
"${steps[season]['CL5FD1'][time]['status']}"     1.97     0.73     2.10
```

```
${steps[season]['CL5FD1'][time]['MW']}
${steps[season]['CL5FD1'][time]['MVar']} "Closed"     0.00     0.00

       12 "Critical load-5,7 A" "1" "1" "2 "
"${steps[season]['CL7FD1'][time]['status']}"     2.13     0.90     2.31
${steps[season]['CL7FD1'][time]['MW']}
${steps[season]['CL7FD1'][time]['MVar']} "Closed"     0.00     0.00

       13 "Critical load-5,7 D" "1" "1" "1 "
"${steps[season]['CL5FD2'][time]['status']}"     1.45     0.51     1.56
${steps[season]['CL5FD2'][time]['MW']}
${steps[season]['CL5FD2'][time]['MVar']} "Closed"     0.00     0.00

       13 "Critical load-5,7 D" "1" "1" "2 "
"${steps[season]['CL7FD2'][time]['status']}"     2.21     0.90     2.38
${steps[season]['CL7FD2'][time]['MW']}
${steps[season]['CL7FD2'][time]['MVar']} "Closed"     0.00     0.00

       14 "Critical load-5,7 B" "1" "1" "1 "
"${steps[season]['CL7FD3'][time]['status']}"     2.55     1.00     2.74
${steps[season]['CL7FD3'][time]['MW']}
${steps[season]['CL7FD3'][time]['MVar']} "Closed"     0.00     0.00

       14 "Critical load-5,7 B" "1" "1" "2 "
"${steps[season]['CL5FD3'][time]['status']}"     2.10     0.70     2.21
${steps[season]['CL5FD3'][time]['MW']}
${steps[season]['CL5FD3'][time]['MVar']} "Closed"     0.00     0.00

       15 "Critical load-5,7 C" "1" "1" "1 "
"${steps[season]['CL5FD4'][time]['status']}"     2.00     0.80     2.15
${steps[season]['CL5FD4'][time]['MW']}
${steps[season]['CL5FD4'][time]['MVar']} "Closed"     0.00     0.00

       15 "Critical load-5,7 C" "1" "1" "2 "
"${steps[season]['CL7FD4'][time]['status']}"     2.25     0.94     2.44
${steps[season]['CL7FD4'][time]['MW']}
${steps[season]['CL7FD4'][time]['MVar']} "Closed"     0.00     0.00

       18 "Critical load-8,9 B" "1" "1" "1 " "${steps[season]['Critical
load-8'][time]['status']}"     9.49     2.86     9.91
${steps[season]['Critical load-8'][time]['MW']}
${steps[season]['Crtiical load-8'][time]['MVar']} "Closed"     0.00
0.00

       19 "Critical load-8,9 C" "1" "1" "1 " "${steps[season]['Critical
load-9'][time]['status']}"     8.18     2.86     8.67
${steps[season]['Critical load-9'][time]['MW']}
${steps[season]['Critical load-9'][time]['MVar']} "Closed"     0.00
0.00

       22 "PST12F1 B2" "1" "1" "1 " "Open"     0.00     0.00     0.00
3.02    -0.08 "Closed"     0.00     0.00

       24 "SH Load" "1" "1" "1 "
"${steps[season]['Hospital1'][time]['status']}"     5.80     1.10     5.90
${steps[season]['Hospital1'][time]['MW']}
${steps[season]['Hospital1'][time]['MVar']}"Closed"     0.00     0.00

       25 "PST12F1 L1" "1" "1" "1 " "Open"     0.00     0.00     0.00
1.04     0.39 "Closed"     0.00     0.00
```

```
       26 "C&W L1" "1" "1" "1 " "Open"     0.00     0.00     0.00     0.80
0.40 "Closed"     0.00     0.00

       27 "J&CH L" "1" "1" "1 " "${steps[season]['Critical load-
1'][time]['status']}"     1.50     0.60     1.62
${steps[season]['Critical load-1'][time]['MW']}
${steps[season]['Critical load-1'][time]['MVar']} "Closed"     0.00
0.00

       28 "PS12F1L2" "1" "1" "1 " "Open"     0.00     0.00     0.00
0.57     0.21 "Closed"     0.00     0.00

       29 "C&W12F3 B1" "1" "1" "1 " "Open"     0.00     0.00     0.00
2.96     0.58 "Closed"     0.00     0.00

       30 "C&W12F3 L1" "1" "1" "1 " "Open"     0.00     0.00     0.00
0.17     0.07 "Closed"     0.00     0.00

       33 "PST12F1 L3" "1" "1" "1 " "Open"     0.00     0.00     0.00
1.04     0.39 "Closed"     0.00     0.00

       34 "Critical load-6" "1" "1" "1 " "${steps[season]['Critical load-
6'][time]['status']}"     5.70     0.34     5.71
${steps[season]['Critical load-6'][time]['MW']}
${steps[season]['Critical load-6'][time]['MVar']} "Closed"     0.00
0.00

       35 "3HT12F1 B1" "1" "1" "1 " "Open"     0.00     0.00     0.00
1.88     0.66 "Closed"     0.00     0.00

       36 "3HT12F1 L1" "1" "1" "1 " "Open"     0.00     0.00     0.00
0.41     0.14 "Closed"     0.00     0.00

       46 "Hospital3" "1" "1" "1 "
"${steps[season]['Hospital3'][time]['status']}"     2.80     0.85     2.93
${steps[season]['Hospital3'][time]['MW']}
${steps[season]['Hospital3'][time]['MVar']} "Closed"     0.00     0.00

       47 "Hospital4" "1" "1" "1 "
"${steps[season]['Hospital4'][time]['status']}"     0.30     0.18     0.35
${steps[season]['Hospital4'][time]['MW']}
${steps[season]['Hospital4'][time]['MVar']} "Closed"     0.00     0.00

       48 "3HT12F6 L1" "1" "1" "1 " "Open"     0.00     0.00     0.00
2.03     1.18 "Closed"     0.00     0.00

       49 "3HT12F6 L2" "1" "1" "1 " "Open"     0.00     0.00     0.00
4.74     2.28 "Closed"     0.00     0.00

       50 "3HT12F1 L1" "1" "1" "1 " "Open"     0.00     0.00     0.00
1.88     0.65 "Closed"     0.00     0.00

       51 "C&W12F4 L1" "1" "1" "1 " "Open"     0.00     0.00     0.00
0.51     0.30 "Closed"     0.00     0.00

       52 "C&W12F4 L2" "1" "1" "1 " "Open"     0.00     0.00     0.00
3.84     2.05 "Closed"     0.00     0.00

    }
```

```
    DATA (Gen,
[BusNum,BusName,GenID,GenStatus,GenMW,GenMVR,GenVoltSet,GenAGCAble,GenAVRAb
le,

       GenMWMin,GenMWMax,GenMVRMin,GenMVRMax,GenCostModel,GenParFac])

    {

        4 "Solar" "1" "Closed"     ${steps[season]['Solar'][time]['MW']}
0.01  1.00000 "NO " "YES"     0.00  1000.00     0.01     0.01 "None"
10.00

        5 "Generator1" " 2"
"${steps[season]['Generator1'][time]['status']}"
${steps[season]['Generator1'][time]['MW']}     0.00  1.00000 "YES" "YES"
1.00     9.82     0.00     6.00 "None"     0.16

        <SUBDATA ReactiveCapability>

          //MW   MinMVAR   MaxMVAR

          0.2   -9.99   7.14

          0.4   -9.99   7.13

          0.6   -9.98   7.13

          0.8   -9.96   7.12

          1   -9.94   7.11

          1.2   -9.92   7.1

          1.4   -9.9   7.09

          1.6   -9.87   7.07

          1.8   -9.83   7.06

          2   -9.79   7.04

          2.2   -9.75   7.02

          2.4   -9.7   6.99

          2.6   -9.65   6.97

          2.8   -9.6   6.94

          3   -9.53   6.91

          3.2   -9.47   6.88

          3.4   -9.4   6.85

          3.6   -9.32   6.81

          3.8   -9.24   6.78

          4   -9.16   6.74

          4.2   -9.07   6.7

          4.4   -8.97   6.65
```

```
          4.6   -8.87   6.61
          4.8   -8.77   6.56
          5   -8.66   6.51
          5.2   -8.54   6.46
          5.4   -8.41   6.4
          5.6   -8.28   6.35
          5.8   -8.14   6.29
          6   -8   6.23
          6.2   -7.84   6.16
          6.4   -7.68   6.1
          6.6   -7.51   6.03
          6.8   -7.33   5.96
          7   -7.14   5.89
          7.2   -6.93   5.81
          7.4   -6.72   5.73
          7.6   -6.49   5.65
          7.8   -6.25   5.57
          8   -6   5.49
          8.2   -5.72   5.4
          8.4   -5.42   5.31
          8.6   -5.1   5.1
          8.8   -4.74   4.74
          9   -4.35   4.35
          9.2   -3.91   3.91
          9.4   -3.41   3.41
          9.6   -2.8   2.8
          9.8   -1.98   1.98
          10   0   0
        </SUBDATA>
        6 "Generator2" "1" "${steps
[season]['Generator1'][time]['status']}"
${steps[season]['Generator1'][time]['MW']}     0.00  1.00000 "YES" "YES"
0.50    15.60     0.00     4.80 "None"    10.00
        <SUBDATA ReactiveCapability>
          //MW   MinMVAR   MaxMVAR
```

0.31	-15.59	10.58
0.62	-15.58	10.57
0.93	-15.57	10.57
1.24	-15.54	10.55
1.56	-15.52	10.54
1.87	-15.48	10.52
2.18	-15.44	10.50
2.49	-15.39	10.47
2.80	-15.34	10.44
3.12	-15.28	10.41
3.43	-15.21	10.37
3.74	-15.14	10.33
4.05	-15.06	10.29
4.36	-14.97	10.24
4.68	-14.88	10.19
4.99	-14.77	10.13
5.30	-14.67	10.07
5.61	-14.55	10.01
5.92	-14.42	9.95
6.24	-14.29	9.88
6.55	-14.15	9.8
6.86	-14.00	9.72
7.17	-13.85	9.64
7.48	-13.68	9.56
7.80	-13.50	9.47
8.11	-13.32	9.38
8.42	-13.12	9.28
8.73	-12.92	9.18
9.04	-12.70	9.08
9.36	-12.48	8.97
9.67	-12.23	8.85
9.98	-11.98	8.74
10.29	-11.71	8.61

```
            10.6   -11.43   8.49

            10.92   -11.14   8.36

            11.23   -10.82   8.22

            11.54   -10.49   8.08

            11.85   -10.13   7.94

            12.16   -9.76   7.79

            12.48   -9.36   7.64

            12.79   -8.92   7.48

            13.1   -8.46   7.32

            13.41   -7.96   7.15

            13.72   -7.4   6.97

            14.04   -6.79   6.79

            14.35   -6.11   6.11

            14.66   -5.32   5.32

            14.97   -4.36   4.36

            15.28   -3.1   3.1

            15.6   0   0

        </SUBDATA>

        53 "Battery1" "1" "${(!
(parseFloat(steps[season]['Battery1'][time]['MW']) === 0.00) && Crtiical
load-6Batt) ? 'Closed': 'Open'}"     ${steps [season] ['Battery1']
[time]['MW']}     0.00  1.00000 "YES" "YES"     0.00  1000.00 -9900.00
9900.00 "None"    10.00

        54 "Battery2" "1"
"${(!(parseFloat(steps[season]['Battery2'][time]['MW']) === 0.00)
&& !Crtiical load-6Batt) ? 'Closed': 'Open'}"     ${steps [season]
['Battery2'] [time]['MW']}     2.00  1.00000 "YES" "YES"     0.00  1000.00
-9900.00  9900.00 "None"    10.00

    }

    DATA (Shunt,
[BusNum,BusName,ShuntID,SSRegNum,SSStatus,SSCMode,SSRegulates,SSAMVR,SSVHig
h,

       SSVLow,SSRegVolt,SSDEV,SSNMVR,SSMaxMVR,SSMinMVR])

    {

           3 "Substation-2" "1"        3 "Open" "Fixed" "Volt"    15.00
1.0000   0.9900   1.0000   0.0000    ${steps [season] ['Cap Sub-2'] [time]
['MW']}    50.00     0.00
```

```
        23 "Critical-3" "1"       23 "Closed" "Fixed" "Volt"     1.50
1.0000   0.9900   1.0000   0.0000     ${steps [season] ['Cap Hospital1']
[time] ['MW']}     3.00     0.00

          34 "Critical load-6" "1"       34 "Closed" "Fixed" "Volt"
0.00   1.0000   0.9900   1.0000   0.0000     ${steps [season]['Cap Critical
load-6'][time]['MW']}     3.00     0.00

          46 "Hospital3" "1"        46 "Closed" "Fixed" "Volt"    15.00
1.0000   0.9900   1.0000   0.0000    ${steps [season]['Cap
Hospital3'][time]['MW']}    50.00     0.00

    }

    DATA (Branch,
[BusNum,BusName,BusNum:1,BusName:1,LineCircuit,LineXFType,LineStatus,LineTa
p,


LinePhase,XFAuto,XFRegBus,XFRegValue,XFRegError,XFRegMin,XFRegMax,XFTapMin,

       XFTapMax,XFStep])

     {

         1 "Sub-1."     5 "Genbus1" "2" "Fixed" "Closed"   1.00000
0.00000 "No"     0   0.00000 -0.51000   0.51000   1.50000   0.51000
1.50000   0.00625

         1 "Sub-1."     6 "Genbus2" " 1" "Fixed" "Closed"   1.00000
0.00000 "No"     0   0.00000  -0.51000   0.51000   1.50000   0.51000
1.50000   0.00625

         1 "Sub-1."    12 "Critical load-5,7 A" " 1" "Fixed" "Closed"
${steps[season]['Taps PST'][time]['MW']}   0.00000 "No"     0   0.00000  -
0.51000   0.51000   1.50000   0.51000   1.50000   0.00625

         1 "Sub-1."    13 "Critical load-5,7 D" " 1" "Fixed" "Closed"
${steps[season]['Taps PST'][time]['MW']}   0.00000 "No"     0   0.00000  -
0.51000   0.51000   1.50000   0.51000   1.50000   0.00625

         2 "Sub-4"     7 "C&W Bus 2" " 1" "Fixed" "Closed"   1.00000
0.00000 "No"     0   0.00000  -0.51000   0.51000   1.50000   0.51000
1.50000   0.00625

         2 "Sub-4"     8 "C&W Bus 1" " 1" "Fixed" "Closed"   1.00000
0.00000 "No"     0   0.00000  -0.51000   0.51000   1.50000   0.51000
1.50000   0.00625

         3 "Sub-2"     9 "T&H Bus 1" " 1" "Fixed" "Closed"   1.00000
0.00000 "No"     0   0.00000  -0.51000   0.51000   1.50000   0.51000
1.50000   0.00625

         3 "Sub-2"    10 "T&H Bus 2" " 1" "Fixed" "Closed"   1.00000
0.00000 "No"     0   0.00000  -0.51000   0.51000   1.50000   0.51000
1.50000   0.00625

         3 "Sub-2"    11 "T&H Bus 3" " 1" "Fixed" "Closed"   1.00000
0.00000 "No"     0   0.00000  -0.51000   0.51000   1.50000   0.51000
1.50000   0.00625
```

```
         4 "Sub-3"    16 "MET Bus A" " 1" "Fixed" "Closed"
${steps[season]['Taps M1'][time]['MW']}   0.00000 "No"     0   0.00000  -
0.51000   0.51000   1.50000   0.51000   1.50000   0.00625

         4 "Sub-3"    17 "MET Bus D" " 1" "Fixed" "Closed"
${steps[season]['Taps M2'][time]['MW']}   0.00000 "No"     0   0.00000  -
0.51000   0.51000   1.50000   0.51000   1.50000   0.00625

        21 "Crtiical load-1"    27 "J&CH L" " 1" "Fixed" "Closed"   1.00000
0.00000 "No"     0   0.00000  -0.51000   0.51000   1.50000   0.51000
1.50000   0.00625

        23 "Hospital1 Bus"    24 "SH Load" " 1" "Fixed" "Closed"   1.00000
0.00000 "No"     0   0.00000  -0.51000   0.51000   1.50000   0.51000
1.50000   0.00625

        32 "PST12F1 B4"    34 "Crtiical load-6 campus" " 1" "Fixed"
"Closed"   1.00000   0.00000 "No"     0   0.00000  -0.51000   0.51000
1.50000   0.51000   1.50000   0.00625

        43 "Hospital3 & Hospital4"    46 "Hospital3" " 1" "Fixed" "Closed"
1.00000   0.00000 "No"     0   0.00000  -0.51000   0.51000   1.50000
0.51000   1.50000   0.00625

        43 "Hospital3 & Hospital4"    47 "Hospital4" " 1" "Fixed" "Closed"
1.00000   0.00000 "No"     0   0.00000  -0.51000   0.51000   1.50000
0.51000   1.50000   0.00625

     }

     DATA (OverExcitationLimiter_OEL1,
[BusNum,GenID,TSDeviceStatus,TSFlag,TSIfdref,TSIfdmax,TSTpickup,TSRunBack,T
STmax,

        TSTset,TSIfcont,TSAlarm])

     {

          6 "1" "Active" 0 2.1 2.15 -10 0 30 20 2.1 0

     }

     DATA (PlantController_REPC_A,
[BusNum,GenID,WhoAmI,WhoAmI:1,TSDeviceStatus,RefFlag,VcompFlag,FreqFlag,TST
f,TSKp,
TSKi,Tft,TSTfv,TSVfrz,TSRc,TSXc,TSKc,TSMaxerr,TSMinerr,Dbd,TSQmax,TSQmin,Kp
g,
Kig,TSTp,Dbd:1,Dbd:2,Femax,Femin,TSPmax,TSPmin,TSTlag,Ddn,Dup,TSMWCap])

     {

         53 "1" "none" "none" "Active" 1 1 0 0.05 10 10 0 3 0.7 0 0 1 1 -1
0 1 -1 10 10 0 0 0 1 -1 2 0 3 20 0 0

         54 "1" "none" "none" "Active" 1 1 0 0.05 10 10 0 3 0.7 0 0 1 1 -1
0 1 -1 10 10 0 0 0 1 -1 2 0 3 20 0 0

     }

     DATA (Gen, [BusNum,GenID,GenMVABase,TSGovRespLimit])

     {
```

```
          6 "1" 15.6 "Normal"

         53 "1" 100 "Normal"

         54 "1" 100 "Normal"

     }

     DATA (Exciter_EXST4B,
[BusNum,GenID,TSDeviceStatus,TSTr,TSKpr,TSKir,TSTa,TSVrMax,TSVrMin,TSKpm,TS
Kim,

        TSVmmax,TSVmmin,TSKg,TSKp,TSAngleP,TSKi,TSKc,TSXl,TSVbMax])

     {

          6 "1" "Active" 0 15 15 0.02 1 -0.87 1 0 1 -0.87 0 3.5 0 0 0.01 0
99

     }

     DATA (Gen, [BusNum,GenID,GenMVABase,TSGovRespLimit])

     {

          6 "1" 15.6 "Normal"

     }

     DATA (Governor_HYGOV,
[BusNum,GenID,TSDeviceStatus,TSTrate,TSRperm,TSRtemp,TSTr,TSTf,TSTg,TSVelm,
TSGmax,TSGmin,TSTw,TSAt,TSDturb,TSQnl,TSTtur,TSTn,TSTnp,TSDb:1,TSEps,TSDb:2
,TSGv,TSPgv,TSGv:1,TSPgv:1,TSGv:2,TSPgv:2,TSGv:3,TSPgv:3,TSGv:4,TSPgv:4,TSG
v:5,TSPgv:5,TSHdam,TSBgv,TSBgv:1,TSBgv:2,TSBgv:3,TSBgv:4,TSBgv:5,TSBmax,TST
blade])

     {

          5 " 2" "Not active" 0 0.04 0.3 5 0.05 0.5 0.2 1 0 1 1.2 0.5 0.05
0.5 0 0 0 0 0 0 0 0 0 0 0 0 0 0 0 0 0 1 0 0 0 0 0 0 0 0 100

          6 "1" "Active" 0 0.04 0.3 5 0.05 0.5 0.2 1 0 1 1.2 0.5 0.05 0.5 0
0 0 0 0 0 0 0 0 0 0 0 0 0 0 0 0 0 1 0 0 0 0 0 0 0 0 100

     }

     DATA (Gen, [BusNum,GenID,GenMVABase,TSGovRespLimit])

     {

          5 " 2" 100 "Normal"

          6 "1" 15.6 "Normal"

     }

     DATA (MachineModel_GENCLS,
[BusNum,GenID,TSDeviceStatus,TSH,TSD,TSRa,TSXd:1,TSRcomp,TSXcomp])

     {

          4 "1" "Active" 3 0 0 0.2 0 0

     }
```

```
     DATA (MachineModel_GENTPJ,
[BusNum,GenID,TSDeviceStatus,TSH,TSD,TSRa,TSXd,TSXq,TSXd:1,TSXq:1,TSXd:2,TS
Xq:2,


TSXl,TSTdo,TSTqo,TSTdo:1,TSTqo:1,TSS1,TSS1:1,TSRcomp,TSXcomp,TSAccFactor,

        TSKis])

     {

          5 " 2" "Active" 3 0 0 2 0.4762 0.2 0.4762 0.1714 0.18 0.1429 7
0.75 0.035 0.05 0 0 0 0 0.4 0

          6 "1" "Active" 2.75 0 0 0.9 0.6 0.293 0.6 0.268 0.268 0.23 5 0
0.03 0.05 0.2 0.55 0 0 0.5 0.06

     }

     DATA (Gen, [BusNum,GenID,GenMVABase,TSGovRespLimit])

     {

          4 "1" 100 "Normal"

          5 " 2" 100 "Normal"

          6 "1" 15.6 "Normal"

     }

    `let fileName = season+'_'+time.replace(':00','')+'.aux'

    jx(true,files,{ [season] : { [time] : [fileName] } })

    let fileDir = 'aux/'

    fs.writeFile(fileDir+fileName,content,'utf8', (err) => {

      console.log(fileName +' (#'+ fileCount +') is complete!')

      fileCount--

      if(!fileCount) console.log('All Files have completed!')

    })

  }

}

function range(start, end) {

    var foo = [];

    for (var i = start; i <= end; i++) {

        foo.push(i);

    }

    return foo;

}
```